Studies on non-supersymmetric D1-D5-P gravitational bound states

By

Bidisha Chakrabarty

PHYS07201204001

Institute of Physics, Bhubaneswar

A thesis submitted to the

Board of Studies in Physical Sciences

In partial fulfillment of requirements

For the Degree of

DOCTOR OF PHILOSOPHY

of

HOMI BHABHA NATIONAL INSTITUTE

July, 2017

Homi Bhabha National Institute

Recommendations of the Viva Voce Board

As members of the Viva Voce Board, we certify that we have read the dissertation prepared by Bidisha Chakrabarty entitled "Studies on non-supersymmetric D1-D5-P gravitational bound states" and recommend that it maybe accepted as fulfilling the dissertation requirement for the Degree of Doctor of Philosophy.

____ Date:

Chairman -

____ Date:

Guide/Convener -

____ Date:

External examiner -

____ Date:

Member 1 -

____ Date:

Member 2 -

Final approval and acceptance of this dissertation is contingent upon the candidate's submission of the final copies of the dissertation to HBNI.

I hereby certify that I have read this dissertation prepared under my direction and recommend that it may be accepted as fulfilling the dissertation requirement.

Date:

Place: Guide

STATEMENT BY AUTHOR

This dissertation has been submitted in partial fulfillment of requirements for an advanced degree at Homi Bhabha National Institute (HBNI) and is deposited in the Library to be made available to borrowers under rules of the HBNI.

Brief quotations from this dissertation are allowable without special permission, provided that accurate acknowledgement of source is made. Requests for permission for extended quotation from or reproduction of this manuscript in whole or in part may be granted by the Competent Authority of HBNI when in his or her judgement the proposed use of the material is in the interests of scholarship. In all other instances, however, permission must be obtained from the author.

Bidisha Chakrabarty

DECLARATION

I, hereby declare that the investigation presented in the thesis has been carried out by me. The work is original and has not been submitted earlier as a whole or in part for a degree / diploma at this or any other Institution / University.

Bidisha Chakrabarty

List of Publications arising from the thesis:

- **Published in Journal**

  1. **Bidisha Chakrabarty**, David Turton and Amitabh Virmani, *"Holographic description of non-supersymmetric orbifolded D1-D5-P solutions"*, *JHEP 11(2015) 063*.
  2. **Bidisha Chakrabarty** and Amitabh Virmani, *"Geroch Group Description of Black Holes"*, *JHEP 11(2014)068*.
  3. **Bidisha Chakrabarty**, Jorge Rocha and Amitabh Virmani, *"Smooth non-extremal D1-D5-P solutions as charged gravitational instantons"*, *JHEP 08(2016)027*.

- **Talks given in Conferences**

  1. **Non-BPS D1-D5-P solutions and Gravitational Instantons**
     Indian Strings Meeting – IISER Pune, India (12/2016).
  2. **On orbifolded fuzzball geometry**
     National strings meeting – IISER, Mohali, India (12/2015).
  3. **On orbifolded fuzzball geometry**
     Young Researcher's conference – IOP, Bhubaneswar, India (09/2015).
  4. **Geroch group description of Black holes**
     Indian Strings Meeting – Puri, India (12/2014).
  5. **Geroch group description of Black holes**
     Field theoretic aspects of Gravity – IISER Mohali, India (12/2014).

Bidisha Chakrabarty

DEDICATIONS

To my family

ACKNOWLEDGEMENTS

I am thankful to my Ph.D supervisor Dr Amitabh Virmani for his continuous guidance, support and encouragement throughout the course of my doctoral studies. I thank my parents, my sister and my friends for the motivation and support they have provided in my ups and downs. I would like to thank all my collaborators, working with whom have been a good learning experience for me. I wish to thank the Theoretical Physics group at IOP for useful discussions and support during my academic pursuit. Finally I acknowledge the help of IOP community and the fellowship from the administration during the course of my Ph.D.

SYNOPSIS

Ever since the birth of General Relativity (GR) it has been of great interest to understand its dynamics, its exact solutions and their properties. Einstein's equations being coupled, non-linear partial differential equations are nontrivial to solve unless there is sufficient symmetry present in the system. Over the years enormous effort has been invested to discover solution generating techniques that make use of symmetries to construct new exact solutions of GR including interesting black hole solutions. Although classical GR is a beautiful theory that admits various black hole solutions, we need a viable quantum theory of Gravity to understand the microscopic origin of black hole entropy, to resolve the spacetime singularities that appear in classical GR and to describe phenomenon like Hawking evaporation via unitary evolution.

Superstring theory is so far the most powerful framework to describe quantum gravity. String theory has been quite successful in explaining the microscopic origin of black hole entropy for certain extremal and near-extremal black holes. The first example appeared in the seminal paper by Strominger and Vafa where the area-entropy relation was derived for a class of five dimensional extremal black holes by counting microscopic degeneracy of BPS states. One might wonder that the black hole in a supergravity and microstates in string theory are at two different regimes of coupling, so how to compare the entropy of these two quantities? The answer is that the BPS states do not jump discontinuously as one varies the moduli and coupling constants of the theory. As a result one can count the degeneracy of BPS states in string theory having a fixed charge at weak coupling and extrapolate the result to strong coupling where the states have a black hole description with the same charge. Since the work of Strominger and Vafa, the so-called D1-D5 system has been extensively studied in the string theory literature.

The goal of this thesis is to investigate various features of nonsupersymmetric smooth D1-D5-P supergravity solutions, taking motivation from AdS/CFT. We also present novel approaches to construct these solutions systematically using group theory techniques. This work is organised as follows.

Introduction: Chapter 1 and chapter 2 of the thesis are devoted to discussing the motivation and introductory material on black hole information paradox, the fuzzball conjecture, hidden symmetries in gravitational theories and integrability in $2D$ gravity.

Holographic description of orbifolded JMaRT: Black holes have temperature, hence they radiate. In this process they lose mass and finally evaporate away completely. Stephen Hawking in 1974 has argued that laws of quantum mechanics are violated in black hole formation and evaporation process. This is known as the black hole 'Information loss Paradox'. However, quantum mechanics is one of the most successful and critically tested framework. Consequently there have been many proposals to resolve the information puzzle, one of the promising proposals is known as the 'Fuzzball conjecture' [1]. According to the conjecture, associated with a black hole of entropy S there are e^S horizon-free nonsingular configurations that asymptotically look like the black hole but start differing from it at the horizon scale. With this picture the would be horizon is no longer in a vacuum state, so the radiation that comes out of it, carries information and there is no information loss. The singularity resolution at the horizon scale for the geometries seems astonishing, however, it should not be too surprising as there are solutions in the context of string theory where timelike singularities are resolved in a similar manner.

For supersymmetric (BPS) black holes, the fuzzball picture is well explored. Scaling solutions with long AdS throats resembling black holes have been constructed. Multicenter bubbling geometries and families of superstratum solutions have also been obtained [2]. Examples of almost BPS smooth solutions have also been constructed. Non-extremal black hole microstates are of great interest in order to resolve the information puzzle as extremal black holes do not Hawking radiate. Though much less is known about them.

The most notable example of nonextremal smooth geometry is the so called JMaRT solution found by Jejjala, Madden, Ross and Titchener [3]. In chapter 3 of the thesis we explore certain orbifolds of JMaRT solution and study their smoothness properties. This chapter is based on the work we have pursued in [4]. In the decoupling limit, JMaRT geometry reduces to $AdS_3 \times S^3$. Using the AdS/CFT correspondence we identify the dual CFT states of orbifolded JMaRT and we find exact agreement of the conserved charges calculated from the gravity and CFT sides. The CFT states are described by fractionally filled Fermi levels on Ramond-Ramond (RR) ground state. It is known that JMaRT solution has an ergoregion with a classical instability. We study this instability in the cases of orbifolds with the most general form of the probe scalar wave function and find exact matching between the emission rates calculated from the gravity and CFT sides. We also study pair creation like picture of ergoregion emission including all three charges, orbifolding and two rotations. Our results represent the largest class of non-BPS black hole microstate geometries with identified dual CFT states presently known.

Exact solution generation techniques: Higher dimensional gravity theories when dimensionally reduced to two dimensions manifest infinite number of symmetries. The infinite dimensional symmetry group is known as the Geroch group and the associated Lie algebra is a Kac-Moody algebra. The origin of this infinite dimensional symmetry lies in the fact that there are two inequivalent ways to reduce pure gravity to $2D$ from higher dimensions, known as the Ehlers and Matzner-Misner reduction schemes. The symmetries resulting from these two reduction schemes do not commute because they are realized on different field variables. These variables are related by a non-local transformation called the Kramer-Neugebauer transformation. The intertwining of the two sets of non-commuting symmetries give rise to the enhanced affine symmetry. It has been argued that the Geroch symmetry transformations act transitively on the solution space of Einstein gravity with requisite symmetry. Thus exploiting these symmetry transformations it is possible to systematically construct new exact solutions of GR and supergravity starting from a simple seed (e.g. Minkowski space in $D = 4$). A recipe is provided by Breitenlohner and Maison [5–7].

In general, a D dimensional gravity-matter system with k number of commuting Killing symmetries can be dimensionally reduced to $D - k$ dimensions and the reduced theory admits an enhanced symmetry group, known as the group of hidden symmetries. For example $4D$ gravity reduced to $3D$ has an $SL(2, R)$ hidden symmetry, $11D$ supergravity reduced to $3D$ has the exceptional group $E_{8(8)}$ as the hidden symmetry group. These hidden symmetries have been exploited to construct various black hole solutions in $4D$ and $5D$, see e.g. [8, 9].

In chapter 4 of the thesis certain aspects of the 2D symmetries are explored. In particular we consider black holes in $5D$ vacuum gravity and $4D$ Einstein-Maxwell theory and study their Geroch group description. The chapter is based on our work [10]. We have identified the relation between space-time Monodromy matrices and constant Geroch group matrices. We have constructed Geroch group $SL(3, R)$ matrices for the $5D$ Myers-Perry and Kaluza-Klein black holes and the Geroch group $SU(2, 1)$ matrix for the $4D$ Kerr-Newman black hole. All these cases are two soliton solutions where the solitons sit at the two poles of the Geroch group matrix with residues of rank one. We further demonstrate the Riemann-Hilbert factorization of Geroch group matrices for the above examples. In all of these cases the Geroch group matrices become constants at spatial infinity. The subleading asymptotic form of the Geroch group matrix determines the charge matrix. We present certain non-trivial relations between the Geroch group matrices and charge matrices for the examples we consider.

Non-extremal smooth solutions as charged gravitational instantons: In solving the black hole entropy puzzle and the information loss paradox, it is useful to understand black hole microstates from different perspectives. Such a study has been very useful for BPS microstates in $6D$ supergravity. In [11] it was shown that a class of solutions can be cast in a suggestive base-fiber form. This rewriting paved the way to the construction of multi-center bubbling solutions.

As the number of microstates of a black hole is very large, it is useful to classify some of them in a systematic way. For a large class of known microstates only spacelike Killing vectors degenerate. This gives rise to the possibility of relating them to gravitational instanton, where also only spacelike Killing vectors degenerate. Gravitational instantons are smooth Euclidean solutions of the vacuum Einstein's equation with or without a cosmological constant. Gravitational instantons in $4D$ are well explored in Euclidean Gravity paradigm, but their higher-dimensional cousins are not so well studied.

In chapter 5 of the thesis we look at the non-supersymmetric D1-D5-P JMaRT solution from a new point of view, namely as a charged gravitational instanton. The discussion in this chapter is based on our work [12]. Here we present an inverse scattering construction of the non-supersymmetric three charge, doubly rotating JMaRT solution and show that these solutions can be thought of as charged Euclidean $5D$ Myers-Perry instanton. We present an explicit construction of the Myers-Perry (MP) instanton metric in Euclidean $5D$ gravity using Belinski-Zakharov solution generating technique starting from a Euclidean Schwarzschild solution. The BZ technique is based on the same group theory techniques discussed in the previous chapter. The MP instanton is then uplifted to $6D$ by adding a flat timelike direction. We add charges on the $6D$ metric using appropriate $SO(4,4)$ hidden symmetry transformations. The $SO(4,4)$ hidden symmetry arises upon dimensional reduction from $6D$ to $3D$. The $6D$ theory we work with, is a consistent truncation of IIB supergravity compactified on T^4. It has metric, dilaton and the RR 2-form. We analyze the rod structures of the solutions constructed and compare them with black holes. The angular momentum bounds in our construction perfectly agree with the ones necessary for the smooth microstate geometries, and various smoothness requirements precisely give the JMaRT solution.

Conclusion: A summary and possible future directions are discussed in chapter 6. We have studied non-BPS D1-D5-P system closely and have systematically constructed the JMaRT solution using solution generating techniques. Using related techniques we have also investigated certain black hole solutions.

Contents

Chapter 1

Introduction

It has been more than hundred years since the advent of General relativity (GR). The predictions of GR have been successfully tested to remarkable accuracy in several astronomical observations such as the perihelion precession of planetary orbits, the bending of light around massive objects, the gravitational redshift and so on. Classical GR admits interesting solutions known as black holes. Such an object possesses a region of space-time where the gravitational attraction is so strong that classically no particle or signal can escape from that region. Hence it has not been possible to observe black holes in direct astrophysical observations so far. An exciting development in this direction is the experimental detection of gravitational waves in 2016. Gravitational waves were predicted as early as 1916. They were detected recently at the LIGO experiment [13]. The observed gravitational waves originated from a pair of coalescing black holes.

Though classical GR is an elegant theory, it is not complete by itself. Black holes for instance possess singularities that are shielded from the physical world by an event horizon. It is expected that a theory of gravity that also incorporates the laws of quantum mechanics, i.e., a quantum theory of gravity, is required to resolve the black hole singularities. In the usual formulation of quantum field theory in four space-time dimensions, perturbative gravity is non-renormalisable because Newton's constant has negative mass dimensions.

In 1974 Hawking did a semiclassical analysis by considering quantum field theory in a classical black hole background and showed that black holes emit thermal radiation like that of a black body [14]. As black hole evaporates completely via this thermal radiation, the fundamental laws of quantum mechanics appear to be violated. This is known as the black hole information loss paradox. General relativity and quantum mechanics are not consistent together.

Black holes have a temperature and entropy. The macroscopic entropy of a black hole is given by the Bekenstein-Hawking formula $S = \frac{A}{4G\hbar}$, where A is the horizon area [15]. According to the "no hair" theorem, a black hole is completely characterized by its mass M, charges Q_i and angular momentum J. This is reminiscent of quantum numbers that characterize microscopic states in statistical mechanics. One wonders if the Bekenstein-Hawking entropy of the black hole has a statistical interpretation, i.e., a microscopic origin.

A consistent theory of quantum gravity is expected to address many of the puzzles that we face in modern physics, namely resolution of the black hole information paradox, origin of microscopic entropy of black holes, resolution of spacetime singularities and so on. String theory is the best candidate theory for quantum gravity so far. It has successfully provided methods and avenues to address many of the challenges faced in quantum gravity. In the following sections we briefly review black holes in general relativity in four spacetime dimensions, the information puzzle, and also provide an brief introduction to string theory.

1.1 Black holes

Black holes in general relativity appear as solutions of Einstein's equations

$$R_{\mu\nu} - \frac{1}{2}Rg_{\mu\nu} = 8\pi G T_{\mu\nu} \,, \tag{1.1}$$

where $R_{\mu\nu}$ and $R = g^{\mu\nu}R_{\mu\nu}$ are the four dimensional Ricci tensor and Ricci scalar for the metric $g_{\mu\nu}$ respectively. $T_{\mu\nu}$ is the energy momentum tensor for the matter fields and G is the four dimensional Newton's constant. Black holes have curvature singularities at the center at $r = 0$ where classical GR breaks down. Near the singularity quantum gravity effects are expected to become strong. Hence black holes are useful objects in the study of quantum gravity. The singularity of a black hole is cloaked by an event horizon that acts a causal boundary between points in spacetime. Any observer outside an event horizon of a classical black hole has no information about the interior region. Uniqueness theorems in GR limit the number of possible black hole solutions in four dimensions. They are Schwarzschild black hole ($M \neq 0, Q = 0, J = 0$), Reissner-Nördstrom black hole ($M \neq 0, Q \neq 0, J = 0$), Kerr black hole ($M \neq 0, Q = 0, J \neq 0$) and Kerr-Newman black hole ($M \neq 0, Q \neq 0, J \neq 0$).

As an example consider a 3 + 1 dimensional Schwarzschild black hole. According to Birkhoff's theorem this is the unique spherically symmetric vacuum ($T_{\mu\nu} = 0$) black hole solution of Einstein's equation in four spacetime dimensions. The metric outside the black hole is given by

$$ds^2 = -\left(1 - \frac{2GM}{r}\right)dt^2 + \frac{dr^2}{\left(1 - \frac{2GM}{r}\right)} + r^2(d\theta^2 + \sin^2\theta d\phi^2). \tag{1.2}$$

The horizon is located at $r = 2GM$ where the g_{tt} component of the metric becomes zero and the g_{rr} component diverges. This divergence of the metric component is just a coordinate artifact. One can go to Kruskal-Szekeres coordinates for maximally extended Schwarzschild metric that covers both the outside and inside of the black hole. In these coordinates the metric is completely smooth across $r = 2GM$. Looking at the metric (1.2) it becomes clear that for $r < 2GM$ the radial and the time coordinates get interchanged. Hence $t = const$ spacelike slices outside the horizon becomes timelike in the interior of black hole and similarly $r = const$ timelike slices outside becomes spacelike in the interior. The Schwarzschild metric components do not depend on t and hence ∂_t is a Killing vector in the geometry.

The next example we consider is that of a 3 + 1 dimensional Reissner-Nördstrom (RN) black hole. It is the unique spherically symmetric static charged black hole solution of Einstein gravity coupled to Maxwell field in $3+1$ dimensions. The metric and gauge field are given by

$$ds^2 = -\left(1 - \frac{2GM}{r} + \frac{Q^2G}{r^2}\right)dt^2 + \frac{dr^2}{\left(1 - \frac{2GM}{r} + \frac{Q^2G}{r^2}\right)} + r^2(d\theta^2 + \sin^2\theta d\phi^2)\ ,$$
$$A_t = \frac{Q}{r}. \tag{1.3}$$

Again the metric has a curvature singularity at $r = 0$ and the horizons are located at

$$r_\pm = GM \pm \sqrt{(GM)^2 - Q^2G}. \tag{1.4}$$

There are three possible cases. When $GM^2 < Q^2$, $r_\pm$ has no real roots and the curvature singularity at $r = 0$ becomes a 'naked singularity', that is not surrounded by any horizon. According to the cosmic censorship conjecture in GR, such solutions do not form in a realistic gravitational collapse. When $GM^2 > Q^2$, $r_\pm$ are real roots. These roots correspond to location of the outer and inner horizons of the black hole. The outer horizon $r = r_+$ serves to be the event horizon. When $GM^2 = Q^2$ the two horizons coincide as $r_+ = r_- = MG$. This limit is called the extremal limit. An extremal black hole has minimum mass M for a given charge Q. The near horizon region of extremal RN is $AdS_2 \times S^2$.

For a given mass M, charges Q_i and angular momentum J, a black hole is completely characterized (no hair theorem). Hence many initial configurations of matter upon gravitational collapse can give rise to the same black hole. One wonders what happens to the information about various states of matter that create the black hole. Hawking in 1974 sharpened this question, when he considered quantum field theory in the background of a classical Schwarzschild black hole. He showed that the black hole radiates thermally with a temperature $T_H = \frac{\hbar\kappa}{2\pi}$ where κ is the surface gravity of the black hole [14]. In the case of extremal black holes surface gravity vanishes, and hence they do not Hawking radiate.

Black holes have entropy given by $S = \frac{A}{4G\hbar}$ where A is the horizon area [15]. Bekenstein came up with the idea of area-entropy relation by considering a "thought experiment". Consider a box full of heat radiation being lowered towards a black hole horizon quasistatically. Once it reaches the horizon the box is opened, its content is thrown inside the black hole and the box is taken back to a safe distance from the black hole. Heat energy produces disorder in the molecules and hence contributes to entropy. The heat energy transferred to the black hole can never come out of it. To save the second law of thermodynamics that says total entropy of the universe always increases in any irreversible process, the black hole has to be assigned an entropy. Since the heat flows in through the horizon area, he conjectured that the entropy of the black hole has to be proportional to the area. In general black hole entropy is a function of black hole charges. All these ideas combined together give rise to the laws of black hole thermodynamics [16, 17].

According to the zeroth law of black hole mechanics κ remains constant on the horizon of stationary black holes. This resembles the zeroth law of thermodynamics for usual bodies that states that for a system in thermal equilibrium the temperature is a constant across the system. The first law of thermodynamics is the law of conservation of total energy. The first law in case of a rotating, charged black hole takes the form,

$$dM = \kappa \frac{dA}{8\pi G} + \Omega dJ + \Phi dQ, \tag{1.5}$$

where Ω is the angular velocity of the black hole and Φ is the electrostatic potential. κ, Ω and Φ are constants on the horizon of a stationary black hole. κ plays the role of temperature, A is related to the entropy. The first law tells us how a black hole responds to an infinitesimal perturbation of mass dM. In close analogy to the second law of thermodynamics, the second law of black hole mechanics says that the horizon area of a black hole never decreases in any classical process. Bekenstein also conjectured a generalized second law (GSL) that states $\delta S_{outside} + \delta S_{BH} \geq 0$ and this strictly holds true when quantum effects are included. The third law of black hole physics says that black holes with zero surface gravity cannot be obtained following a finite number of steps. Note that extremal black holes have zero surface gravity with non-zero entropy.

In Hawking's semiclassical calculations, particle-antiparticle pairs are produced at the black hole horizon from vacuum due to quantum fluctuations in the presence of strong gravitational field of the black hole. This is very similar to the Schwinger pair creation that happens from vacuum when a strong electric field is applied. In the case of a black hole the particle having negative energy falls in the black hole and the outgoing particles give rise to a thermal radiation at infinity. If we assume that the black hole was created from a pure state, then it appears that its final state of evolution being thermal radiation, is a mixed state. Such an evolution violates laws of unitarity in quantum mechanics. Since we cannot extract any information from thermal radiation (which is random), it appears that all the information that went into the creation of the black hole cannot be retrieved. Thus Hawking's semiclassical analysis suggests that information is lost in black hole evaporation process. In the following section we discuss the information loss puzzle in more details. For further details and for more precise statements on the laws of black hole mechanics we refer the reader to [18].

1.2 Information paradox

Consider a Schwarzschild black hole of mass M that has formed from a gravitational collapse. The conformal diagram of a black hole formed by a gravitational collapse is shown in figure 1.1. The initial matter that collapsed to form the black hole is lost in the curvature singularity. At late times, away from the singularity there is vacuum everywhere including at the horizon. The horizon is locally described by the so-called "Unruh vacuum". Due to vacuum fluctuations particle-antiparticle pair creation can take place at the event horizon. Particles that are produced just inside the horizon falls into the black

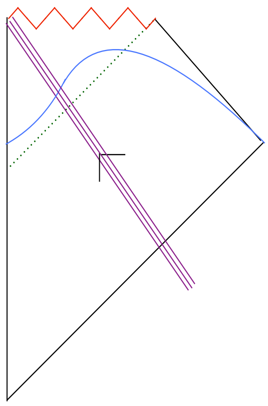

Figure 1.1: Penrose diagram of a black hole formed by gravitational collapse of null matter.

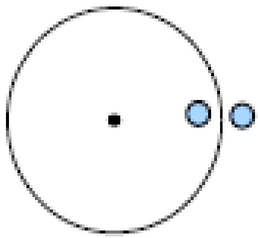

Figure 1.2: Pair creation from horizon.

hole, and the particle created outside can float off to infinity in the form of Hawking radiation [14]. See figure 1.2. In this process the mass and entropy of the black hole decrease. After sufficiently long time the black hole evaporates completely into thermal radiation at infinity. Since the pair creation happens from vacuum the final radiation has no memory of the initial composition of matter that forms the black hole. This leads to information loss. The initial pure matter has evolved into a mixed thermal state. This is not an unitary evolution. In quantum mechanics given an initial state, one acts with the time evolution operator e^{-iHt} on that to construct the final state and vice-versa. In the black hole evaporation process there can be many initial states that give rise to the thermal radiation at the end. It appears that the laws of quantum mechanics are in conflict with the black hole formation and evaporation process.

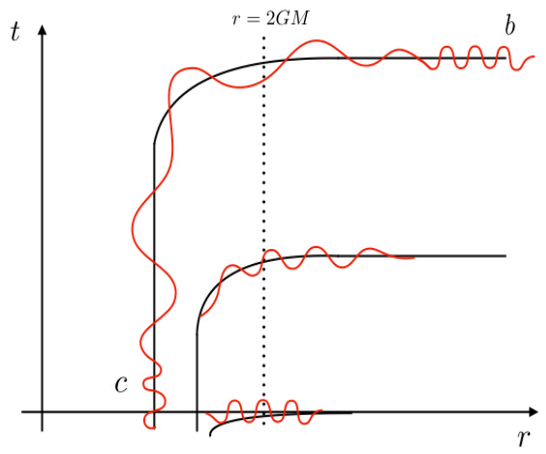

Figure 1.3: Nice slices in a black hole spacetime

Let us try to understand the pair creation phenomenon in a little more detail. We consider nice spacelike slices that cover both the outside and inside of the black hole as given in the figure 1.3. In the outside of the black hole $t = constant$ is a spacelike slice whereas in the interior $r < 2GM$ the spacelike slices are $r = constant$ slices. Note that a later slice with higher value of t (schematic time) had to stretch compared to an earlier slice with smaller t. This stretching of nice slices across the horizon gives rise to particle creation when we study quantum fields in the black hole background.

The produced pair (b, c) is in an entangled state. One can not talk about b particle states alone. When the entire black hole is evaporated away, the radiation (b-particles) is entangled with nothing since there are no c-particles to entangle with. This never happens in quantum mechanics. The entangled state of the first bc-pair is

$$|\psi\rangle_1 = Ce^{\gamma \hat{b}_1^\dagger \hat{c}_1^\dagger}|0\rangle_{b_1}|0\rangle_{c_1}, \tag{1.6}$$

where C and γ are constants. As more and more particle pairs are created the total state of the system becomes a direct product of all the individual pairs

$$|\psi\rangle = |\psi\rangle_1 \otimes |\psi\rangle_2 \otimes |\psi\rangle_3 \otimes \dots \qquad . \tag{1.7}$$

This is clearly a mixed state and not a factored state. Hence unitarity seems to be violated at the end of evaporation process. Information paradox presents a fundamental inconsistency between general relativity and quantum mechanics that a viable quantum theory of gravity is expected to address.

1.3 String theory

String theory is one of the best candidate for a quantum theory of gravity. In the framework of string theory the fundamental objects that describe our nature are one dimensional strings. The energy per unit length of the string is called the string tension $T = \frac{1}{2\pi l_s^2}$ where l_s is string length. The string length l_s is an independent parameter. It is expected to be of the order of Planck length, i.e., 10^{-35}m. Strings are not yet observed in experiments since at present even the best available particle accelerators cannot probe such a small length. Unlike point particle interactions, string interactions are UV finite. The string length l_s acts as a short distance cutoff.

Strings can be of two kinds: open or closed. The motion of the strings sweeps out a two-dimensional worldvolume in spacetime known as the string worldsheet. In its simplest form, the string action is given by the area of the worldsheet. First quantization of the string gives rise to 1 + 1 dimensional quantum field theory on the worldsheet where the spatial direction σ has a finite extent. From the world sheet point of view the target space coordinates X^μ appear as fields. Since along the compact spatial coordinate σ, momentum p is quantized, each worldsheet field is thought of as a collection of harmonic oscillators with momentum p. These oscillator modes are the creation and annihilation operators. Acting with the creation operators on the vacuum one can generate an infinite

Type	IIA			IIB		
Form Fields	B_2	C_1	C_3	B_2	C_2	C_4
Electric	$F1$	$D0$	$D2$	$F1$	$D1$	$D3$
Magnetic	$NS5$	$D6$	$D4$	$NS5$	$D5$	$D3$

Table 1.1: A summary of the form fields of type IIA and IIB supergravity, together with electrically and magnetically charged branes under those form fields.

tower of states. The infinite tower contains both massive and massless states. The massive states with mass proportional to the inverse of l_s are extremely heavy. For low energy considerations we focus on the massless sector. The massless excitations of open strings contain gauge fields and that of closed strings contain spin-2 Graviton $g_{\mu\nu}$, Neveu-Schwarz Neveu-Schwarz (NS-NS) field $B_{\mu\nu}$ and the scalar dilaton ϕ. Thus quantization of strings give rise to gravity.

Bosonic string theory does not have a stable ground state. When fermions are added to the worldsheet introducing supersymmetry, the theory is called superstring theory. On a closed string, fermions can have either periodic or antiperiodic boundary conditions. These are known as Ramond and Neveu Schwarz sectors respectively. The classical action of superstrings has superconformal invariance. At the quantum level superconformal invariance requires the theory to live in 10 space-time dimensions. The known consistent superstring theories are of five kinds namely type I, type IIA, type IIB, heterotic $SO(32)$ and heterotic $E_8 \times E_8$. Type I and the two heterotic theories have $\mathcal{N} = (1,0)$ supersymmetry on the worldsheet. Since in ten dimensions minimal spinor is Majorana Weyl with 16 independent components, the above three superstring theories preserve 16 real supercharges. Type IIA and type IIB have $\mathcal{N} = (1,1)$ and $\mathcal{N} = (2,0)$ supersymmetry, respectively, with 32 real supercharges. Type IIA theory is nonchiral that means it has both left handed and right handed fermions, the other four theories have chiral spinors.

The low energy limit of superstring theory is supergravity. Apart from $(g_{\mu\nu}, \phi)$, these theories also contain form fields. The form field content of type IIA and IIB supergravity is summarized in table 1.1.

1.3.1 D-branes

Open strings have two end points where two different types of boundary conditions can be imposed.

- Neumann boundary conditions: $\partial_\sigma X^\mu = 0$ at $\sigma = 0, \pi$ where σ is the spatial world-sheet coordinate and X^μ are the target space coordinates. This condition allows the end points of the open string to move freely.
- Dirichlet boundary conditions: $\delta X^\mu = 0$ at $\sigma = 0, \pi$ that keep the end points of the open string fixed.

Consider a D dimensional space-time on which we impose Neumann boundary conditions on $p+1$ coordinates say $a = 0, 1, ..., p$ and Dirichlet boundary conditions on the rest of the $D-p-1$ coordinates $b = p+1, .., D-1$. Then the end points of the open string lie on a $p+1$ dimensional hypersurface. This hypersurface is called a D-brane (D comes from Dirichlet). See figure 1.4. D-branes are non-perturbative, solitonic objects in string theory. They have mass $M \propto \frac{1}{g_s}$ where g_s is the string coupling. In perturbative string theory these objects are extremely heavy and not seen in the spectrum. They are revealed when we study the theory nonperturbatively.

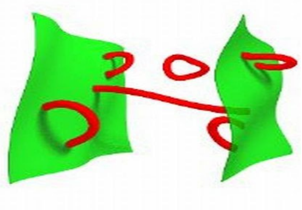

Figure 1.4: String and Brane: closed string and open strings on D-branes.

Dirichlet boundary condition breaks Lorentz invariance of the theory partially. The presence of a $D-p$ brane in spacetime breaks $ISO(D,1)$ to $ISO(p,1)$. Consequently $D-p$

scalar fields appear on the brane world volume that behave like Goldstone bosons for the broken symmetries.

Let us mention how branes couple to form fields. In general, a p-brane couples to $p+1$-form field electrically and to $(D-p-3)$-form field magnetically as described in the following diagram.

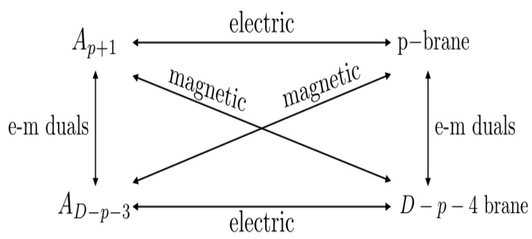

Figure 1.5: Electric and magnetic couplings to form fields.

1.3.2 AdS/CFT duality

The AdS/CFT correspondence as conjectured by Maldacena in 1997 [19–21] is a remarkable equivalence between type IIB superstring theory in the background of $AdS_5 \times S^5$ and $\mathcal{N}=4$ $SU(N)$ super Yang-Mills (SYM) theory living on the boundary of AdS. The isometry group of $\mathcal{N}=4$ SYM has a bosonic subgroup $SO(2,4)$. Note that $SO(2,4)$ is the conformal group in four dimensions. The R-symmetry group of the SYM is $SU(4)_R$. This matches with the isometry group of $AdS_5 \times S^5$ since symmetry group of AdS_5 is $SO(2,4)$ and that of S^5 is $SO(6) \simeq SU(4)_R$. The parameters of the two theories are related as follows. The closed string coupling constant g_s is related to the Yang-Mills coupling g_{YM} as $g_s = g_{YM}^2$. The equal radii R of AdS_5 and S^5 are related to the rank N of gauge group through $R^4 = 4\pi g_s N \alpha'^2$ where $\alpha' = l_s^2$. The five-form Ramond-Ramond (RR) flux through S^5 is quantized and is equal to N. The duality is also called a open-close duality since in AdS the RR fields correspond to the massless modes of closed string whereas in the CFT the Yang Mills gauge fields are the massless open string modes.

The above duality is the strong form of the conjecture and is valid for all values of N and g_s. String theory on $AdS_5 \times S^5$ is a difficult and unsolved problem as it involves quantization on a curved manifold in the presence of of RR fields. The utility and solvability of the conjecture increases if we consider two further limits to arrive at a weaker but more practical form of the conjecture. The first limit is the 't Hooft limit in the SYM side where 't Hooft coupling $\lambda \equiv g_{YM}^2 N = g_s N$ is held fixed while taking $N \to \infty$ limit. In this case only planar diagrams (genus $g = 0$) contribute in the SYM side since non-planar diagrams in the large N limit are suppressed by $\frac{1}{N^{2g}}$. In the AdS side this corresponds to taking $g_s \to 0$, that is no string loops. This limit gives rise to classical string theory on $AdS_5 \times S^5$ instead of the full quantum string theory. Further simplification happens when along with $N \to \infty$, we also take $\lambda \to \infty$. In this limit the SYM is strongly coupled and non-perturbative. Classical string theory reduces to supergravity on $AdS_5 \times S^5$. This is due to the fact that in the $\lambda \to \infty$ limit for a finite R, $\alpha' \sim \lambda^{-\frac{1}{2}} \to 0$. So higher curvature terms (stringy corrections) in the Lagrangian do not contribute and string theory becomes supergravity. In this limit the gauge theory is strongly coupled but the gravity side is weakly coupled. Using this strong-weak duality we can study strongly coupled quantum field theories in D dimensions by mapping them to weakly coupled gravity in $D + 1$ dimensions.

The duality maps fields on the bulk theory to operators in the boundary theory. This is known as the Field-Operator correspondence. In particular the boundary value of the bulk field sources the operator in the field theory. For example, the graviton is related to the stress tensor in the boundary theory, while the dilaton is related to the boundary operator $\mathrm{tr}(F_{\mu\nu}F^{\mu\nu})$.

Similar duality exists between type IIB superstring theory in the background of $AdS_3 \times S^3$ and 1 + 1 dimensional $\mathcal{N} = (4, 4)$ super conformal field theory (SCFT) with 8 supercharges. This duality is the most relevant for the purpose of this thesis.

1.4 Structure of the thesis

The thesis is organized as follows. In Chapter 2 of the thesis we review the fuzzball proposal in string theory that attempts to resolve the black hole information paradox followed by a discussion on supersymmetric and non supersymmetric smooth D1-D5-P supergravity solutions. Towards the end of chapter 2, we discuss hidden symmetries that appear in dimensional reduction of higher dimensional gravitational theories to three dimensions. When we further reduce to two dimensions these theories become integrable. This discussion of hidden symmetries is useful in the context of exact solution generating techniques in GR and supergravity where they are explicitly used to construct various black hole solutions. These symmetries are also expected to generate smooth solutions (fuzzballs) in the same spirit.

In chapter 3 we present our work on holographic description of non-BPS orbifolded D1-D5-P solutions [4]. We have identified the holographic description (via AdS/CFT) of the general class of non-supersymmetric orbifolded D1-D5-P supergravity solutions found by Jejjala, Madden, Ross and Titchener (JMaRT). This class of solutions includes both smooth solutions and solutions with conical defects, and in the near-decoupling limit these solutions describe degrees of freedom in the cap region. The CFT description involves a general class of states obtained by fractional spectral flow in both left and right-moving sectors. This generalizes an earlier work that studied special cases in this class [22]. We also compute the massless scalar emission spectrum and emission rates in both gravity and CFT and find perfect agreement. This result is a strong evidence for our proposed identification. We also investigate the physics of ergoregion emission as pair creation for these orbifolded solutions. Our results represent the largest class of non-supersymmetric black hole microstate geometries with identified CFT duals presently known. We will return to the JMaRT discussion in chapter 5 where we describe the JMaRT solution from a different perspective as a gravitational instanton.

In chapter 4 we take a useful digression and discuss group theory methods to generate black hole solutions in four and five dimensions. The techniques used in this chapter will be implemented in the case of JMaRT in the next chapter where the method becomes more challenging. In chapter 4 we consider four and five dimensional black holes from two dimensional Geroch group point of view [10]. On one hand the Geroch group allows one to associate spacetime independent matrices with gravitational configurations that effectively only depend on two coordinates. This class includes stationary axisymmetric four and five dimensional black holes. On the other hand, a recently developed inverse scattering method [6] allows one to factorize these matrices and explicitly construct the corresponding spacetime configurations. In this chapter we demonstrate the construction as well as the factorization of Geroch group matrices for a wide class of black hole examples. In particular, we obtain the Geroch group $SL(3,\mathbb{R})$ matrices for the five-dimensional Myers-Perry and Kaluza-Klein black holes and the Geroch group SU(2, 1) matrix for the four-dimensional Kerr-Newman black hole. We also present certain non-trivial relations between the Geroch group matrices and charge matrices for these black holes.

In chapter 5 we revisit the three charge JMaRT solution and describe it from a new point of view, namely as a charged gravitational instanton [12]. We use an inverse scattering method and group theory techniques to present an alternative and more direct construction of the non-supersymmetric D1-D5-P supergravity solutions known as JMaRT. We show that these solutions — with all three charges and both rotations turned on — can be viewed as a charged version of the Myers-Perry instanton. We also present an inverse scattering construction of the Myers-Perry instanton metric in Euclidean five-dimensional gravity. The angular momentum bounds in this construction are precisely the ones necessary for the smooth microstate geometries. We add charges on the Myers-Perry instanton using appropriate SO(4, 4) hidden symmetry transformations.

Finally in chapter 6, we conclude with the summary of our work and future open problems.

Chapter 2

Black holes in string theory

In this chapter we provide a brief overview of topics in black holes in string theory relevant for the thesis.

2.1 The small corrections theorem

Hawking did a semiclassical analysis and showed that the expectation value of the number operator for the outgoing particles emitted from a black hole is thermal. As a result the full evolution – from infalling matter state to the formation of the black hole and finally to its complete evaporation – seemed nonunitary. For a long time it was speculated that quantum gravity effects could play a role by introducing small subleading corrections to Hawking's semi-classical analysis. This can potentially generate small correlations to the outgoing Hawking flux. Since the number of quanta is exponentially large for a black hole, this tiny effect can in principle accumulate over time and as a result radiation can carry black hole information. The subleading corrections could then remove the entanglement between outgoing and infalling particles, solving both the unitarity problem and the information paradox.

Mathur [23] has shown that small corrections to the Hawking's calculation cannot remove the entanglement between the Hawking pairs and hence cannot resolve the loss of unitarity. The main conclusion is that one requires order unity change (nonperturbative) in the horizon state to resolve the information paradox. The horizon is not the local vacuum even at leading order. A proof of this theorem relies on the strong subadditivity (SSA) property of the quantum entanglement entropy. If A, B, and C are three mutually disjoint subsystems that are entangled with the rest of system then

$$S_{ent}(A + B) + S_{ent}(B + C) \geq S_{ent}(A) + S_{ent}(C), \tag{2.1}$$

where $S_{ent}(A)$ is the entanglement entropy of the subsystem A with the rest and so on.

Now consider A, B and C to be specific subsystems as follows of a black hole after the $N-$th step of its evaporation. The subsystem A is the set of Hawking quanta collected at infinity at the end of N-th step: $A = \{b_i\}, i = 1, \ldots, N$. Let the subsystems B and C be the $N + 1$-th Hawking particle moving outside and falling inside the black hole, respectively, i.e., $B = b_{N+1}$ and $C = c_{N+1}$. Then, $S_{ent}(A) = S(\{b_i\})$ is the entanglement entropy of the radiated Hawking quanta $\{b_i\}$ far away from the black hole with the rest of the system after N steps. Applying SSA on the system we obtain

$$S(\{b_i\} + b_{N+1}) + S(b_{N+1} + c_{N+1}) \geq S(\{b_i\}) + S(c_{N+1}). \tag{2.2}$$

The $b - c$ pair was not entangled with the rest of the system, hence we had $S(b_{N+1} + c_{N+1}) = 0$ and $S(c_{N+1}) = \ln 2$. Let us allow for small corrections due to weak entanglement of a Hawking pair with the previously emitted quanta, i.e., $S(b_{N+1} + c_{N+1}) < \epsilon_1$ and $S(c_{N+1}) > \ln 2 - \epsilon_2$ where $\epsilon_1, \epsilon_2 \ll 1$. ϵ_1 and ϵ_2 are the changes in the Hawking states due to entanglement between the emitted pair and early radiation. The previous SSA relation then reduces to

$$S(\{b_i\} + b_{N+1}) \geq S(\{b_i\}) + \ln 2 - (\epsilon_1 + \epsilon_2), \tag{2.3}$$

$$S_{N+1} > S_N + \ln 2 - (\epsilon_1 + \epsilon_2). \tag{2.4}$$

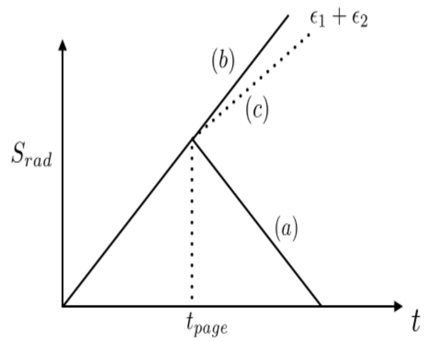

Figure 2.1: Page curve. Entanglement entropy of radiation S_{rad} as a function of time t. Line a represents the behaviour of a normal body, as it burns. Line b represents burning curve for a black hole, when there are no small corrections. Line c schematically represents inclusions of small corrections. The page time t_{page} is the time at which the curve a turns over: entanglement of the radiation with the burning body starts to decrease.

This shows that the entanglement of the Hawking radiation with the remaining black hole keeps on increasing, even after Page time at least by an amount $\ln 2 - (\epsilon_1 + \epsilon_2)$. Hence small corrections cannot change the nature of the Page curve for black holes (line c in the above figure) and make it behave like normal bodies (line a in the figure). Thus, it appears that, small corrections are unable to restore unitarity in black hole evolution and to obtain a pure final state. Hence, one concludes that one needs an order unity change of the horizon state to resolve the information puzzle. It is then reasonable to expect that quantum gravity effects might completely deform the horizon away from vacuum.

2.2 The fuzzball proposal

One of the most promising proposals to resolve the information puzzle in the context of string theory is known as the fuzzball conjecture proposed by Mathur [1, 24]. What lies at the heart of the conjecture is the assertion that quantum gravity effects are not confined within Planck length (l_P) from the centre of a black hole but can extend to a scale of the size of black hole horizon. This can happen due to the large number of microstates (N) associated to a black hole for which the effective length scale of quantum gravity becomes $\sim N^{\alpha} l_P$. This proposal completely changes the picture of the black hole horizon and its interior. In particular, the horizon state is no longer vacuum, but changes to some other state $|\psi\rangle$.

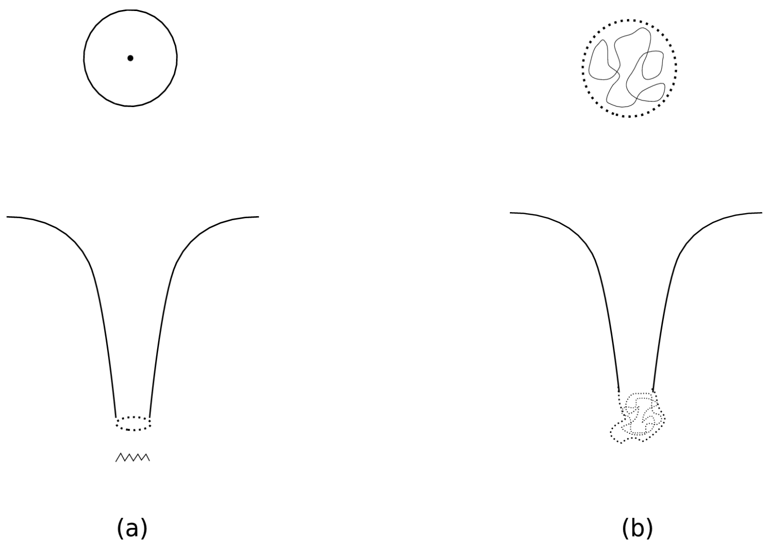

Figure 2.2: Black holes vs fuzzballs.

The pair creation at the horizon scale does not happen from vacuum in the fuzzball picture. It happens from state $|\psi\rangle$ and hence the radiation carries information about $|\psi\rangle$ or initial matter just the way it does in the case of a burning coal. Consequently there will be no information loss and unitarity can be restored. With this idea, gravity and quantum mechanics seem to get along well.

According to the fuzzball conjecture, associated with a black hole of entropy S there are e^S horizon-free, non-singular, non spherically-symmetric configurations that have the same conserved charges and asymptotic structure as that of the black hole. These configurations differ from the black hole structure at the horizon scale. In general fuzzball microstates are complicated string theory solutions; some of them can be well described within supergravity. In a gravitational collapse a shell of matter would tunnel into a fuzzball microstate. This can happen since the possible states to tunnel to is very large $\sim e^S$, so even if the tunnelling probability is very small $\sim e^{-S}$, there is effectively order unity probability for the shell to tunnel into a fuzzball microstate.

2.3 Making black holes in string theory

Black holes in string theory are constructed from wrapping strings and branes on appropriate cycles. We briefly review the 1-charge, 2-charge, and the 3-charge systems below.

In general relativity if a large mass M is placed in a given region, it collapses under its own gravity and forms a black hole. If the matter is a spherical ball of perfect fluid, then it cannot hold up against gravitational collapse once it is confined within a radius $R_{\min} = \frac{9}{4}GM$. This is known as the Buchdahl's theorem.

The fuzzball proposal suggests to replace the black hole with an appropriate horizonless configuration. Let us consider the simplest example of a smooth solution [25] and see how this solution holds up against collapse and bypasses Buchdahl's theorem. Consider the $3+1$ dimensional Euclidean Schwarzschild metric and add a flat timelike direction to it. The five dimensional metric is

$$ds^2 = -dt^2 + \left(1 - \frac{r_0}{r}\right)d\tau^2 + \frac{dr^2}{\left(1 - \frac{r_0}{r}\right)} + r^2(d\theta^2 + \sin^2\theta d\phi^2), \tag{2.5}$$

where Euclidean time τ ia a compact direction with range $0 \leq \tau < 4\pi r_0$. The (r_0, τ) directions form a cigar geometry. The spacetime ends at $r = r_0$ where the τ circle goes to zero size. The five dimensional metric is completely smooth. Performing dimensional

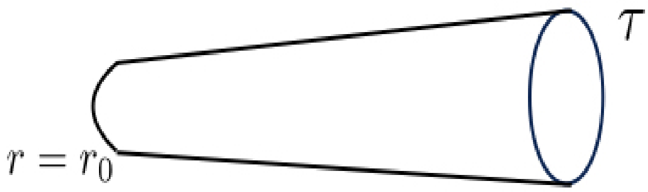

Figure 2.3: Cigar geometry.

reduction on the τ circle we get

$$g_{\tau\tau} = e^{\frac{2}{\sqrt{3}}\phi}, \tag{2.6}$$

$$\phi = \frac{\sqrt{3}}{2}\ln\left(1 - \frac{r_0}{r}\right), \tag{2.7}$$

together with the 3 + 1 dimensional Einstein frame metric

$$\begin{aligned} g^{Ein}_{\mu\nu} &= e^{\frac{\phi}{\sqrt{3}}} g_{\mu\nu} \\ ds^2_{Ein} &= -\left(1 - \frac{r_0}{r}\right)^{\frac{1}{2}} dt^2 + \frac{dr^2}{\left(1 - \frac{r_0}{r}\right)^{\frac{1}{2}}} + r^2\left(1 - \frac{r_0}{r}\right)^{\frac{1}{2}} (d\theta^2 + \sin^2\theta d\phi^2). \end{aligned} \tag{2.8}$$

The stress tensor for the scalar field is

$$T_{\mu\nu} = \partial^\mu\phi\partial^\nu\phi - \frac{1}{2}g^{Ein}_{\mu\nu}\partial_\lambda\phi\partial^\lambda\phi\ .$$

In component form, this gives $T^\mu_\nu = \text{diag}(-\rho, p_r, p_\theta, p_\phi) = \text{diag}(-f, f, -f, -f)$ where $f = \frac{3r_0^2}{8r^4}\left(1 - \frac{r_0}{r}\right)^{\frac{3}{2}}$.

We note that from the point of view of 3+1 dimensions, at $r = r_0$ both the energy density ρ and the pressure p diverge. This is an artifact of the dimensional reduction. The metric in 4+1 dimensions is smooth and free from any singularity. Moreover, from the 3+1 perspective the radial pressure p_r is positive, whereas the pressure in the angular directions p_θ, p_ϕ are negative. Thus the spacetime experiences anisotropic pressure. Observe that Buchdahl's theorem assumes isotropic pressure and does not apply in this case. In addition as $r \to r_0$ the time component of the metric $g_{tt} \to 0$, but never changes sign, thus there is no horizon in the metric. One might argue that in the 4+1 dimensional metric the S^2 has a non zero radius r_0 while in 3+1 dimensions the radius vanishes as $r \to r_0$. This is because the point $r = r_0$ corresponds to a naked singularity in the 3+1 dimensional metric. This is also an artifact of the dimensional reduction. The full 4+1 dimensional metric has no singularities or a horizon.

The crucial point is that in string theory there are extra dimensions with non-trivial topologies. These give rise to smooth solutions without horizon or singularity in a manner similar to the example considered above. These smooth solutions have the same charges and angular momenta as the black hole. The fuzzball proposal, proposes to replace the usual black hole picture with an appropriate such microstate.

2.3.1 One charge solution

Let us consider type IIA string theory compactified on $S^1 \times T^4$. Let us label the S^1 direction to be y with radius R, where $0 \leq y \leq 2\pi R$. We wrap n_1 number of elementary (NS1) strings on y, with no added excitations. The closed string spectrum of this system contains two form $B_{\mu\nu}$ field. The string couples to the $B_{\mu\nu}$ field through $\int B d\mathcal{A}$ where $d\mathcal{A}$ is an elementary area in the string worldsheet. For such configurations the gravitational interaction between two strings having the same tension is exactly cancelled by the coupling of strings to the gauge fields. Hence there is no net force acting between any two strings. The configuration has total mass=total winding charge thereby saturating the BPS (supersymmetric) bound and is labelled by the winding charge of the wrapped strings. In the following we consider a similar BPS solution where a single string is wrapped n_1 times over the y circle. The gravitational configuration produced by this string is given by [26]

$$ds^2_{string} = H_1^{-1}(-dt^2 + dy^2) + dr^2 + r^2 d\Omega_3^2 + \sum_{i=1}^{4} dx_i dx_i \tag{2.9}$$

$$B_{ty} = H_1^{-1} \tag{2.10}$$

$$e^{2\phi} = H_1^{-1} \tag{2.11}$$

where x_i's are coordinates on compact T^4 and (r, Ω_3) are standard polar coordinates along the transverse noncompact space. The string wraps the y direction and is localised at $r = 0$ in the transverse space. $H_1 = 1 + \frac{Q_1}{r^2}$ is a Harmonic function in the noncompact directions. Q_1 is related to the winding charge, $Q_1 = \frac{g^2 \alpha'^3}{V} n_1$ where V is the volume of the compact T^4. In order to obtain a classical geometry we consider n_1 to be very large. Note that the y circle goes to zero size at $r = 0$. This happens due to the fact that the string source is placed at $r = 0$ and the tension of the strings cause the compact circle to squeeze to zero size at that point to minimize the energy. To find the horizon area we consider the above metric in Einstein frame. The Einstein metric is

$$g^{Einstein}_{\mu\nu} = e^{-\frac{\phi}{2}} g^{string}_{\mu\nu} \tag{2.12}$$

$$ds^2_{Einstein} = H_1^{-\frac{3}{4}}(-dt^2 + dy^2) + H_1^{\frac{1}{4}}(dr^2 + r^2 d\Omega_3^2) + H_1^{\frac{1}{4}} \sum_{i=1}^{4} dx_i dx_i. \tag{2.13}$$

Note that the metric does not have a horizon for $r > 0$. To calculate the horizon area, we consider r = constant surface and take $r \to 0$ limit where the strings are wrapped. The horizon area with respect to the Einstein metric is $A_H = 2\pi^2 (2\pi R) V H_1^{\frac{1}{2}} r^3$. Therefore $A_H \to 0$ as $r \to 0$ and the Bekenstein-Hawking entropy $S_{BH} = 0$.

Since we are considering BPS states the microscopic entropy should match with the Bekenstein entropy due to non renormalization theorems [27]. In the microscopic side the contribution to the entropy comes from the zero modes of the string since there are no added excitations. In the eight transverse directions we can have 128 worldsheet fermions and 128 worldsheet bosons contributing to the degeneracy of states [28]. Hence the microscopic entropy becomes $S_{micro} = \ln[256] \simeq 0$. In the limit $n_1 \to \infty$ it matches with the Bekenstein-Hawking entropy. The analysis clearly shows that it is not possible to construct any finite size black hole with only one charge in string theory since the solution has zero horizon area and entropy.

2.3.2 Two-charge solution

In this section we describe the two charge black hole. In order to stabilize the y-circle from pinching off at $r = 0$, one can try attaching gravitons carrying momentum to the strings. The energy associated to the momentum mode of a graviton carrying n_p units of momenta along the y direction with length $L = 2\pi R$ is $E_p = \frac{2\pi n_p}{L}$, in contrast the energy of the wrapped string with tension T is $E_{NS1} = n_1 T L$. For $L = 0$ the total energy is not minimized due to the presence of momentum modes. Consequently, in the string frame the y direction does not pinch off at $r = 0$. The solution describing the $NS1 - P$ bound state is [26]

$$ds^2_{string} = H_1^{-1}[(-dt^2 + dy^2) + K(dt + dy)^2] + (dr^2 + r^2 d\Omega_3^2) + \sum_{i=1}^{4} dx_i dx_i \tag{2.14}$$

$$B_{ty} = H_1^{-1} \tag{2.15}$$

$$e^{2\phi} = H_1^{-1}, \tag{2.16}$$

where $K = \frac{Q_P}{r^2}$ and Q_P is the momentum charge $Q_P = \frac{g^2 \alpha'^4}{VR^2} n_p$.

The Einstein frame metric is

$$ds^2_{Einstein} = H_1^{-\frac{3}{4}}[-dt^2 + dy^2 + K(dt + dy)^2] + H_1^{\frac{1}{4}}(dr^2 + r^2 d\Omega_3^2) + H_1^{\frac{1}{4}} \sum_{i=1}^{4} dx_i dx_i \, . \tag{2.17}$$

In the limit $r \to 0$ horizon area becomes $A_H = 2\pi^2(2\pi R)VQ_P^{\frac{1}{2}}Q_1^{\frac{1}{2}}r$. We see that $A_H \to 0$ as $r \to 0$ and hence the Bekenstein-Hawking entropy vanishes. We have failed to construct a finite size black hole even with two kinds of charges.

The statistical entropy S_{micro} is computed by unwrapping the fundamental string to its full length $L_T = n_1 L$. This allows the string to vibrate in all the transverse directions in various harmonics. It follows that there are many different states for the same total winding and momentum charges. The counting of these states gives the statistical entropy S_{micro}.

Figure 2.4:

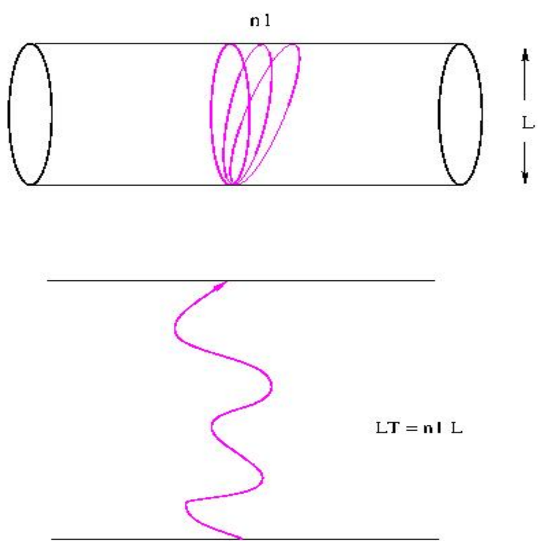

Since the black hole is BPS, S_{micro} has to match with S_{BH}. Note that each vibrational mode in the kth harmonic carries $\frac{2\pi k}{L_T}$ units of momentum. Thus the total momentum on the wrapped string is given by $P = \frac{2\pi n_p}{L} = \frac{2\pi(n_1 n_p)}{L_T}$. The number of ways the total $n_1 n_p$ units of momenta are distributed among all harmonics corresponds to the degeneracy. If the k-th harmonic carries m_k units of excitations then $\sum_{k=1}^{\infty} k m_k = n_1 n_p$. The number of possible vibrations satisfying this constraint gives the precise microscopic degeneracy N. Then $S_{micro} = \ln[N]$. The microscopic degeneracy and entropy evaluate to $N = e^{2\pi\sqrt{2}\sqrt{n_1 n_p}}$, $S_{micro} = 2\pi\sqrt{2}\sqrt{n_1 n_p}$ respectively [24, 29]. Hence there is an apparent mismatch between S_{BH} and S_{micro}.

The answer to this puzzle is not completely settled. We describe the proposed resolution from the point of view of the fuzzball proposal. As per the fuzzball proposal, the above metric does not correctly describe the $NS1-P$ system. One needs to take into account the arbitrary transverse vibrations of the string to write down the correct solution. Supergravity solutions for elementary string carrying arbitrary vibration profile $\mathbf{F}(t-y)$ have been constructed in [30, 31]. Performing a chain of S and T dualities on the $NS1-P$ system we arrive at the $D1-D5$ frame where the correct solution becomes [1]

$$\begin{aligned} ds^2 =& f_1^{-1/2} f_5^{-1/2}[-(dt - A_i dx^i)^2 + (dy + B_i dx^i)^2] + f_1^{1/2} f_5^{1/2} d\mathbf{x}.d\mathbf{x} \\ &+ f_1^{1/2} f_5^{-1/2} d\mathbf{z}.d\mathbf{z} \end{aligned} \tag{2.18}$$

$$e^{2\Phi} = f_1 f_5^{-1}, \tag{2.19}$$

$$C^{(2)}_{ti} = \frac{B_i}{f_1}, C^{(2)}_{ty} = f_1^{-1} - 1, \tag{2.20}$$

$$C^{(2)}_{iy} = -\frac{A_i}{f_1}, C^{(2)}_{ij} = C_{ij} + f_1^{-1}(A_i B_j - A_j B_i) \tag{2.21}$$

where $D1$ branes wrap the y circle and $D5$ branes wrap around y and the compact T^4 coordinates z_i. x^i's are the noncompact $\mathbb{R}^4$ coordinates transverse to both $D1$ and $D5$ branes. The various quantities appearing in the metric are related to the profile function $\mathbf{F}(v)$ as

$$f_5 = 1 + \frac{Q_5}{L}\int_0^L \frac{dv}{|\mathbf{x}-\mathbf{F}|^2}, \quad f_1 = 1 + \frac{Q_5}{L}\int_0^L \frac{|\dot{F}|^2 dv}{|\mathbf{x}-\mathbf{F}|^2}, \quad A_i = -\frac{Q_5}{L}\int_0^L \frac{\dot{F}_i dv}{|\mathbf{x}-\mathbf{F}|^2}, \tag{2.22}$$

and $dC = -*_4 df_5, dB = -*_4 dA$ where $*_4$ is defined with respect to the non-compact flat spatial metric with coordinates x_i. The variable v is a null coordinate along the string $v = t - y$. The upper limit of integration is $L = \frac{2\pi Q_5}{R}$. The $D1$ and $D5$ charges are related as follows

$$Q_1 = Q_5 \langle |\dot{F}|^2 \rangle = Q_5 \frac{1}{L}\int_0^L |\dot{F}|^2 dv. \tag{2.23}$$

The Lunin-Mathur (LM) metric (2.18)–(2.21) describe configurations of n_1 number of $D1$ branes around S^1 and n_5 number of $D5$ branes around $S^1 \times T^4$ in type IIB string theory.

Though it seems that the LM solutions have singularity at $\mathbf{x} = \mathbf{F}(\mathbf{v})$ where the harmonic functions diverge, this is actually a coordinate singularity. To see this note that, with the condition that $\dot{F}(v)$ is always nonzero, the coordinates of the transverse directions can be split into a longitudinal component x_L and a transverse component x_T around $\dot{F}(v_0)$. Close to the singularity we then obtain

$$f_5 \approx \frac{Q_5}{L}\frac{\pi}{|\dot{F}|x_T}, \quad f_1 \approx \frac{Q_5}{L}\frac{\pi|\dot{F}|}{x_T}, \quad A_i \approx -\frac{Q_5}{L}\frac{\pi \dot{F}_i}{x_T|\dot{F}|} \,. \tag{2.24}$$

Using the above expressions it can be shown that the full metric is smooth everywhere [32]. These solutions are asymptotically flat with an inner $AdS_3 \times S^3 \times T^4$ (finite) throat.

The entropy on the supergravity side for the LM solutions has been calculated using geometric quantization of the moduli space of the $D1 - D5$ solutions and by imposing additional consistency conditions [33]. The supergravity entropy with four bosonic excitations along the R^4 gives $S_{Rychkov} = 2\pi\sqrt{\frac{2}{3}n_1 n_5}$.

Rychkov counting does not take into account the four bosonic excitations along T^4 and all the eight fermionic excitations along R^4 and T^4 directions due to the string vibrations. Once these factors are correctly incorporated in the geometric quantization scheme, the modified supergravity entropy would match with the microscopic entropy of the two charge system in the $D1 - D5$ frame $S_{micro,D1-D5} = 2\pi\sqrt{2}\sqrt{n_1 n_5}$.

2.3.3 Three charge system

Strominger and Vafa [34] computed the Bekenstein-Hawking entropy for five dimensional supersymmetric three charge black holes in $N = 4$ theories with a classical horizon in the supergravity approximation and find that it matches with the statistical entropy of a bound state of D-branes. In this section we look at supergravity solutions with three electric charges and angular momenta in the context of eleven dimensional M-theory. In the next section we look at the low energy CFT that describes the relevant bound state of D-branes.

Consider M-theory compactified on T^6 along six spatial directions and wrap three sets of extremal M2 branes along the three orthogonal T^2s inside T^6. It can be shown that the solution preserves one eighth of the supersymmetries. From the non-compact five dimensional point of view this configuration appears as a point mass. Interestingly one can add three sets of M5 branes to this configuration without further breaking any supersymmetry [35, 36]. The M5 branes being electromagnetic duals to M2 branes wrap along the orthogonal spatial compact directions to that of the M2. The full solution contains local magnetic dipole charges due to M5 branes placed perpendicular to the M2 brane background. The fifth direction of the M5 branes wrap a spacelike circle (labelled ψ) in the non-compact five dimensional spacetime. With M5 branes present, configurations are no longer point like from five dimensional point of view. The configuration is described in the table below.

	t	x_1	x_2	x_3	ψ	x_5	x_6	x_7	x_8	x_9	x_{10}
M_2	×	•	•	•	−	×	×	−	−	−	−
M_2	×	•	•	•	−	−	−	×	×	−	−
M_2	×	•	•	•	−	−	−	−	−	×	×
M_5	×	•	•	•	×	−	−	×	×	×	×
M_5	×	•	•	•	×	×	×	−	−	×	×
M_5	×	•	•	•	×	×	×	×	×	−	−

Table 2.1: • → branes localized, − → branes smeared, × → branes wrapped

The full solution is described by,

$$ds_{11}^2 = (Z_1Z_2Z_3)^{-\frac{2}{3}}(dt+k)^2 + (Z_1Z_2Z_3)^{\frac{1}{3}}h_{\mu\nu}dx^\mu dx^\nu + \left(\frac{Z_2Z_3}{Z_1^2}\right)^{1/3}\left(dx_5^2+dx_6^2\right) + \left(\frac{Z_1Z_3}{Z_2^2}\right)^{1/3}\left(dx_7^2+dx_8^2\right) + \left(\frac{Z_1Z_2}{Z_3^2}\right)^{1/3}\left(dx_9^2+dx_{10}^2\right), \tag{2.25}$$

$$A_{(3)} = A^{(1)}\wedge dx_5\wedge dx_6 + A^{(2)}\wedge dx_7\wedge dx_8 + A^{(3)}\wedge dx_9\wedge dx_{10}, \tag{2.26}$$

where Z_I's are warp factors corresponding to the three sets of M2/M5 branes. Z_I's and k are functions of four dimensional base coordinates x^μ and $A_{(3)}$ is the 3-form field in eleven dimensions. M2 and M5 branes couple to $A^{(3)}$ by electric and magnetic coupling respectively. To obtain a BPS solution, the four dimensional base $h_{\mu\nu}$ needs to be hyper-Kähler [37]. The five dimensional one forms $A^{(I)}$ are defined as follows:

$$dA^{(I)} = -d(Z_I^{-1}(dt+k)) + \Theta^{(I)}, \tag{2.27}$$

where the first term is due to the M2 branes and the second term is due to the magnetic dipole field strength of the M5 branes. Given the base metric $h_{\mu\nu}$ one can solve the following set of 'sequentially linear' BPS equations to obtain the full metric [36]

$$\Theta^{(I)} = \star_4 \Theta^{(I)} \tag{2.28}$$

$$\nabla^2 Z_I = \frac{1}{2}C_{IJK}\star_4\left(\Theta^{(J)}\wedge\Theta^{(K)}\right) \tag{2.29}$$

$$dk + \star_4 dk = Z_I\Theta^{(I)} \tag{2.30}$$

where $\star_4$ is the Hodge star in the four dimensional noncompact space and $C_{IJK} = |\epsilon_{IJK}|$.

One of the key steps that advanced the study of three-charge supersymmetric black hole microstates was the rewriting by Giusto and Mathur [38] of the first example of a smooth geometry in the fibered form, thus making the connection with the classification of supersymmetric solutions. This exercise led to the realisation that the four-dimensional base space for such solutions had to be "ambipolar", which paved the way for generalisations to the multi-center solutions [39, 40].

The simplest example of a hyper-Kähler base metric is $\mathbb{R}^4$. We are more interested in multi-center Gibbons-Hawking (GH) metrics as the base [41]. GH metrics are a particular subclass of hyper-Kähler metrics that preserve all three complex structures. The four dimensional GH metrics have the form of a $U(1)$ fibration over flat $\mathbb{R}^3$ base

$$ds_4^2 = h_{\mu\nu}dx^\mu dx^\nu = V^{-1}\left(d\psi + \vec{A}\cdot d\vec{y}\right)^2 + V\left(dx^2 + dy^2 + dz^2\right). \tag{2.31}$$

V is harmonic on $\mathbb{R}^3$ with finite number of isolated sources at location $\vec{y}^{(i)} = (x, y, z)$

$$V = \epsilon_0 + \sum_{j=1}^{N} \frac{q_j}{r_j}. \tag{2.32}$$

The metric (2.31) is hyper-Kähler if $\vec{\nabla}\times\vec{A} = \vec{\nabla}V$.

It is convenient to work with a new set of frames for the GH base and the self-dual and anti self-dual 2-forms in this frame to define magnetic fluxes

$$\hat{e}^1 = V^{-\frac{1}{2}}(d\psi + A) \tag{2.33}$$

$$\hat{e}^{a+1} = V^{\frac{1}{2}}dy^a \tag{2.34}$$

$$\Omega_\pm^{(a)} = \hat{e}^1\wedge\hat{e}^{a+1} \pm \frac{1}{2}\epsilon_{abc}\hat{e}^{b+1}\wedge\hat{e}^{c+1}\,, \qquad a = 1, 2, 3. \tag{2.35}$$

The magnetic field strength is expressed as

$$\Theta^{(I)} \equiv \sum_{a=1}^{3}\left(\partial_a(V^{-1}K^I)\right)\Omega_+^{(a)} \tag{2.36}$$

where K^I's are some functions in $\mathbb{R}^3$. For magnetic dipole two-form field strength $\Theta^{(I)}$ to be exact, K^I's have to be harmonic in $\mathbb{R}^3$ satisfying $\nabla^2 K^I = 0$.

Metric (2.31) appears to be singular at the source points $\vec{y}^{(i)}$ where V diverges. This is only a coordinate singularity. One can consider polar coordinates (ρ, θ, ϕ) on $\mathbb{R}^3$ with $\rho = 2\sqrt{r} = 2\sqrt{|\vec{y} - \vec{y^j}|}$ in terms of which the metric becomes regular. Near the source $(\rho \to 0)$ the metric in polar coordinates looks like an orbifold of $\mathbb{R}^4$ with an appropriate identification of periodicities of the angular coordinates

$$ds^2 \simeq q_j\Big[d\rho^2 + \frac{\rho^2}{4}\Big\{\Big(\frac{d\psi}{q_j} + \cos\theta\, d\phi\Big)^2 + \big(d\theta^2 + \sin^2\theta\, d\phi^2\big)\Big\}\Big], \tag{2.37}$$

$$ds^2 \sim d\rho^2 + \rho^2 d\Omega_3^2. \tag{2.38}$$

In order to avoid singularity at the source the charges q_i have to be integers.

The constant ϵ_0 in (2.32) determines the asymptotic structure of the GH metric. When $\epsilon_0 \neq 0$, the $U(1)$ fibre has a finite size at spatial infinity. The metric becomes asymptotically $\mathbb{R}^3 \times S^1$ and is called asymptotically locally flat (ALF). When $\epsilon_0 = 0$, asymptotically the metric is $\frac{\mathbb{R}^4}{Z_{|q_0|}}$ where q_0 is the total charge. In this case the metric is called asymptotically locally euclidean (ALE).

Figure 2.5: Two-center GH

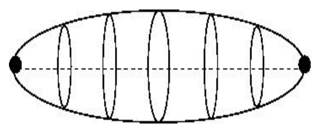

The multicenter GH metric has rich topology. The $U(1)$ fibre shrinks to zero size at the GH centers. Hence any two GH centers are connected by an S^2. So far we have considered GH bases with (+,+,+,+) signature. We can relax this condition by considering negatively charged GH centers. In this case, the base metric changes sign from (+,+,+,+) to (-,-,-,-) in some regions, such metrics are called ambipolar GH metrics. Including negative charges in the metric gives rise to closed timelike curves in general. Even though the four dimensional base becomes pathological, the full eleven dimensional metrics are still well behaved because of the warp factors. See [41, 42] for a detailed discussion of how this comes about.

For BPS black holes that we have discussed so far, the fuzzball picture is well explored. A lot of progress has been made in this direction. Scaling solutions, multicenter bubbling geometries and families of superstratum solutions have been constructed by Bena,Warner, DeBoer, Shigemori, Russo, Giusto and others [39–41, 43–46]. Examples of near BPS smooth solutions have also been constructed by Bena et al [47–49].

Non-supersymmetric smooth solutions are technically much more demanding, only a handful of non-extremal solutions are known so far. The first non-supersymmetric black hole microstate solutions to be discovered were the solutions found by Jejjala, Madden, Ross and Titchener (often abbreviated to JMaRT) [3]. For other studies of non-supersymmetric black hole microstate solutions, see [42, 50, 53, 55, 56, 58]. JMaRT solutions are special cases of the non-BPS rotating three-charge Cvetič-Youm (CY) metrics. Cvetič-Youm solutions are Myers-Perry solutions with three $U(1)$ charges. In general, Cvetič-Youm geometries have singularities, horizons, and closed timelike curves. JMaRT is free from all singularities, horizons, closed timelike curves. Conditions on the parameter space of the Cvetič-Youm geometries give rise to smooth JMaRT geometries. To start with, CY metric in 6D has seven parameters M, a_1, a_2, Q_1, Q_5, Q_P and R. Imposing regularity conditions we get 3-charge JMaRT with five independent parameters m, n, R, Q_1 and Q_5 (except for orbifold parameter k that we allow) where m and n are integer parameters. The near core geometry of JMaRT solutions is $AdS_3 \times S^3$ and they are asymptotically flat. There are interesting limits from these solutions. For instance CY metrics with $J_\phi = J_\psi = 0$ and $M = Q_1 + Q_5 + Q_P$ is same as the Strominger-Vafa system and CY with $J_\phi = J_\psi \neq 0$ and $M = Q_1 + Q_5 + Q_P$ is the BMPV system [61] where the two angular momenta J_ϕ and J_ψ are expressed interms of the rotation parameters a_1, a_2 as discussed in chapter 3. Analogously JMaRT with $m = n + 1$ becomes supersymmetric. This supersymmetric limit is a two-center Bena-Warner system.

2.3.4 The D1-D5 SCFT

The gauge theory that describes the D1-D5 bound state in the infrared is given by the $\mathcal{N} = (4,4)$ super conformal field theory with eight supercharges [62]. The theory enjoys a $SU(2)_L \times SU(2)_R$ R-symmetry, related to the S^3 part of the D1-D5 metric. It also has a broken $SO(4)_I \simeq SU(2)_1 \times SU(2)_2$ internal symmetry related to the presence of the T^4. The D1-D5 CFT has $n_1 n_5$ copies of the $(4,4)$ T^4 SCFT. The T^4 SCFT has four real bosonic (X^1, X^2, X^3, X^4) and four real fermionic excitations in the left sector $(\psi^1, \psi^2, \psi^3, \psi^4)$. Similarly there are four real fermionic excitations $\bar{\psi}^1, \bar{\psi}^2, \bar{\psi}^3, \bar{\psi}^4$ in the right sector. These excitations collectively describe T^4 as the target space. The SCFT has a central charge $c = 6$. The generators of the SCFT in the left sector are the stress tensor T, four fermionic supercurrents $G^{\alpha A}$ and the $SU(2)_L$ R-symmetry current J^a. Similar generators are in the right sector of the SCFT.

The D1-D5 CFT is the $N = n_1 n_5$ copies of the T^4 SCFT orbifolded by the symmetric group S_N. Modular invariance in the orbifolded theory requires one to introduce twisted sectors. The twist operators link different copies of the SCFT with one another. As one circles around a point where a twist operator σ_n is inserted, the n copies of the bosonic and fermionic fields are mapped into each other. On a cylinder the action of the twist field σ_n is given by

$$\begin{aligned} \sigma_n \quad &: \quad X^{(1)} \to X^{(2)} \to \cdots \to X^{(n)} \to X^{(1)} \\ &: \quad \psi^{(1)} \to \psi^{(2)} \to \cdots \to \psi^{(n)} \to \ -\psi^{(1)}. \end{aligned} \tag{2.39}$$

Twisted sector of the theory contains operators with fractional modes and fractional conformal dimensions. For example the R-symmetry generator $J^a_{-\frac{m}{n}}$ has a fractional holomorphic conformal weight $h = \frac{m}{n}$ that can be non-integral. We will use these operators later on in chapter 3 for constructing various fractional spectral flowed states in the D1-D5 CFT.

2.4 Hidden symmetry and integrability

Solutions of a gravity theory coupled to matter in d dimensions that admit k commuting Killing vectors can be thought of as solutions of dimensionally reduced gravity theory in $d - k$ dimensions. Quite often the dimensionally reduced gravity theory admits an enhanced group of symmetries [63, 64], sometimes called hidden symmetries. These hidden symmetries have been fruitfully used to study solutions of higher-dimensional theories for several decades now. Most notably, the hidden symmetry groups in three-dimensions have been used to construct black hole solutions of four and five dimensional theories, see, e.g., the review [65], and references [9, 66] for recent works. They have also been used to obtain uniqueness results for four and five dimensional black holes, see, e.g., [67, 68]. More recently, these symmetry groups have been used to classify BPS and non-BPS solutions of various four-dimensional supergravity theories, see, e.g., the following incomplete list of references [58, 69–72].

The case of $d-2$ commuting Killing vectors is particularly rich, as in that case the hidden symmetry groups are typically infinite dimensional Lie groups [5, 73–78]. We call the two dimensional hidden symmetry groups Geroch groups, by extension of the case of pure gravity in four-dimensions.The corresponding Lie algebras are the affine-extensions of the Lie algebras of the hidden symmetry groups in three dimensions. This is because, the two-dimensional models are often obtained via dimensional reduction from three dimensions over yet another Killing vector. This results in integrable models [5, 77, 79–81]. In the 1990s many authors contributed to the development of Geroch group as symmetries of string theory, see e.g., the following incomplete list of references [82–85].

In this section we review dimensional reduction of vacuum gravity from four to two dimensions and demonstrate the emergence of infinite dimensional symmetry with affine $SL(2, \mathbb{R})$ Lie algebra in two dimensions. The integrability of the two dimensional theory implies that there exists a set of linear Lax equations whose integrability condition gives rise to the Einstein equation in two dimensions. Invoking Lax equations is a crucial step in constructing various exact solutions in GR and supergravity.

Let us consider Einstein gravity in four spacetime dimensions with action

$$S_{EH} = \int d^4x \sqrt{-g}R, \tag{2.40}$$

where g is the determinant of the four dimensional metric and R is Ricci scalar in four dimensions. We consider stationary, axisymmetric spacetimes with two mutually commuting Killing vectors (one timelike ∂_t and one spacelike ∂_ϕ). Such a theory is effectively two dimensional since one can perform Kaluza Klein reduction over the Killing directions from four to two dimensions. The reduction can be done in two inequivalent ways, known as the Ehler's and the Matzner Misner reduction schemes. The two schemes result in two noncommuting $SL(2,\mathbb{R})$ symmetries, whose combination gives rise to an affine $SL(2,\mathbb{R})$ symmetry in two dimensions.

i) **Ehlers reduction:** First we perform reduction from four to three dimensions over t with the metric ansatz

$$ds^2 = -e^{-\phi}(dt + A)^2 + e^{\phi} ds_3^2, \tag{2.41}$$

where ϕ and A are the dilaton and Maxwell 1-form respectively. The three dimensional Lagrangian becomes

$$L_3 = \sqrt{g}\left(R - \frac{1}{2}(\partial\phi)^2 + \frac{1}{4}e^{-2\phi}F^{mn}F_{mn}\right). \tag{2.42}$$

In three dimensions A can be dualized to a scalar field (denoted as χ). For the dualization we treat the 2-form $\mathcal{F} = dA$ as an independent field in the three dimensional Lagrangian L_3 and add a term to L_3 that is proportional to the Bianchi identity for $\mathcal{F}$ with χ as a Lagrange multiplier. Varying the total Lagrangian with respect to $\mathcal{F}$ we get $d\chi = \star_3(e^{-2\phi}\mathcal{F})$. We can substitute for $\mathcal{F}$ from the duality relation back into the full Lagrangian. The resulting three dimensional Lagrangian becomes

$$L_3' = \sqrt{g}\left(R - \frac{1}{2}(\partial\phi)^2 - \frac{1}{2}e^{2\phi}(\partial\chi)^2\right). \tag{2.43}$$

This is the Lagrangian for pure gravity coupled to scalar matter in three dimensions. L_3' has a built in $SL(2,\mathbb{R})$ global symmetry that becomes manifest when written in terms of a complex field $\tau = \tau_1 + i\tau_2 = \chi + ie^{-\phi}$,

$$L_3' = \sqrt{g}\left(R - \frac{2\partial\tau.\partial\bar{\tau}}{(\tau-\bar{\tau})^2}\right) \tag{2.44}$$

This is manifestly invariant under

$$\tau \to \tau' = \frac{a\tau+b}{c\tau+d}, \quad \text{where} \begin{pmatrix} a & b \\ c & d \end{pmatrix} \in SL(2,\mathbb{R}).$$

The emergence of such hidden global symmetries in three dimensions in the process of dimensional reduction followed by the dualization of gauge fields to scalars is due to Ehlers [86].

We now move on to the second step of dimensional reduction from three to two dimensions over ϕ direction. The ansatz for the three-dimensional metric is taken to be

$$ds_3^2 = f_E^2(d\rho^2 + dz^2)^2 + \rho^2 d\phi^2 \tag{2.45}$$

where ρ, z are the Weyl canonical coordinates. In the above we have set the two-dimensional Kaluza Klein gauge field to zero since it has no dynamical degree of freedom. The two dimensional Lagrangian then becomes

$$L^{(2D)}_{\text{Ehlers}} = \sqrt{g^{(2)}}\rho\left(R^{(2)} + 2g^{ab}f_E^{-1}\partial_a f_E \rho^{-1}\partial_b\rho - \frac{1}{2}(\partial\phi)^2 - \frac{1}{2}e^{2\phi}(\partial\chi)^2\right). \tag{2.46}$$

ii) **Matzner Misner reduction:** An alternative way to reduce the theory to two dimensions without dualizing the gauge fields in three dimensions, is known as the Matzner Misner reduction scheme [87]. The idea is to split the 1-form A_m in three dimensions to a two dimensional vector A_a and a scalar axion φ i.e. $A_m = (A_a, \varphi)$. Upon dimensional reduction to two dimensions we get two Maxwell 1-forms: one from the metric and one from the gauge field. In two-dimensions they can set to zero. Therefore, starting from (2.42) and reducing to two dimensions, we have

$$F^{mn}F_{mn} = 2f_E^{-2}\rho^{-2}(\partial\varphi)^2, \tag{2.47}$$

$$\sqrt{g^{(3)}} = f_E^2\rho\sqrt{g^{(2)}}. \tag{2.48}$$

The two dimensional Lagrangian reads

$$L^{(2D)} = \sqrt{g^{(2)}}\rho\left(R^{(2)} + 2g^{ab}f_E^{-1}\partial_a f_E\rho^{-1}\partial_b\rho - \frac{1}{2}(\partial\phi)^2 - \frac{1}{2}\rho^{-2}e^{-2\phi}(\partial\varphi)^2\right). \tag{2.49}$$

The above Lagrangian can be brought to the form (2.46) once we make the field redefinitions $e^{-\tilde{\phi}} = \rho e^{\phi}$, $f_{MM} = f_E\rho^{\frac{1}{4}}e^{\frac{\phi}{2}}$.

The fields in the Ehlers and Matzner Misner reduction schemes are related by Kramer-Neugebauer map defined as

$$e^{-\tilde{\phi}} \to \rho e^{\phi}, \tag{2.50}$$

$$\chi \to \varphi, \tag{2.51}$$

$$f_E \to f_{MM}. \tag{2.52}$$

2.4.1 Infinite dimensional symmetry

In two dimensions Ehlers and Matzner Misner reduction schemes give rise to two different isometry groups $SL(2,\mathbb{R})_E$ and $SL(2,\mathbb{R})_{MM}$ respectively. The combination of these two groups gives rise to infinite dimensional Geroch group in two dimensions. One has to act with $SL(2,\mathbb{R})_E$ generators (e_0, h_0, f_0) on φ and $SL(2,\mathbb{R})_{MM}$ generators (e_1, h_1, f_1) on χ to understand the origin of the infinite dimensional symmetries. The action of e_0 and h_0 are linear in the fields and local. The difference comes from the action of f_0 on φ, that is nonlinear and non-local [88, 89]. The full set of transformation rules are identified with an affine $SL(2,\mathbb{R})$ Kac-Moody algebra [90].

Integrability in two dimensions implies that there exists linear Lax pair of equations whose compatibility condition is equivalent to the integrable Einstein equation in two dimensions. In chapter 4 and 5 of the thesis we will focus on Breitenlohner Maison [5] and Belinsky Zakharov [79] Lax equations for two-dimensional gravity. These Lax pair lead to solution generating techniques. The methods rely on the inverse scattering technique; generating new solutions for a given seed solution.

Chapter 3

Holographic description of non-supersymmetric orbifolded D1-D5-P solutions

The black hole information paradox [91] is a profound and long-standing problem in quantum gravity. String theory has had many successes in black hole physics, including the microscopic derivation of the entropy of the large supersymmetric D1-D5-P black hole [34]. The evidence from constructions of black hole microstates in string theory points to a resolution of the information paradox whereby the true quantum bound state has a size of order the event horizon of the naive classical solution, and so the black hole event horizon and interior are replaced by quantum degrees of freedom. This is known as the fuzzball conjecture [1,92,96].

To probe the quantum degrees of freedom of the black hole, one often studies semi-classical microstates, which may be described within supergravity. There has been significant progress in the study of three-charge BPS black hole microstates [2,36,98,100,102], culminating in the recent first explicit construction of a 'superstratum' [46].

Given a supergravity solution with the same charges as a black hole, it is important to establish whether the solution describes a bound state. In an AdS/CFT setup [19,20,107], one can do this by identifying a state in the holographically dual CFT. At present, there are many more such supergravity solutions than there are solutions with identified CFT duals. In the case of the superstratum, there is a proposal for the dual CFT states, evidence for which has recently been obtained [108] using precision holography techniques [109].

In this chapter we identify the CFT duals of the general class of orbifolded JMaRT solutions. Physically, the $k > 1$ states are of particular interest; although the whole family of CFT states we study are atypical, states with larger k are closer to typical states than states with smaller k. This is because the typical three-charge state is in the maximally twisted sector, $k = n_1 n_5$, so states with higher k are closer to typicality.

We work in the D1-D5 system on T^4. In the holographically dual orbifold CFT [19, 34, 111], it has been proposed that semiclassical states obtained by the action of the superconformal algebra generators on Ramond-Ramond (R-R) ground states are dual to bulk solutions involving diffeomorphisms that do not vanish at the boundary of the AdS throat [112]. Similarly, solutions involving non-trivial deformations (with respect to a reference R-R ground state) in the region deep inside the AdS throat known as the 'cap' should be dual to CFT states that cannot be expressed in terms of superconformal algebra generators acting on R-R ground states; examples of three-charge BPS states which support this proposal were found in [22].

The CFT states studied in [22] involve fractional spectral flow in the left-moving sector, starting from the twisted R-R ground states studied in [115]. The dual geometries are the BPS orbifold solutions found in [3, 100]. It was anticipated in [22] that applying fractional spectral flow in both left- and right-moving sectors of the CFT, one should obtain states dual to the general orbifolded JMaRT geometries. In this chapter we confirm this expectation, make precise the map between gravity and CFT, and provide strong evidence for the identification by studying the emission spectrum and emission rates of the states in both gravity and CFT. Although our main interest is in R-R states, the general class of CFT states we study also contains NS-NS states.

Since non-BPS, non-extremal states may be expected to be generically unstable, it is far from clear how many states might be described by stationary supergravity solutions. However the decay of such states is an opportunity to gain insight into the unitary mechanism that should replace Hawking radiation for generic states. In the case of the $k = 1$ JMaRT solutions, soon after the discovery of these solutions it was shown that these geometries decay via a classical ergoregion instability [117].

A microscopic dual CFT explanation of the instability was proposed in [118]: the unitary CFT process of Hawking radiation is enhanced for the atypical CFT states dual to the JMaRT solutions, such that it manifests in the bulk as the ergoregion instability. Certain aspects of the CFT arguments were somewhat heuristic at the time, but were later made more precise in a series of papers [119–122]. The spectrum and emission rate of minimal scalars from the microscopic considerations were found to be in exact agreement with the instability found on the gravity side. In this chapter we extend these studies to the general $k > 1$ case.

Finally, we explore the physical picture of ergoregion emission as pair creation [123, 124]. This picture was investigated in reference [119] for the two-charge $k = 1$ JMaRT solutions. It was shown that to a good approximation, radiation from these solutions can be split into two distinct parts. One part escapes to infinity, and the other remains deep inside the AdS region, at the cap. In the present work, we generalize this picture to include all three charges and the orbifolding parameter k, and consider the most general form of the probe scalar wavefunction. We confirm that also in this more elaborate set-up, the radiation splits into two distinct parts: one part escapes to infinity and the other part remains deep inside in the AdS region.

Our results generalize various previous studies (already mentioned above) of both BPS and non-BPS states arising from spectral flow of R-R ground states. We comment in detail on the relation of our work to these previous works after we have introduced the CFT states in full detail in Section 3.2.

There has been a resurgence of interest in the black hole information paradox in recent years, in particular with regard to the experience of an infalling observer; see [23,125,126, 128–131] and references within. Our results develop further the AdS/CFT dictionary for non-BPS black hole microstates, and such technical progress may ultimately shed light on these questions.

The remainder of this chapter is organized as follows. In Section 3.1 we study the general family of orbifolded JMaRT solutions and solve the wave equation on these backgrounds. In Section 3.2 we identify the CFT description of these geometries. The emission spectrum and rates obtained from the CFT are shown to be in perfect agreement with the gravity computation. In Section 3.3 we analyze the pair creation picture of ergoregion emission for these orbifolds. We close with a brief discussion in Section 3.4.

3.1 Orbifolded JMaRT solutions

After a brief review of the supergravity solutions in Section 3.1.1, we study the near-decoupling limit in Section 3.1.2 in which the geometries have a large AdS inner region, weakly coupled to flat asymptotics. In Section 3.1.3 we analyze the smoothness properties and categorize the possible orbifold singularities of the solutions. In Section 3.1.4 we study the scalar wave equation on these orbifolds. We obtain the real and imaginary parts of the instability eigen-frequencies in the near-decoupling limit.

3.1.1 Supergravity solutions

The JMaRT solutions [3] are special cases of the non-extremal rotating three-charge Cvetič-Youm [132] solutions. In general, Cvetič-Youm geometries can have singularities, horizons, and closed timelike curves. Reference [3] derived the conditions that need to be imposed on the parameter space of the Cvetič-Youm geometries so that we get smooth solitonic solutions, possibly with orbifold singularities.

We consider type IIB string theory compactified on

$$M_{4,1} \times \mathrm{S}^1 \times \mathrm{T}^4 \,. \tag{3.1}$$

We consider the S^1 to be macroscopic, and consider the T^4 to be string-scale. We consider n_1 D1-branes wrapped on S^1, n_5 D5-branes wrapped on $\mathrm{S}^1 \times \mathrm{T}^4$, and n_p units of momentum P along the S^1. We parameterize the S^1 with coordinate y and the T^4 with coordinates z^i.

Our supergravity analysis begins with the general non-extremal three-charge Cvetič-Youm metric, lifted to type IIB supergravity [132, 133]. The 10D string frame metric is [3]

$$\begin{aligned} ds^2 \;=\;& -\frac{f}{\sqrt{\tilde{H}_1\tilde{H}_5}}(dt^2 - dy^2) + \frac{M}{\sqrt{\tilde{H}_1\tilde{H}_5}}(s_p dy - c_p dt)^2 \\ & + \sqrt{\tilde{H}_1\tilde{H}_5}\left(\frac{r^2 dr^2}{(r^2+a_1^2)(r^2+a_2^2) - Mr^2} + d\theta^2\right) \\ & + \left(\sqrt{\tilde{H}_1\tilde{H}_5} - (a_2^2 - a_1^2)\frac{(\tilde{H}_1 + \tilde{H}_5 - f)\cos^2\theta}{\sqrt{\tilde{H}_1\tilde{H}_5}}\right)\cos^2\theta d\psi^2 \\ & + \left(\sqrt{\tilde{H}_1\tilde{H}_5} + (a_2^2 - a_1^2)\frac{(\tilde{H}_1 + \tilde{H}_5 - f)\sin^2\theta}{\sqrt{\tilde{H}_1\tilde{H}_5}}\right)\sin^2\theta d\phi^2 \\ & + \frac{M}{\sqrt{\tilde{H}_1\tilde{H}_5}}(a_1\cos^2\theta d\psi + a_2\sin^2\theta d\phi)^2 \\ & + \frac{2M\cos^2\theta}{\sqrt{\tilde{H}_1\tilde{H}_5}}[(a_1c_1c_5c_p - a_2s_1s_5s_p)dt + (a_2s_1s_5c_p - a_1c_1c_5s_p)dy]d\psi \\ & + \frac{2M\sin^2\theta}{\sqrt{\tilde{H}_1\tilde{H}_5}}[(a_2c_1c_5c_p - a_1s_1s_5s_p)dt + (a_1s_1s_5c_p - a_2c_1c_5s_p)dy]d\phi \\ & + \sqrt{\frac{\tilde{H}_1}{\tilde{H}_5}}\sum_{i=1}^{4} dz_i^2 \,, \end{aligned} \tag{3.2}$$

where we use the shorthand notation $c_i = \cosh\delta_i$, $s_i = \sinh\delta_i$, for $i = 1, 5, p$, and where

$$f \;=\; r^2 + a_1^2\sin^2\theta + a_2^2\cos^2\theta \,, \qquad \tilde{H}_1 \;=\; f + M\sinh^2\delta_1 \,, \qquad \tilde{H}_5 \;=\; f + M\sinh^2\delta_5 \tag{3.3}$$

Explicit expressions for the six-dimensional dilaton and Ramond-Ramond two-form field can be found, e.g., in [3]; we will not need those details in our discussion below. Upon compactification to five dimensions, one obtains asymptotically flat configurations carrying three U(1) charges, corresponding to D1, D5, and P. These charges are given by $Q_i = M s_i c_i$.

The y circle will play a key role in the following; we take it to have radius R at spacelike infinity, $y \sim y + 2\pi R$. In addition, we take the volume of T^4 to be $(2\pi)^4 V$ at spacelike infinity. The integer quantization of the three charges is then given by

$$Q_1 = \frac{g_s \alpha'^3}{V} n_1, \qquad Q_5 = g_s \alpha' n_5, \qquad Q_p = \frac{g_s^2 \alpha'^4}{V R^2} n_p. \tag{3.4}$$

The ADM mass and angular momenta of the five-dimensional asymptotically flat configurations are

$$\begin{aligned} M_{\text{ADM}} &= \frac{\pi M}{4G_5}\left(s_1^2 + s_5^2 + s_p^2 + \frac{3}{2}\right), & (3.5)\\ J_\psi &= -\frac{\pi M}{4G_5}(a_1 c_1 c_5 c_p - a_2 s_1 s_5 s_p), & (3.6)\\ J_\phi &= -\frac{\pi M}{4G_5}(a_2 c_1 c_5 c_p - a_1 s_1 s_5 s_p), & (3.7) \end{aligned}$$

where G_5 is the five-dimensional Newton constant. The ten-dimensional Newton constant is as usual $G_{10} = 8\pi^6 g_s^2 \alpha'^4$, so we have $G_5 = \frac{\pi g_s^2 \alpha'^4}{4VR}$. To have positive ADM mass we take $M \geq 0$, and without loss of generality we take $\delta_1, \delta_5, \delta_p \geq 0$ and $a_1 \geq a_2 \geq 0$.

The singularities $\tilde{H}_1 = 0$ and $\tilde{H}_5 = 0$ in metric (3.2) are curvature singularities, and there are also singularities where the function

$$g(r) \equiv (r^2 + a_1^2)(r^2 + a_2^2) - M r^2 \tag{3.8}$$

has roots, i.e. at

$$r_\pm^2 = \frac{1}{2}\left[(M - a_1^2 - a_2^2) \pm \sqrt{(M - a_1^2 - a_2^2)^2 - 4a_1^2 a_2^2}\right]. \tag{3.9}$$

To find a smooth solution without curvature singularities, consider the metric with $\tilde{H}_1 > 0$ and $\tilde{H}_5 > 0$ everywhere. Further smooth geometries without horizons are obtained by demanding that at $r = r_+$ an S^1 should shrink smoothly, with the singularity at $r = r_+$ being that of polar coordinates at the origin of a two-dimensional factor of the metric [3]. The parameter analysis is slightly different for the two-charge ($Q_p = 0$) and three-charge cases; in this chapter we focus on the general case of three non-vanishing charges. In this case four conditions on the parameters must be satisfied for the geometries to be smooth (up to possible orbifold singularities). We now present a brief summary of the analysis of [3]; for further details we refer the reader to that reference.

The function $g(r)$ has real roots if and only if $M > (a_1 + a_2)^2$ or $M < (a_1 - a_2)^2$. For $r = r_+$ to be an origin, rather than a horizon, the determinant of the metric in the constant t and r subspace must vanish at $r = r_+$. This rules out the case $M > (a_1 + a_2)^2$ and gives the first condition on the parameters,

$$M = a_1^2 + a_2^2 - a_1 a_2 \frac{c_1^2 c_5^2 c_p^2 + s_1^2 s_5^2 s_p^2}{s_1 c_1 s_5 c_5 s_p c_p}\,. \tag{3.10}$$

In order that $r = r_+$ be an origin, a spacelike Killing vector with closed orbits must smoothly degenerate there. The most general Killing vector with closed orbits is

$$\xi_{\text{Killing}} = \partial_y - \alpha\partial_\psi - \beta\partial_\phi, \tag{3.11}$$

and the one that degenerates at $r = r_+$, given the condition (3.10), is given by

$$\alpha = -\frac{s_p c_p}{(a_1 c_1 c_5 c_p - a_2 s_1 s_5 s_p)}, \qquad \beta = -\frac{s_p c_p}{(a_2 c_1 c_5 c_p - a_1 s_1 s_5 s_p)}. \tag{3.12}$$

We introduce new coordinates appropriate to the neighborhood of $r = r_+$,

$$\bar{\psi} \equiv \psi - \frac{s_p c_p}{(a_1 c_1 c_5 c_p - a_2 s_1 s_5 s_p)} y, \qquad \bar{\phi} \equiv \phi - \frac{s_p c_p}{(a_2 c_1 c_5 c_p - a_1 s_1 s_5 s_p)} y. \tag{3.13}$$

Then the coordinate which shrinks at $r = r_+$ is y at constant $\bar{\psi}$, $\bar{\phi}$.

In order to find the most general smooth solutions and to allow for the possibility of orbifold singularities at $r = r_+$, we introduce a positive integer k and impose that $y \to y + 2\pi k R$ at constant $\bar{\psi}$, $\bar{\phi}$, is a closed orbit. This gives two further conditions,

$$\frac{s_p c_p}{(a_1 c_1 c_5 c_p - a_2 s_1 s_5 s_p)}(kR) = n \in \mathbb{Z}\,, - \frac{s_p c_p}{(a_2 c_1 c_5 c_p - a_1 s_1 s_5 s_p)}(kR) = m \in \mathbb{Z}\,. \tag{3.14}$$

Furthermore, demanding regularity at the origin $r = r_+$ under $y \to y + 2\pi k R$ fixes the size of the y-circle at infinity,

$$R = \frac{1}{k} \frac{M s_1 c_1 s_5 c_5 (s_1 c_1 s_5 c_5 s_p c_p)^{1/2}}{\sqrt{a_1 a_2}(c_1^2 c_5^2 c_p^2 - s_1^2 s_5^2 s_p^2)}\,. \tag{3.15}$$

To summarize, the full regularity conditions for the three-charge orbifolded case are

$$(a) \qquad a_1 a_2 = \frac{Q_1 Q_5}{k^2 R^2} \frac{s_1^2 c_1^2 s_5^2 c_5^2 s_p c_p}{(c_1^2 c_5^2 c_p^2 - s_1^2 s_5^2 s_p^2)^2}, \tag{3.16}$$

$$(b) \qquad M = a_1^2 + a_2^2 - a_1 a_2 \frac{c_1^2 c_5^2 c_p^2 + s_1^2 s_5^2 s_p^2}{s_1 c_1 s_5 c_5 s_p c_p}, \tag{3.17}$$

$$(c) \qquad \frac{s_p c_p}{(a_1 c_1 c_5 c_p - a_2 s_1 s_5 s_p)}(kR) = n \in \mathbb{Z}, \tag{3.18}$$

$$(d) \qquad -\frac{s_p c_p}{(a_2 c_1 c_5 c_p - a_1 s_1 s_5 s_p)}(kR) = m \in \mathbb{Z}. \tag{3.19}$$

The metric describes a smooth non-singular geodesically complete spacetime after imposing the above four conditions. Using these conditions we record here some relations between the parameters which will be useful in what follows,

$$r_+^2 = -a_1 a_2 \frac{s_1 s_5 s_p}{c_1 c_5 c_p}, \quad r_-^2 = -a_1 a_2 \frac{c_1 c_5 c_p}{s_1 s_5 s_p}, \quad M = a_1 a_2 nm \left(\frac{c_1 c_5 c_p}{s_1 s_5 s_p} - \frac{s_1 s_5 s_p}{c_1 c_5 c_p} \right)^2 . \tag{3.20}$$

The ADM angular momenta, in terms of the parameters introduced above, take the following simple form,

$$J_\psi = -\frac{m}{k} n_1 n_5, \qquad\qquad J_\phi = \frac{n}{k} n_1 n_5. \tag{3.21}$$

3.1.2 The near-decoupling limit

In order to study AdS/CFT in this system one must isolate low-energy excitations of the D1-D5 bound state, which is achieved by taking the large R limit. In the gravity description, this corresponds to taking the near-decoupling limit in which one obtains a large inner region involving an $\mathrm{AdS}_3 \times \mathrm{S}^3 \times \mathrm{T}^4$ throat, weakly coupled to the flat asymptotics.

The large R limit is defined by keeping Q_1, Q_5 fixed and taking $R \gg (Q_1 Q_5)^{\frac{1}{4}}$, which makes R the largest scale in the problem. We then have the small dimensionless parameter

$$\epsilon = \frac{(Q_1 Q_5)^{\frac{1}{4}}}{R} \ll 1. \tag{3.22}$$

In the Cvetic-Youm metric, the near-decoupling limit is obtained by taking

$$a_1^2, a_2^2, M \ll Q_1, Q_5 \qquad \Rightarrow \qquad s_1 \simeq c_1 \gg 1\,, \quad s_5 \simeq c_5 \gg 1. \tag{3.23}$$

We refer to the limit (3.22), (3.23) as the large R limit or the near-decoupling limit.

In this limit we can identify the region $r^2 \ll Q_1, Q_5$ as an asymptotically AdS region. This amounts to taking $\tilde{H}_1 \approx Q_1$ and $\tilde{H}_5 \approx Q_5$ and using approximations (3.23) in the metric

(3.2). We thus obtain an asymptotically $AdS_3 \times S^3$ metric,

$$ds^2 = -\left(\rho^2 - M_3 + \frac{J_3^2}{4\rho^2}\right)d\tau^2 + \left(\rho^2 - M_3 + \frac{J_3^2}{4\rho^2}\right)^{-1} d\rho^2 + \rho^2\left(d\varphi - \frac{J_3}{2\rho^2}d\tau\right)^2$$
$$+ \sqrt{Q_1Q_5}\left\{d\theta^2 + \sin^2\theta\left[d\phi + \frac{R}{\sqrt{Q_1Q_5}}(a_1c_p - a_2s_p)d\varphi + \frac{R}{\sqrt{Q_1Q_5}}(a_2c_p - a_1s_p)d\tau\right]^2\right.$$
$$\left. + \cos^2\theta\left[d\psi + \frac{R}{\sqrt{Q_1Q_5}}(a_2c_p - a_1s_p)d\varphi + \frac{R}{\sqrt{Q_1Q_5}}(a_1c_p - a_2s_p)d\tau\right]^2\right\} \quad (3.24)$$

where we have defined new coordinates

$$\varphi = \frac{y}{R}, \quad \tau = \frac{t}{R}, \quad (3.25)$$

$$\rho^2 = \frac{R^2}{Q_1Q_5}[r^2 + (M - a_1^2 - a_2^2)\sinh^2\delta_p + a_1a_2\sinh 2\delta_p]. \quad (3.26)$$

The AdS length and the size of the S^3 is $(Q_1Q_5)^{\frac{1}{4}}$. In writing the above expressions we have also defined

$$M_3 = \frac{R^2}{Q_1Q_5}[(M - a_1^2 - a_2^2)\cosh 2\delta_p + 2a_1a_2\sinh 2\delta_p], \quad (3.27)$$

$$J_3 = \frac{R^2}{Q_1Q_5}[(M - a_1^2 - a_2^2)\sinh 2\delta_p + 2a_1a_2\cosh 2\delta_p]. \quad (3.28)$$

The regularity conditions (3.16)–(3.19) simplify in the large R limit as follows,

$$(a') \qquad a_1a_2 \simeq \frac{Q_1Q_5}{k^2R^2}s_pc_p, \quad (3.29)$$

$$(b') \qquad M \simeq a_1^2 + a_2^2 - a_1a_2\frac{c_p^2 + s_p^2}{s_pc_p}, \quad (3.30)$$

$$(c') \qquad \frac{s_pc_p}{c_1c_5(a_1c_p - a_2s_p)}(kR) \simeq n \in \mathbb{Z}, \quad (3.31)$$

$$(d') \qquad -\frac{s_pc_p}{c_1c_5(a_2c_p - a_1s_p)}(kR) \simeq m \in \mathbb{Z}. \quad (3.32)$$

A useful form of condition (3.30) via (3.20) is

$$M \simeq \frac{Q_1 Q_5}{(kR)^2}\frac{nm}{s_p c_p}, \tag{3.33}$$

and another expression that will be useful later is

$$r_+^2 - r_-^2 \simeq \frac{Q_1 Q_5}{k^2 R^2}. \tag{3.34}$$

Substituting conditions (3.29)–(3.32) into (3.24) we find that the geometry is an orbifold of $AdS_3 \times S^3$,

$$\begin{aligned} ds^2 \;=\; & \sqrt{Q_1 Q_5}\left[-\left(\frac{1}{k^2}+\rho^2\right)d\tau^2 + d\rho^2\left(\frac{1}{k^2}+\rho^2\right)^{-1} + \rho^2 d\varphi^2 \right. \\ & \left. + d\theta^2 + \sin^2\theta\left(d\phi + \frac{m}{k}d\varphi - \frac{n}{k}d\tau\right)^2 + \cos^2\theta\left(d\psi - \frac{n}{k}d\varphi + \frac{m}{k}d\tau\right)^2\right]. \end{aligned} \tag{3.35}$$

We will analyze the smoothness properties of these orbifold geometries in the next subsection.

Let us now look at how various physical quantities behave in the large R limit. It is only in this limit that we expect physical parameters in the gravity description to be reproduced by a dual CFT analysis. In this limit the mass above the mass of the D1 and D5 branes is

$$\Delta M_{\mathrm{ADM}} \simeq \frac{\pi M}{4G_5}\left(s_p^2 + \frac{1}{2}\right) \simeq \frac{n_1 n_5}{R}\frac{m^2+n^2-1}{2k^2}, \tag{3.36}$$

and the 6D ADM linear momentum P_{ADM} is

$$P_{\mathrm{ADM}} = \frac{n_p}{R} = \frac{\pi M}{4G_5}s_p c_p \simeq \frac{n_1 n_5}{R}\frac{mn}{k^2}. \tag{3.37}$$

In Section 3.2 we will observe agreement between the gravity quantities (3.21), (3.36), and (3.37) from the CFT description.

3.1.3 Smoothness analysis

As observed above, the decoupling limit of the general JMaRT orbifolded solution is an orbifold of $AdS_3\times S^3$, with metric (3.35). These orbifolds were briefly discussed in [3]; here we present a detailed smoothness analysis following [22]. For convenience let us introduce the coordinates

$$\tilde{\psi} \equiv \psi - \frac{n}{k}\varphi + \frac{m}{k}\tau, \qquad \tilde{\phi} \equiv \phi + \frac{m}{k}\varphi - \frac{n}{k}\tau. \tag{3.38}$$

Working in the covering space for coordinates $(\varphi, \tilde{\psi}, \tilde{\phi})$, the periodicities of (φ, ψ, ϕ) translate into the following identifications:

$$A: \quad (\varphi, \tilde{\psi}, \tilde{\phi}) \to (\varphi, \tilde{\psi}, \tilde{\phi}) + 2\pi\left(1, -\frac{n}{k}, \frac{m}{k}\right), \tag{3.39}$$

$$B: \quad (\varphi, \tilde{\psi}, \tilde{\phi}) \to (\varphi, \tilde{\psi}, \tilde{\phi}) + 2\pi(0, 1, 0), \tag{3.40}$$

$$C: \quad (\varphi, \tilde{\psi}, \tilde{\phi}) \to (\varphi, \tilde{\psi}, \tilde{\phi}) + 2\pi(0, 0, 1). \tag{3.41}$$

Note that the coordinate φ in the metric (3.35) is ill-defined at $\rho = 0$, where a conical singularity can occur; the periodicity required for smoothness is $\varphi \to \varphi + 2\pi k$ at fixed $\tilde{\psi}, \tilde{\phi}$. Conical singularities only occur at points that remain invariant under the operation

$$A^{m_A} B^{m_B} C^{m_C} \tag{3.42}$$

for some $m_I \in \mathbb{Z}$. The conical singularities all arise at $\rho = 0$ and may be localized at $\theta = 0$ and/or $\theta = \frac{\pi}{2}$, or may occur everywhere in θ. We will continue to focus on the case of three non-zero charges; the two-charge case is discussed in [3].

<u>**Case 1:** $\gcd(k,m) = \gcd(k,n) = 1$</u>

If there are no common divisors between the pairs (m,k) and (n,k), then there are no conical singularities and the spacetime is completely smooth.

To see this, we first examine the possibility of having a fixed point where $\tilde{\phi}$ has a non-zero size, i.e., at $\rho = 0, \theta \neq 0$. For a fixed point to occur here, $\tilde{\phi}$ must remain invariant under (3.42). This implies that $\frac{m}{k}m_A + m_C = 0$. Since m_C is an integer this requires $\frac{m_A}{k}$ to be an integer; we write $m_A = km'_A$. The periodic identifications of φ and $\tilde{\psi}$ are then

$$\varphi \;\; \to \;\; \varphi + 2\pi k m'_A\,, \qquad\qquad \tilde{\psi} \;\to\; \tilde{\psi} + 2\pi\left(m_B - n m'_A\right). \tag{3.43}$$

In the range $0 < \theta < \frac{\pi}{2}$, $\tilde{\psi}$ also has a finite size. So for a fixed point to occur there, $\tilde{\psi}$ must also remain invariant. This fixes $m_B = nm'_A$, and as a result the above identification becomes

$$\varphi \;\; \to \;\; \varphi + 2\pi k m'_A\,, \tag{3.44}$$

which, being an integer multiple of $2\pi k$, is the correct identification for smoothness. At $\theta = \frac{\pi}{2}$, $\tilde{\psi}$ has zero size. Thus, under the diffeomorphism (3.43) the point $\rho = 0, \theta = \frac{\pi}{2}$ is a fixed point. The relevant identification is simply (3.44) and we again have smoothness. It remains to examine $\rho = 0, \theta = 0$. Here $\tilde{\phi}$ has zero size but $\tilde{\psi}$ has non-zero size. Requiring $\tilde{\psi}$ to be invariant fixes $-\frac{n}{k}m_A + m_B = 0$. Since m_B is an integer, this implies m_A should be an integer multiple of k; we again write it as $m_A = km'_A$. The relevant identification is again (3.44). This shows that the spacetime is free of conical singularity here also.

In summary, there are no conical singularities anywhere, and so the spacetime is completely smooth. From the point of view of the $k = 1$ JMaRT solitons, one can say that the $\mathbb{Z}_k$ quotient is freely acting in this case [3].

Case 2: $\gcd(k, m) > 1,\ \gcd(k, n) = 1$

If $\gcd(k, m) \equiv l_1 > 1$ and $\gcd(k, n) = 1$, there is a $\mathbb{Z}_{l_1}$ orbifold singularity at $\rho = 0, \theta = \frac{\pi}{2}$ and the spacetime is otherwise smooth.

To see this, we first note that at $\rho = 0, \theta = 0$, the analysis is the same as in Case 1, and there is no orbifold singularity at these points.

Next, let us write $k = l_1\hat{k}$, $m = l_1\hat{m}$. For a fixed point at $\rho = 0, \theta \neq 0$, $\tilde{\phi}$ must remain invariant. This fixes $m_A = \hat{k}m'_A$, $m_C = -\hat{m}m'_A$. At points $\theta \neq \frac{\pi}{2}$, $\tilde{\psi}$ also has a non-zero size, so it must also remain invariant. This fixes $-\frac{n}{k}(\hat{k}m'_A) + m_B = 0$, i.e, $m_B = \frac{n}{l_1}m'_A$. Since m_B is an integer, m'_A must be an integer multiple of l_1, i.e., $m'_A = l_1 m''_A$. Then the φ identification $\varphi \to \varphi + 2\pi m_A$ becomes $\varphi \to \varphi + (2\pi k)m''_A$ since we have

$$m_A = \hat{k}m'_A = \hat{k}l_1 m''_A = km''_A. \tag{3.45}$$

Hence we have smoothness at $\rho = 0,\ 0 < \theta < \frac{\pi}{2}$.

For $\rho = 0, \theta = \frac{\pi}{2}$, $\tilde{\psi}$ has zero size. Invariance of $\tilde{\phi}$ gives $m_A = \hat{k}m'_A$. So the φ identification $\varphi \to \varphi + 2\pi m_A$ becomes $\varphi \to \varphi + 2\pi(\hat{k}m'_A)$, i.e.,

$$\varphi \quad \to \quad \varphi + (2\pi k)\frac{m'_A}{l_1}. \tag{3.46}$$

Since m'_A is a general integer, there is a $\mathbb{Z}_{l_1}$ orbifold singularity at $\rho = 0, \theta = \frac{\pi}{2}$.

Case 3: $\gcd(k, m) = 1,\ \gcd(k, n) > 1$

If $\gcd(k, m) = 1$ and $\gcd(k, n) \equiv l_2 > 1$, there is a $\mathbb{Z}_{l_2}$ orbifold singularity at $\rho = 0, \theta = 0$ and the spacetime is otherwise smooth.

To see this, firstly an analysis similar to Case 2 shows that there are no conical singularities at $\rho = 0, \theta = \frac{\pi}{2}$ or at $\rho = 0,\ 0 < \theta < \frac{\pi}{2}$.

Next, let us write $k = l_2\hat{k}$, $n = l_2\hat{n}$. For $\rho = 0, \theta = 0$ to be a fixed point $\tilde{\psi}$ must remain invariant. This fixes $m_A = \hat{k}m'_A, m_B = \hat{n}m'_A$. The φ identification $\varphi \to \varphi + 2\pi m_A$ then becomes $\varphi \to \varphi + 2\pi\hat{k}m'_A$, which is

$$\varphi \quad \to \quad \varphi + (2\pi k)\frac{m'_A}{l_2}. \tag{3.47}$$

This results in a $\mathbb{Z}_{l_2}$ orbifold singularity at $\rho = 0, \theta = 0$.

Case 4: $\gcd(k,m) > 1,\ \gcd(k,n) > 1,\ \gcd(k,m,n) = 1$

When both $\gcd(k,m) \equiv l_1 > 1$ and $\gcd(k,n) \equiv l_2 > 1$, the spacetime has both a $\mathbb{Z}_{l_1}$ orbifold singularity at $\rho = 0, \theta = \frac{\pi}{2}$ and a $\mathbb{Z}_{l_2}$ orbifold singularity at $\rho = 0, \theta = 0$. Away from these points the metric is smooth. The analysis is similar to the previous two cases.

Case 5: $\gcd(k,m) > 1,\ \gcd(k,n) > 1\ \ \gcd(k,m,n) > 1$

When $\gcd(k,m) \equiv l_1 > 1$, $\gcd(k,n) \equiv l_2 > 1$, and $\gcd(k,m,n) \equiv l_3 > 1$, then the orbifold has a rich singularity structure with

- $\mathbb{Z}_{l_1}$ orbifold singularity at $\rho = 0,\ \theta = \frac{\pi}{2}$,
- $\mathbb{Z}_{l_2}$ orbifold singularity at $\rho = 0,\ \theta = 0$, and
- $\mathbb{Z}_{l_3}$ orbifold singularity at $\rho = 0,\ 0 < \theta < \frac{\pi}{2}$.

Thus at $\rho = 0$ there is at least a $\mathbb{Z}_{l_3}$ orbifold singularity all over the three-sphere[1], which may be enhanced to a singularity of higher degree at the poles if l_1 and/or l_2 are greater than l_3.

To see this, we first observe that an analysis similar to Cases 2 and 3 shows that there is a $\mathbb{Z}_{l_1}$ orbifold singularity at $\rho = 0,\ \theta = \frac{\pi}{2}$ and a $\mathbb{Z}_{l_2}$ orbifold singularity at $\rho = 0,\ \theta = 0$.

[1]Note that the orbifold singularity at $\rho = 0,\ 0 < \theta < \frac{\pi}{2}$ only arises in the non-BPS case, since in the BPS limit we have $m = n + 1$ and so m and n have no common divisors.

To see the orbifold singularity at $\rho = 0,\ 0 < \theta < \frac{\pi}{2}$ we introduce the following notation,

$$m = l_1 \hat{m}, \qquad n = l_2 \hat{n}, \qquad l_1 = l_3 \hat{l}_1, \qquad l_2 = l_3 \hat{l}_2, \qquad k = l_3 \hat{l}_1 \hat{l}_2 \hat{k}. \tag{3.48}$$

To have a fixed point at $\rho = 0,\ 0 < \theta < \frac{\pi}{2}$, both $\tilde{\psi}$ and $\tilde{\phi}$ must remain invariant. From the invariance of $\tilde{\phi}$ we get

$$\frac{m}{k} m_A + m_C \ = \ 0 \qquad \Rightarrow \qquad \frac{\hat{m}}{\hat{l}_2 \hat{k}} m_A + m_C \ = \ 0\,. \tag{3.49}$$

Since m_C is an integer, m_A must be a multiple of $\hat{l}_2 \hat{k}$, so we write $m_A = \hat{l}_2 \hat{k} m'_A$. This gives $m_C = -\hat{m} m'_A$.

Similarly, from the invariance of $\tilde{\psi}$ we get

$$-\frac{n}{k} m_A + m_B \ = \ 0 \qquad \Rightarrow \qquad -\frac{\hat{n} \hat{l}_2}{\hat{l}_1} m'_A + m_B \ = \ 0. \tag{3.50}$$

Since m_B is an integer, m'_A must be a multiple of $\hat{l}_1$, i.e., $m'_A = \hat{l}_1 m''_A$. This implies $m_A = \hat{l}_1 \hat{l}_2 \hat{k} m''_A$, and $m_B = \hat{n} \hat{l}_2 m''_A$. The φ identification now becomes

$$\varphi \ \rightarrow \ \varphi + 2\pi \hat{l}_1 \hat{l}_2 \hat{k} m''_A = \varphi + (2\pi k) \frac{m''_A}{l_3}. \tag{3.51}$$

Hence there is a $\mathbb{Z}_{l_3}$ orbifold at $\rho = 0$ and $\theta \neq 0, \theta \neq \frac{\pi}{2}$.

We finally note that although we presented the above analysis for the decoupled asymptotically $\mathrm{AdS}_3 \times \mathrm{S}^3$ geometries, it applies equally well to the asymptotically flat geometries before taking the decoupling limit using (3.13).

3.1.4 Scalar wave equation

We next study a minimally coupled scalar in six dimensions on the general orbifolded JMaRT solutions. For the $k = 1$ solutions, such a computation showed that these geometries suffer from a classical ergoregion instability [117]. We extend this study to the case of general k, m, n, obtaining the real and imaginary parts of the instability eigen-frequencies in the large R limit. We will later reproduce these results from the CFT.

Let us consider a minimally coupled complex scalar Ψ in six dimensions, on the background of the dimensionally reduced 6D Einstein frame metric. If one takes the 10D string frame metric written in (3.2) and discards the T^4 directions, one obtains exactly the 6D Einstein frame metric, and so we will not rewrite it here. Such a minimal scalar arises for example from the dimensional reduction of the ten-dimensional IIB graviton having both its indices along the four-torus. We can separate variables using the ansatz,

$$\Psi = \exp\left[-i\omega t + im_\psi \psi + im_\phi \phi + i\frac{\lambda}{R} y\right]\chi(\theta)h(r), \tag{3.52}$$

which gives equation for the angular part

$$\frac{1}{\sin 2\theta}\frac{d}{d\theta}\left(\sin 2\theta \frac{d}{d\theta}\chi\right) + \left[\left(\omega^2 - \frac{\lambda^2}{R^2}\right)(a_1^2 \sin^2\theta + a_2^2 \cos^2\theta) - \frac{m_\psi^2}{\cos^2\theta} - \frac{m_\phi^2}{\sin^2\theta}\right]\chi = -\Lambda\chi. \tag{3.53}$$

We are looking for wave functions with frequency $\omega \sim \frac{1}{R}$. In the large R limit, in terms of ϵ defined in (3.22), we observe that

$$\left(\omega^2 - \frac{\lambda^2}{R^2}\right)a_i^2 \ \sim \ \epsilon^4 \tag{3.54}$$

and so we find

$$\Lambda \ = \ l(l+2) + O(\epsilon^4)\,. \tag{3.55}$$

The radial equation takes the form

$$\frac{1}{r}\frac{d}{dr}\left(\frac{g(r)}{r}\frac{d}{dr}h\right) - \Lambda h + \left[\left(\omega^2 - \frac{\lambda^2}{R^2}\right)(r^2 + Ms_1^2 + Ms_5^2) + \left(\omega c_p - \frac{\lambda}{R}s_p\right)^2 M\right] h$$
$$-k^2\frac{r_+^2 - r_-^2}{r^2 - r_+^2}\left(-\lambda - \frac{n}{k}m_\psi + \frac{m}{k}m_\phi\right)^2 h + k^2\frac{r_+^2 - r_-^2}{r^2 - r_-^2}\left(\omega\varrho R - \lambda\vartheta - \frac{n}{k}m_\phi + \frac{m}{k}m_\psi\right)^2 h = 0, \tag{3.56}$$

where $g(r) = (r^2 - r_+^2)(r^2 - r_-^2)$. Introducing the dimensionless variable x for the radial coordinate via

$$x = \frac{1}{k^2}\left(\frac{r^2 - r_+^2}{r_+^2 - r_-^2}\right), \tag{3.57}$$

we can write the radial equation in the form

$$\partial_x\left[x\left(x + \frac{1}{k^2}\right)\partial_x h\right] + \frac{1}{4}\left[\kappa^2 x + 1 - \nu^2 + \frac{\xi^2}{x + k^{-2}} - \frac{\zeta^2}{x}\right] h = 0, \tag{3.58}$$

with

$$\kappa^2 = \left(\omega^2 - \frac{\lambda^2}{R^2}\right)(r_+^2 - r_-^2)k^2, \tag{3.59}$$
$$\xi = \omega\varrho R - \lambda\vartheta - m_\phi\frac{n}{k} + m_\psi\frac{m}{k}, \tag{3.60}$$
$$\zeta = -\lambda - m_\psi\frac{n}{k} + m_\phi\frac{m}{k}, \tag{3.61}$$
$$\varrho = \frac{c_1^2 c_5^2 c_p^2 - s_1^2 s_5^2 s_p^2}{s_1 c_1 s_5 c_5}, \tag{3.62}$$
$$\vartheta = \frac{c_1^2 c_5^2 - s_1^2 s_5^2}{s_1 c_1 s_5 c_5} s_p c_p, \tag{3.63}$$
$$\nu^2 = 1 + \Lambda - \left(\omega^2 - \frac{\lambda^2}{R^2}\right)(r_+^2 + Ms_1^2 + Ms_5^2) - \left(\omega c_p - \frac{\lambda}{R}s_p\right)^2 M. \tag{3.64}$$

For later use, we note from (3.64) that the correction to ν is $O(\epsilon^2)$,

$$\nu = l + 1 + O(\epsilon^2)\,. \tag{3.65}$$

The radial differential equation (3.58) cannot be solved exactly. It can however be solved via matched asymptotic expansion. This is done in detail in Appendix A.1. The instability frequencies are given by solutions to the transcendental equation (A.16). To the leading order in the large R expansion, we let one of the Γ functions in the denominator of (A.16) develop a pole,

$$\frac{1}{2}(1 + \nu + k|\zeta| + k\xi) \simeq -N, \tag{3.66}$$

with N a non-negative integer. From equations (3.62) and (3.63) we see that in the large R limit $\varrho \to 1$ and $\vartheta \sim \epsilon^2$. Hence to leading order one obtains

$$\xi \simeq \omega R - m_\phi \frac{n}{k} + m_\psi \frac{m}{k} \,. \tag{3.67}$$

Substituting this relation along with (3.65) into equation (3.66), we get the real part ω_R of the instability frequencies to leading order, which are given by

$$\omega_R \simeq \frac{1}{kR}\Big(-l - m_\psi m + m_\phi n - \big|-k\lambda - m_\psi n + m_\phi m\big| - 2(N+1)\Big). \tag{3.68}$$

For certain values of the parameters, ω_R can become negative or zero. For those cases there is no emission.

One obtains the imaginary part ω_I of the instability frequencies to leading order by iterating the above approximation to the next order, setting $N \to N + \delta N$. This computation is discussed in detail in Appendix A.1. The result is

$$\omega_I \simeq \frac{1}{kR}\frac{\pi}{2^{2l+1}(l!)^2}\left[\left(\omega^2 - \frac{\lambda^2}{R^2}\right)\frac{Q_1 Q_5}{k^2 R^2}\right]^{l+1} \binom{N+l+1}{l+1}\binom{N+k|\zeta|+l+1}{l+1}. \tag{3.69}$$

Since $\omega_I > 0$, we have an instability: i.e., an exponentially growing perturbation. In the following section we reproduce (3.68) and (3.69) from the dual CFT.

3.2 CFT description of orbifolded JMaRT solutions

3.2.1 The D1-D5 system on T^4 and the orbifold CFT

In order to discuss the CFT interpretation of the general orbifolded JMaRT solutions, we next review some properties of the D1-D5 system on T^4 and the corresponding orbifold CFT. We follow in places the presentations of [134] and [22].

As mentioned in the previous section, we work in type IIB string theory compactified on $M_{4,1} \times S^1 \times T^4$, with n_1 D1-branes wrapped on S^1 and n_5 D5-branes wrapped on $S^1 \times T^4$. We work in the limit of large R, which corresponds to the low-energy limit of the gauge theory on the D-brane bound state.

At low energies, the gauge theory on the bound state flows to a $(4,4)$ SCFT. It is conjectured that there is a point in moduli space where this SCFT is a symmetric product orbifold theory, consisting of $n_1 n_5$ symmetrized copies of a free $(4,4)$ SCFT with target space T^4 [34, 111].

Each copy of T^4 gives 4 bosonic fields X^1, X^2, X^3, X^4, along with 4 left-moving fermionic excitations $\psi^1, \psi^2, \psi^3, \psi^4$ and the corresponding right-moving excitations, which we denote with a bar ($\bar{\psi}^1$, etc.). The total central charge of the CFT is $c = 6n_1n_5$.

The CFT has a small $\mathcal{N} = 4$ superconformal symmetry in both the left and right-moving sectors. The small $\mathcal{N} = 4$ superconformal algebra is generated by four bosonic and four fermionic generators. The bosonic generators are the energy-momentum tensor $T(z)$ and three $SU(2)$ R-symmetry currents $J^i(z)$ and the fermionic generators are the four supercurrents $G^a(z)$ and $G^{b^\dagger}(z)$ respectively. The operator product expansions of the algebra are given by [62]

$$
\begin{aligned}
T(z)T(w) &= \frac{\partial T(w)}{z-w} + \frac{2T(w)}{(z-w)^2} + \frac{c}{2(z-w)^4}, \\
G^a(z)G^{b\dagger}(w) &= \frac{2T(w)\delta_{ab}}{z-w} + \frac{2\bar{\sigma}^i{}_{ab}\partial J^i}{z-w} + \frac{4\bar{\sigma}^i{}_{ab}J^i}{(z-w)^2} + \frac{2c\delta_{ab}}{3(z-w)^3}, \\
J^i(z)J^j(w) &= \frac{i\epsilon^{ijk}J^k}{z-w} + \frac{c}{12(z-w)^2}, \\
T(z)G^a(w) &= \frac{\partial G^a(w)}{z-w} + \frac{3G^a(z)}{2(z-w)^2}, \\
T(z)G^{a\dagger}(w) &= \frac{\partial G^{a\dagger}(w)}{z-w} + \frac{3G^{a\dagger}(z)}{2(z-w)^2}, \\
T(z)J^i(w) &= \frac{\partial J^i(w)}{z-w} + \frac{J^i}{(z-w)^2}, \\
J^i(z)G^a(w) &= \frac{G^b(z)(\sigma^i)^{ba}}{2(z-w)}, \\
J^i(z)G^{a\dagger}(w) &= -\frac{(\sigma^i)^{ab}G^{b\dagger}(w)}{2(z-w)}
\end{aligned}
\tag{3.70}
$$

where c is the central charge, σ's are the Pauli matrices and $\bar{\sigma}$'s are their complex conjugates.

Since each superconformal algebra contains an R-symmetry $SU(2)$, hence we have the global symmetry $SU(2)_L \times SU(2)_R$, whose quantum numbers we denote as

$$
SU(2)_L : \ (j_L, m_L); \qquad SU(2)_R : \ (j_R, m_R). \tag{3.71}
$$

In addition there is a broken $SO(4) \simeq SU(2) \times SU(2)$ symmetry, corresponding to rotations in the four directions of the T^4. We label this symmetry by

$$
SU(2)_1 \times SU(2)_2. \tag{3.72}
$$

We use indices $\alpha, \dot{\alpha}$ for $SU(2)_L$ and $SU(2)_R$ respectively, and indices $A, \dot{A}$ for $SU(2)_1$ and $SU(2)_2$ respectively. The 4 real fermion fields of the left sector are grouped into complex fermions $\psi^{\alpha A}$. The right fermions are grouped into fermions $\bar{\psi}^{\dot{\alpha}A}$. The boson fields X^i

are a vector in T^4 and have no charge under $SU(2)_L$ or $SU(2)_R$, so are grouped as $X_{A\dot{A}}$. Different copies of the $c = 6$ CFT are denoted with a copy label in brackets, e.g.,

$$X^{(1)}\,,\; X^{(2)}\,,\; \cdots\,,\; X^{(n_1 n_5)}\,. \tag{3.73}$$

It will be convenient to describe the states of interest in terms of spectral flow [135]. Under a spectral flow transformation on the left-moving sector with parameter α, the dimensions and charges of states change as follows:

$$h' = h + \alpha m_L + \alpha^2 \frac{c}{24}\,, \qquad m'_L = m_L + \alpha \frac{c}{12}\,. \tag{3.74}$$

An independent spectral flow operation exists in the right-moving sector, with parameter $\bar{\alpha}$.

3.2.2 Twisted Ramond sector ground states

We next briefly review the construction of twist operators and twisted Ramond sector ground states by mapping to a local covering space [134,136]. Let us consider the permutation $(123\ldots k)$. The bare twist operator σ_k corresponding to this permutation imposes the following periodicity conditions on the cylinder:

$$\begin{aligned} &X^{(1)} \to X^{(2)} \to \cdots \to X^{(k)} \to X^{(1)} \\ &\psi^{(1)} \to \psi^{(2)} \to \cdots \to \psi^{(k)} \to \; -\psi^{(1)}. \end{aligned} \tag{3.75}$$

Note that the last sign in the second line above is minus, and is the only physically meaningful sign, as the intermediate signs can be absorbed by field redefinitions[2]. This state is then in the NS sector in the covering space, which we will sometimes refer to simply as the NS sector. A similar expression holds for the right-moving fermions; for ease of

[2]One of the authors (DT) thanks Oleg Lunin for a discussion on this point.

presentation we will write only the left-moving expressions in various places in the following. It is convenient to describe these k twisted copies of the CFT as a 'component string' of length k. One defines the bare twist operator σ_k by mapping first to the plane with coordinate $z = e^w$ and then to a local covering plane with coordinate t via a map of the local form

$$z - z_* \approx b_* \, (t - t_*)^k \,, \tag{3.76}$$

where z_* and t_* are the respective images of w_* in the z plane and the t plane. The k bosonic fields in (3.75) map to one single-valued bosonic field $X(t)$ in the t plane, and similarly for the fermions. In the t plane, one inserts the identity operator at the point t_*, obtaining the lowest-dimension operator in the k-twisted sector. If we take $t_* = 0$, we obtain the NS-NS vacuum in the covering space. We thus refer to it as the "k-twisted NS-NS vacuum", and denote it by $|0_k\rangle^{(r)}_{\text{NS}}$, where r is an index labelling the different component strings. The quantum numbers of this state are

$$h \;=\; \bar{h} \;=\; \frac{1}{4}\left(k - \frac{1}{k}\right) \,, \qquad\qquad m_L \;=\; m_R \;=\; 0 \,. \tag{3.77}$$

We next define an excited (spin-)twist operator σ_k^α as follows. Follow the procedure used to define the bare twist σ_k, but in the covering t plane, insert a spin field[3] S^α at t_*. If we take $t_* = 0$, we obtain the (left-moving) R vacuum $|0_{\text{R}}^\pm\rangle_t$ of the t plane. We write

$$\sigma_k^\alpha = S_k^\alpha \sigma_k \,, \qquad \alpha = +, - \,. \tag{3.78}$$

Back on the original cylinder, with coordinate w, as the fields circle the operator $\sigma_k^\pm$, they transform as

$$X^{(1)} \to X^{(2)} \to \cdots \to X^{(k)} \to X^{(1)}$$

[3] If $b_* \neq 1$ in (3.76), one must also include an appropriate normalization factor [136].

$$\psi^{(1)} \to \psi^{(2)} \to \cdots \to \psi^{(k)} \to +\psi^{(1)}. \tag{3.79}$$

The fields are thus in the Ramond sector in the covering space; as before, we will sometimes refer to this simply as the Ramond sector. We write the corresponding state on the original cylinder (with coordinate w) as $|0_k^{\pm}\rangle_{\rm R}^{(r)}$.

Adding in the right-moving sector, we obtain the full spin-twist field

$$\sigma_k^{\alpha\dot{\alpha}} = S_k^{\alpha}\bar{S}_k^{\dot{\alpha}}\sigma_k \tag{3.80}$$

and we denote the corresponding twisted R-R ground state by $|0_k^{\alpha\dot{\alpha}}\rangle_{\rm R}^{(r)}$.

3.2.3 Non-BPS states generated by general fractional spectral flow

We now consider spectral flow operations in the k-fold covering space. Spectral flow by α_c units in the k-fold covering space corresponds to an effective spectral flow in the base space by an amount [22]

$$\alpha = \frac{\alpha_c}{k}\,. \tag{3.81}$$

On the base space, this may then be described as 'fractional spectral flow'; for previous discussions of fractional spectral flow, see [122, 137, 138].

Using this operation we now describe the general AdS/CFT dictionary for the $k > 1$ JMaRT solutions. All of the states we consider consist of $n_c = N_1N_5/k$ component strings of length k, with each component string in the same state[4]; spectral flow acts simultaneously on all component strings. On a component string of length k, excitations are spaced in units of $1/k$. Fractional spectral flow generates states with filled Fermi seas with this fractional moding, as we will see explicitly shortly.

[4]In this chapter we consider parameters such that n_c is an integer.

Let us first define the reference state from which we will perform the fractional spectral flows. This state has all of its component strings in the k-twisted NS-NS vacuum:

$$|0_k\rangle_{\rm NS} \;=\; |0_k\rangle^{(1)}_{\rm NS} \otimes |0_k\rangle^{(2)}_{\rm NS} \otimes \cdots \otimes |0_k\rangle^{(n_c)}_{\rm NS} \,. \tag{3.82}$$

The quantum numbers of this state are (here $c = 6n_1n_5$ for the full CFT)

$$h \;=\; \bar{h} \;=\; \frac{c}{24}\left(1-\frac{1}{k^2}\right), \qquad m_L \;=\; m_R \;=\; 0\,. \tag{3.83}$$

The AdS dual of this state is the decoupled orbifolded AdS solution (3.35) with $m = n = 0$. The full asymptotically flat JMaRT solitonic solutions exist only when $|m| \neq |n|$ (if one works with $a_1 \geq a_2 \geq 0$, this becomes $m > n \geq 0$), so this solution does not directly come from the decoupling limit of an asymptotically flat JMaRT solution[5].

The states we are interested in are obtained by general fractional spectral flow from $|0_k\rangle_{\rm NS}$. The map to the JMaRT solutions is that the spectral flow parameters are given by

$$\alpha \;=\; \frac{m+n}{k}\,, \qquad \bar{\alpha} \;=\; \frac{m-n}{k}\,. \tag{3.84}$$

Using (3.74), the quantum numbers of the spectral flowed states are

$$h \;=\; \frac{c}{24}\left[1+\frac{(m+n)^2-1}{k^2}\right], \qquad m_L \;=\; \frac{c}{12}\frac{m+n}{k}\,, \tag{3.85}$$

$$\bar{h} \;=\; \frac{c}{24}\left[1+\frac{(m-n)^2-1}{k^2}\right], \qquad m_R \;=\; \frac{c}{12}\frac{m-n}{k}\,. \tag{3.86}$$

Therefore the CFT energy above the R-R ground state and momentum are

$$\Delta E \;=\; \frac{\Delta h + \Delta\bar{h}}{R} \;=\; \frac{n_1 n_5}{R}\frac{m^2+n^2-1}{2k^2}\,, \qquad P \;=\; \frac{h-\bar{h}}{R} \;=\; \frac{n_1n_5}{R}\frac{mn}{k^2}\,. \tag{3.87}$$

Note that in the orbifold CFT, the momentum on each component string must be an integer

[5] It is however related to the other decoupled JMaRT solutions by (fractional) spectral flow coordinate transformations, which do not go to zero at the boundary of AdS.

(see e.g. [139]), so in the orbifold CFT one has $mn/k \in \mathbb{Z}$.

Using the map between CFT and gravity SU(2) quantum numbers,

$$m_\psi \;=\; -(m_L + m_R)\,, \qquad m_\phi \;=\; (m_L - m_R)\,, \tag{3.88}$$

these parameters exactly match those computed on the gravity side in (3.21), (3.36) and (3.37), providing a first check on our proposed identification.

The above states are R-R in the covering space when $m + n$ is odd, and NS-NS in the covering space when $m + n$ is even. Our main interest is in the R-R states; in order to connect with the discussion in [22], let us present the free fermion description of these states, focussing on the states with positive m_L and m_R.

Let us first consider a single component string. Recall that on a component string of length k, excitations are spaced in units of $1/k$. The state on the component string involves Fermi seas filled to a general fractional level s/k in both species of fermions, ψ^{+1} and ψ^{+2}, and similarly to a level $\bar{s}/k$ for the right-movers:

$$\begin{aligned} |\Phi_{s,\bar{s},k}\rangle^{(r)} \;=\; & \Big[(\psi^{+1}_{-\frac{s}{k}}\psi^{+2}_{-\frac{s}{k}})\ldots(\psi^{+1}_{-\frac{2}{k}}\psi^{+2}_{-\frac{2}{k}})(\psi^{+1}_{-\frac{1}{k}}\psi^{+2}_{-\frac{1}{k}})\Big] \\ & \times\Big[(\bar{\psi}^{+1}_{-\frac{\bar{s}}{k}}\bar{\psi}^{+2}_{-\frac{\bar{s}}{k}})\ldots(\bar{\psi}^{+1}_{-\frac{2}{k}}\bar{\psi}^{+2}_{-\frac{2}{k}})(\bar{\psi}^{+1}_{-\frac{1}{k}}\bar{\psi}^{+2}_{-\frac{1}{k}})\Big]|0^{++}_k\rangle^{(r)}_{\mathrm{R}}\,. \end{aligned} \tag{3.89}$$

Then as before the state of the full CFT is obtained by taking all $n_c = N_1 N_5/k$ component strings to be in the same state:

$$|\Psi_{s,\bar{s},k}\rangle \;=\; |\Phi_{s,\bar{s},k}\rangle^{(1)} \otimes |\Phi_{s,\bar{s},k}\rangle^{(2)} \otimes \cdots \otimes |\Phi_{s,\bar{s},k}\rangle^{(n_c)}\,. \tag{3.90}$$

The twisted R-R ground state $|0^{++}_k\rangle^{(r)}_{\mathrm{R}}$ may be obtained from the twisted NS-NS vacuum $|0_k\rangle_{\mathrm{NS}}$ by performing fractional spectral flow with parameters $\alpha = 1/k$, $\bar{\alpha} = 1/k$. The above state $|\Psi_{s,\bar{s},k}\rangle$ is generated by a further fractional spectral flow with parameters $\alpha =$

$2s/k$, $\bar{\alpha} = 2s/k$. So in total, $|\Psi_{s,\bar{s},k}\rangle$ is generated by starting with the state $|0_k\rangle_{\rm NS}$ and performing fractional spectral flow with parameters

$$\alpha = \frac{2s+1}{k}\,, \qquad \bar{\alpha} = \frac{2\bar{s}+1}{k}\,. \tag{3.91}$$

We then have the relations

$$m+n = 2s+1\,, \qquad m-n = 2\bar{s}+1\,. \tag{3.92}$$

The NS-NS states obtained for even $m+n$ have analogous Fermi sea representations, built on the twisted NS-NS vacuum $|0_k\rangle_{\rm NS}$.

We now return to our main discussion. For general k, m, n, we have observed the agreement of conserved charges above. As was noted in [22] in the BPS case however, generically these states are degenerate and so further evidence is required to support the identification. In principle, one could compute the one-point functions of operators following [109], however the states we are considering are R-charge eigenstates, and therefore all one-point functions of R-charged operators vanish [109]. Instead, we provide further evidence for our proposed identification by matching the scalar excitation spectrum between gravity and CFT.

3.2.4 Emission spectrum and emission rates from CFT

The vertex operator for emission (or absorption) of a minimal scalar of angular momentum l has the following form [121]. It involves a chiral primary in the twisted sector of degree $(l+1)$, $\tilde{\sigma}_{l+1}$, dressed with fermion and supercurrent excitations $G^{+\dot{A}}_{-\frac{1}{2}}\psi^{-A}_{-\frac{1}{2}}\bar{G}^{+\dot{B}}_{-\frac{1}{2}}\bar{\psi}^{-B}_{-\frac{1}{2}}$ which add the T^4 polarization indices, and further dressed with powers of SU(2) current zero modes J_0, $\bar{J}_0$ which fill out the SU(2) representation. There is also a non-trivial normalization factor; the explicit form can be found in [121].

Since the vertex operator involves a twisted chiral primary $\tilde{\sigma}_{l+1}$, when it acts on a state it introduces new fractionated degrees of freedom. It is thus capable of lowering the energy of the state, with the remainder energy being carried away by the emitted particle.

Our initial state (3.89) is composed of component strings which are all of length k. In the limit of a large number of component strings, $n_c = n_1 n_5/k \gg 1$, the process which dominates is that in which $\tilde{\sigma}_{l+1}$ acts on $l+1$ distinct component strings, combining them into a component string of length $k(l+1)$. There is a family of resulting final states labelled by left- and right-moving excitation numbers N_L, N_R, which correspond to acting with the Virasoro generators L_{-1}, $\bar{L}_{-1}$ in the form $L_{-1}^{N_L}\bar{L}_{-1}^{N_R}$ on the final state of lowest possible energy.

This CFT amplitude, corresponding to emission of a minimal scalar, can be mapped to a technically simpler amplitude by spectral flow and hermitian conjugation. This technique has been employed in the special case of excited R-R states arising from integer spectral flow of the state $|0_k^{++}\rangle_{\rm R}$, i.e., when s and $\bar{s}$ are multiples of k. This was first done for $k=1$ in [121] and then for $k>1$ in [122]. For the $k>1$ case, the calculation involved mapping the amplitude to a covering space, and using the method of [136, 140][6]. In each case one observes a Bose enhancement effect: the probability for emission of the $\mathbf{N}^{\rm th}$ quantum is $\mathbf{N}$ times the probability for emission of the first quantum [118]. Since the CFT is a symmetric product orbifold, one must also take care of various combinatorial factors in computing the amplitude.

Having proposed the identification of the general orbifolded JMaRT solutions with the general fractional spectral flowed CFT states, we can now make a straightforward generalization of the results of [122] to fractional spectral flowed CFT states. We do this by simply taking the emission spectrum, expressed in terms of α, $\bar{\alpha}$, and substituting the values appropriate for the general fractional spectral flowed states that we study. This technique works because all of the states under consideration are fractional spectral flows

[6]For a recent application of this method in a different context, see [134, 141].

of the twisted NS-NS vacuum $|0_k\rangle_{\rm NS}$.

The emission spectrum computed in [122] for the integer spectral flowed $k > 1$ JMaRT states, translated into our conventions[7], is

$$\begin{aligned}
\omega &= \frac{1}{kR}\left[\frac{1}{2}\alpha k(m_\phi - m_\psi) - \frac{1}{2}\bar{\alpha}k(m_\phi + m_\psi) - (l + 2 + N_L + N_R)\right], \\
\lambda &= \frac{1}{kR}\left[\frac{1}{2}\alpha k(m_\phi - m_\psi) + \frac{1}{2}\bar{\alpha}k(m_\phi + m_\psi) + N_R - N_L\right].
\end{aligned} \qquad (3.93)$$

We now generalize this by substituting the parameters appropriate to fractional spectral flow from the twisted NS vacuum $|0_k\rangle_{\rm NS}$,

$$\alpha = \frac{m+n}{k}, \qquad \bar{\alpha} = \frac{m-n}{k}, \qquad (3.94)$$

which yields the spectrum

$$\begin{aligned}
\omega &= \frac{1}{kR}\left[-m_\psi m + m_\phi n - (l + 2 + N_L + N_R)\right] \\
\lambda &= \frac{1}{k}\left[m_\phi m - m_\psi n + N_R - N_L\right].
\end{aligned} \qquad (3.95)$$

Now, generalizing the discussion in [118], note that $\zeta = (N_L - N_R)/k$. If $\zeta > 0$, may be written as

$$\omega = \frac{1}{kR}\left[-l - m_\psi m + m_\phi n - 2 - k\zeta - 2N_R\right] \qquad (3.96)$$

and if $\zeta < 0$, may be written as

$$\omega = \frac{1}{kR}\left[-l - m_\psi m + m_\phi n - 2 + k\zeta - 2N_L\right]. \qquad (3.97)$$

[7] The map between conventions is given in Appendix A.3.

In either case, has the form

$$\omega = \frac{1}{kR}\Big(-l - m_\psi m + m_\phi n - \big|-k\lambda - m_\psi n + m_\phi m\big| - 2(N+1)\Big) \tag{3.98}$$

for some $N \geq 0$, which exactly matches the real part of the instability frequencies computed from the gravity side, given in Eq. (3.68).

The CFT emission rate computed in [122] for the $\mathbf{N}^{\text{th}}$ particle, writing $\delta(\omega;\lambda)$ as a schematic delta function which imposes that ω and λ must take their specific allowed values, in our conventions takes the form

$$\frac{d\Gamma}{d\omega} \;=\; \mathbf{N}\frac{1}{kR}\frac{2\pi}{2^{2l+1}(l!)^2}\left[\left(\omega^2 - \frac{\lambda^2}{R^2}\right)\frac{Q_1 Q_5}{k^2R^2}\right]^{l+1}\binom{N_L+l+1}{l+1}\binom{N_R+l+1}{l+1}\delta(\omega;\lambda)\,. \tag{3.99}$$

In this form, the expression for the emission rate immediately generalizes to the present situation of fractional spectral flowed states, with the allowed frequencies and wavelengths given in (3.95).

Treating separately the cases for $\zeta > 0$ and $\zeta < 0$ as above, one finds

$$\binom{N_L+l+1}{l+1}\binom{N_R+l+1}{l+1} \;=\; \binom{N+l+1}{l+1}\binom{N+k|\zeta|+l+1}{l+1}. \tag{3.100}$$

The imaginary part of the frequency ω_I is given by 1/2 the value of the emission rate for the first quantum, as discussed in [118]. Thus we have

$$\omega_I \;\simeq\; \frac{1}{kR}\frac{\pi}{2^{2l+1}(l!)^2}\left[\left(\omega^2 - \frac{\lambda^2}{R^2}\right)\frac{Q_1 Q_5}{k^2R^2}\right]^{l+1}\binom{N+l+1}{l+1}\binom{N+k|\zeta|+l+1}{l+1}, \tag{3.101}$$

in exact agreement with the value (3.69) obtained from the gravity calculation.

Relation to previous work

We pause here to comment on the relation of our results to previous literature.

The class of states generated by (3.84) is the general set of R-R and NS-NS states obtained by fractional spectral flow from the twisted NS-NS vacuum $|0_k\rangle_{\rm NS}$. Various special cases of this class of CFT states have been studied previously in the literature, as we now describe. For BPS states, the two-charge states ($k \in \mathbb{Z}^+, m = 1, n = 0$) were studied in [115]. The three-charge family ($k = 1$; $s \in \mathbb{Z}$; $\bar{s} = 0$) was studied in [98]. The family ($k \in \mathbb{Z}^+$; $s = nk, n \in \mathbb{Z}$; $\bar{s} = 0$) was studied in [100]. Such values of s correspond to integer spectral flow of the states $|0_k^{\alpha\dot{\alpha}}\rangle_{\rm R}$. The general BPS family obtained from fractional spectral flow, ($k \in \mathbb{Z}^+$ $s \in \mathbb{Z}$; $\bar{s} = 0$) was studied in [22].

For non-BPS states, the CFT states obtained by setting $k = 1$ in (3.82)–(3.84) were proposed to be the dual CFT states of the $k = 1$ JMaRT solutions in the original paper [3] and the CFT emission was studied in [118, 121]. The two-charge family ($k \in \mathbb{Z}^+$; $s = \bar{s} = \hat{n}k, \hat{n} \in \mathbb{Z}$) was studied in [120]. The family ($k \in \mathbb{Z}^+$; $s = \hat{n}k, \hat{n} \in \mathbb{Z}$; $\bar{s} = \bar{n}k, \bar{n} \in \mathbb{Z}$) was studied in [122]. Again, such values of $s, \bar{s}$ correspond to integer spectral flow of the states $|0_k^{\alpha\dot{\alpha}}\rangle_{\rm R}$.

The general non-BPS family of R-R and NS-NS states arising from fractional spectral flow of $|0_k\rangle_{\rm NS}$ (or $|0_k^{\alpha\dot{\alpha}}\rangle_{\rm R}$) is the subject of the present work.

Regarding the wave equation calculation on the gravity side, for $k = 1$ the instability was first derived in [117], and was revisited in slightly different forms in [118, 119]. The two-charge case with $k > 1$ was studied in [120]. In the present work we have analyzed the general three-charge case with arbitrary k, m, n.

3.3 Ergoregion emission as pair creation

Having demonstrated that the general class of orbifolded JMaRT solutions decay via an ergoregion instability, with emission spectrum and emission rate in agreement with the dual CFT, we now examine more explicitly some features of the produced radiation. In particular we investigate the physical picture of ergoregion emission as pair creation [123, 124].

The ergoregion contains negative energy excitations as measured by the Killing vector that generates time translations at spatial infinity. The pair creation picture involves a positive energy excitation that escapes to infinity and a negative energy excitation that remains in the ergoregion. The two excitations also carry equal and opposite values of other conserved charges.

For two-charge, $k = 1$ JMaRT solutions, this picture was investigated in [119] for the simplest form of the probe scalar wavefunction. It was shown that to a good approximation, the radiation from these solutions can be split into two distinct parts. One part escapes to infinity and the other remains deep inside in the AdS region. The two parts carry equal and opposite energy and angular momentum. For large angular momenta, when the wavefunctions can be thought of as approximately localized, it was argued that the inner region part has its main support in the ergoregion.

In this section we generalize this discussion to include three non-zero charges, two non-zero angular momenta, the orbifolding parameter k, and the most general form of the wavefunction. We start with a summary of the solutions of the scalar wave equation in Section 3.3.1. We then compute the contributions to angular momenta (Section 3.3.2) and energy (Section 3.3.3) from the inner and asymptotic regions due to the scalar perturbation.

3.3.1 Solutions of the wave equation

In order to calculate the contributions to conserved charges from the inner and asymptotic regions (which are defined in Appendix A.1), we need the explicit form of the wavefunctions in these regions. We work exclusively in the large R limit, as only in this limit is there a clear separation between the inner and asymptotic regions.

Let us start by relating the different radial coordinates so that we can easily change from one to the other. The coordinate transformation (3.26) upon using (3.20) and (3.30) is simply

$$\rho^2 = \frac{R^2}{Q_1 Q_5}(r^2 - r_+^2)\,. \tag{3.102}$$

In terms of the dimensionless radial variable x used in Section 3.1.4, this relation is $x = \rho^2$.

The metric in the inner region is (3.35), and from (A.6) the wavefunction in the inner region is

$$\Psi_{\rm in} = \exp\left[-i\omega t + i\frac{\lambda}{R}y + im_\psi\psi + im_\phi\phi\right]\chi(\theta)\left(\rho^2 + \frac{1}{k^2}\right)^{\frac{k\xi}{2}}\rho^{k|\zeta|}\left[{}_2F_1(a,b,c,-k^2\rho^2)\right], \tag{3.103}$$

where

$$a \;=\; \frac{1}{2}(1+\nu+k|\zeta|+k\xi), \qquad b \;=\; \frac{1}{2}(1-\nu+k|\zeta|+k\xi), \qquad c \;=\; 1+k|\zeta| \tag{3.104}$$

with ξ, ζ, ν defined in (4.43), (3.61), (3.64). Recall also from (3.65), (3.66) that to leading order in ϵ we have

$$\nu \;\simeq\; l+1, \qquad\qquad 1+\nu+k|\zeta|+k\xi \;\simeq\; -2N. \tag{3.105}$$

For small ρ, we have $\Psi_{\rm in} \sim \rho^{k|\zeta|}$, and for large ρ, using (A.8) and (3.105) we have

$\Psi_{\rm in} \sim \rho^{-(l+2)}$. The norm of the wavefunction is

$$(\Psi\Psi^*)_{\rm in} = \rho^{2k|\zeta|}\left(\rho^2 + \frac{1}{k^2}\right)^{k\xi} |\chi(\theta)|^2 e^{2\omega_I t}\Big({}_2F_1(-N, -N-l-1, 1+k|\zeta|, -k^2\rho^2)\Big)^2 , \quad (3.106)$$

where as before ω_I is the imaginary part of the frequency ω.

In the asymptotic region the metric is flat spacetime to leading order. Using the asymptotic region wavefunction (A.12) together with the requirement of only outgoing waves (A.15), in terms of a normalization constant C_2 and the quantity κ defined in (B.26), the wavefunction is

$$\Psi_{\rm out} = C_2 \exp\left[-i\omega t + im_\psi\psi + im_\phi\phi + i\frac{\lambda}{R}y\right]\chi(\theta)\frac{1}{\sqrt{2\pi\kappa}}\frac{1}{\rho^{\frac{3}{2}}}e^{i\kappa\rho}e^{-i\frac{\pi}{4}}\left(e^{i\frac{\pi\nu}{2}} - e^{-i\frac{3\pi\nu}{2}}\right). \quad (3.107)$$

Therefore the norm of the wavefunction is

$$(\Psi\Psi^*)_{\rm out} = |C_2|^2|\chi(\theta)|^2 e^{2\omega_I t}\frac{2}{\pi|\kappa|}\frac{1}{\rho^3}e^{i(\kappa-\kappa^*)\rho}\sin^2(\pi\nu)\,. \quad (3.108)$$

We next fix the normalization of Ψ in the asymptotic region given its form in the inner region. This is done in detail in Appendix A.2. For our purposes we do not need an expression for C_2 itself, but only its norm. From (A.35) we have

$$|C_2|^2\sin^2(\pi\nu) = \frac{\pi}{2}k^{4N+2\nu}(kR)\omega_I\,\frac{\Gamma(1+k|\zeta|)^2\,\Gamma(N+1)\,\Gamma(N+\nu+1)}{\Gamma(N+\nu+1+k|\zeta|)\,\Gamma(N+1+k|\zeta|)}\,, \quad (3.109)$$

where ω_I takes the value given in (3.69). Finally we note that in the asymptotic region $\rho^2 \simeq \frac{R^2}{Q_1Q_5}r^2$, and as a result the exponent in (3.108) can be written as

$$i(\kappa-\kappa^*)\rho \simeq -\frac{2\omega_R\omega_I}{\sqrt{\omega_R^2 - \frac{\lambda^2}{R^2}}}r\,, \quad (3.110)$$

where as before ω_R is the real part of the frequency ω and takes the value given in (3.68). In the neck region, the exponent (3.110) is very small, $|(\kappa-\kappa^*)\rho| \sim \omega_I(Q_1Q_5)^{1/4} \sim \epsilon^{4l+5}$.

3.3.2 Angular momenta of the perturbation

The general JMaRT solution has four Killing vectors, namely $\partial_t, \partial_y, \partial_\phi, \partial_\psi$. In general the geometries carry angular momentum in both ϕ and ψ directions and momentum in the y direction. As in the previous sections, we consider scalar perturbations that also carry all these charges. The conserved quantities for the scalar perturbation associated to the two angular momenta are

$$L_\psi = \int T_\psi{}^\nu dS_\nu, \qquad L_\phi = \int T_\psi{}^\nu dS_\nu, \tag{3.111}$$

where $T_\mu{}^\nu$ is the energy momentum tensor of the (complex) scalar field,

$$T_{\mu\nu} = \partial_\mu \Psi \partial_\nu \Psi^* + \partial_\nu \Psi \partial_\mu \Psi^* - g_{\mu\nu} \partial_\alpha \Psi \partial^\alpha \Psi^*. \tag{3.112}$$

The integrals in (3.111) extend over a spacelike hypersurface in the spacetime. We choose the surface to be simply given by t = constant. It was shown in reference [3] that $g^{tt} < 0$ everywhere, therefore the t = constant surface is everywhere spacelike.

Substituting the separation ansatz (3.52) in (3.112), we find the following expressions for angular momenta of the scalar perturbation,

$$L_\psi = 2m_\psi \int \sqrt{-g} dr d\mathcal{A} \left(-g^{tt}\omega_R + g^{t\psi} m_\psi + g^{t\phi} m_\phi + g^{ty} \frac{\lambda}{R} \right) \Psi \Psi^*, \tag{3.113}$$

$$L_\phi = 2m_\phi \int \sqrt{-g} dr d\mathcal{A} \left(-g^{tt}\omega_R + g^{t\psi} m_\psi + g^{t\phi} m_\phi + g^{ty} \frac{\lambda}{R} \right) \Psi \Psi^*, \tag{3.114}$$

where $d\mathcal{A} = d\theta d\psi d\phi dy$. Note that the integrals involved in computing L_ψ and L_ϕ are the same. For this reason we focus on L_ψ; the discussion for L_ϕ is entirely analogous.

In the asymptotic region the metric is flat spacetime to leading order. We have $\sqrt{-g} = r^3 \cos\theta \sin\theta$. There are no cross terms in the metric, so the integral (3.113) simply becomes

$$(L_\psi)_{\rm out} = 2m_\psi\omega_R\int_{\rm out} drd\mathcal{A}(r^3\cos\theta\sin\theta)(\Psi\Psi^*)_{\rm out},$$
$$= 4\pi m_\psi\omega_R R C e^{2\omega_I t}\int_{\rm out} dr(r^3 h(r)h(r)^*)_{\rm out}, \qquad (3.115)$$

where $C = \int_{S^3} d\theta d\phi d\psi \cos\theta\sin\theta|\chi(\theta)|^2$. Using relations (3.108) and (3.110) expression (3.115) becomes

$$(L_\psi)_{\rm out} = \frac{8Q_1Q_5 m_\psi\omega_R C}{R\sqrt{\omega_R^2-\frac{\lambda^2}{R^2}}}e^{2\omega_I t}|C_2|^2\sin^2(\pi\nu)\int_{(Q_1Q_5)^{\frac{1}{4}}}^{\infty} dr\exp\left(-\frac{2\omega_R\omega_I}{\sqrt{\omega_R^2-\frac{\lambda^2}{R^2}}}r\right)(3.116)$$

To leading order in the large R limit this integral gives

$$(L_\psi)_{\rm out} \simeq 2\pi m_\psi Q_1Q_5 C e^{2\omega_I t}k^{4N+2l+3}\frac{\Gamma(1+k|\zeta|)^2\,\Gamma(N+1)\,\Gamma(N+l+2)}{\Gamma(N+k|\zeta|+l+2)\,\Gamma(N+k|\zeta|+1)}, \qquad (3.117)$$

where we have used the normalization (3.109). This is our final expression for the angular momentum L_ψ of the scalar perturbation that flows off to infinity. For $N=0$, $k=1$, and $|\zeta|=0$ this expression reduces to the corresponding expression of reference [119].

Exactly the same expression but with opposite sign is obtained from the inner region. Using the coordinate definitions (3.102) and (3.25), and the metric in the inner region (3.35), the integral (3.113) in the inner region becomes

$$(L_\psi)_{\rm in} = 2m_\psi Q_1Q_5\left(\omega_R R+\frac{m}{k}m_\psi-\frac{n}{k}m_\phi\right)\int_0^{1/\epsilon}\rho d\rho\int d\mathcal{A}\cos\theta\sin\theta\left(\rho^2+\frac{1}{k^2}\right)^{-1}(\Psi\Psi^*)_{\rm in}.$$

Substituting the norm (3.106) of the inner region wavefunction, we observe that the integrand falls off in the large ρ limit as ρ^{-2l-5}. Thus to leading order in ϵ we can set the upper limit of the ρ integration to infinity. Thus we obtain

$$\begin{aligned}(L_\psi)_{\rm in} &\simeq 4\pi m_\psi Q_1 Q_5 C e^{2\omega_I t}\left(\omega_R R + \frac{m}{k}m_\psi - \frac{n}{k}m_\phi\right)\times \\ &\int_0^\infty d\rho\rho^{2k|\zeta|+1}\left(\rho^2+\frac{1}{k^2}\right)^{k\xi-1}\left({}_2F_1(-N,-N-l-1,1+k|\zeta|,-k^2\rho^2)\right)^2.\end{aligned}$$

Making the substitution $\tilde{\rho} = k\rho$ and using the integer relations (3.105), this expression can be converted to the form

$$\begin{aligned}(L_\psi)_{\rm in} &\simeq 4\pi m_\psi Q_1 Q_5 C e^{2\omega_I t}\left(\omega_R R + \frac{m}{k}m_\psi - \frac{n}{k}m_\phi\right)k^{4N+2l+4}\times \\ &\int_0^\infty d\tilde{\rho}\tilde{\rho}^{2k|\zeta|+1}\left(\tilde{\rho}^2+1\right)^{-2N-l-k|\zeta|-3}\left({}_2F_1(-N,-N-l-1,1+k|\zeta|,-\tilde{\rho}^2)\right)^2.\end{aligned}$$

This integral can be calculated using the hypergeometric function identity (A.36). We get

$$\begin{aligned}(L_\psi)_{\rm in} &\simeq 4\pi m_\psi Q_1 Q_5 C e^{2\omega_I t}\left(\omega_R R + \frac{m}{k}m_\psi - \frac{n}{k}m_\phi\right)k^{4N+2l+4}\times \\ &\frac{1}{2(2N+k|\zeta|+l+2)}\frac{\Gamma(1+k|\zeta|)^2\,\Gamma(N+1)\,\Gamma(N+l+2)}{\Gamma(N+k|\zeta|+l+2)\,\Gamma(N+k|\zeta|+1)}.\end{aligned} \tag{3.118}$$

Using the definition of ξ from (4.43) and the integer relations (3.105), we obtain a contribution that is exactly the opposite of (3.117),

$$(L_\psi)_{\rm in} \simeq -2\pi m_\psi Q_1 Q_5 C e^{2\omega_I t}k^{4N+2l+3}\frac{\Gamma(1+k|\zeta|)^2\,\Gamma(N+1)\,\Gamma(N+l+2)}{\Gamma(N+k|\zeta|+l+2)\,\Gamma(N+k|\zeta|+1)}. \tag{3.119}$$

At a technical level the analysis presented above is significantly more involved compared to that of [119], however various technical pieces precisely fit together to give exactly equal and opposite contributions to L_ψ (and hence L_ϕ) from the inner and asymptotic regions.

3.3.3 Energy and linear momentum of the perturbation

A similar set of considerations applies to energy and linear momentum along y. Let us start with linear momentum along y. The conserved linear momentum associated to the scalar perturbation is

$$P_y = \int_{t=\text{const}} \sqrt{-g} dr d\mathcal{A}\, T^t{}_y. \tag{3.120}$$

Using the separation ansatz (3.52) in the scalar stress tensor (3.112), the linear momentum expression reduces to

$$P_y = \frac{2\lambda}{R} \int \sqrt{-g} dr d\mathcal{A} \left(-g^{tt}\omega_R + g^{t\psi} m_\psi + g^{t\phi} m_\phi + g^{ty} \frac{\lambda}{R} \right) \Psi\Psi^*. \tag{3.121}$$

Since the integral involved is exactly what we discussed above, it follows that the inner and asymptotic region wavefunctions give equal and opposite contributions to the linear momentum.

The conserved energy of the scalar field Ψ is

$$H = -\int_{t=\text{const}} \sqrt{-g} dr d\mathcal{A}\, T^t{}_t\,. \tag{3.122}$$

It is convenient to write this expression as a part which involves the integral already computed for the angular momentum, plus a remainder which is a total derivative [119]. We denote these as the bulk and boundary terms respectively,

$$H = H_{\text{bulk}} + H_{\text{bdy}}\,, \tag{3.123}$$

where

$$H_{\text{bulk}} = -\int \sqrt{-g} dr d\mathcal{A} \left[g^{tt} \partial_t \Psi \partial_t \Psi^* \right] - \frac{1}{2} \int dr d\mathcal{A} \left[\Psi \partial_i \left(\sqrt{-g} g^{ij} \partial_j \Psi^* \right) + \Psi^* \partial_i \left(\sqrt{-g} g^{ij} \partial_j \Psi \right) \right],$$

$$H_{\rm bdy} = \frac{1}{2}\int dr d\mathcal{A}\, \partial_i \Big[\sqrt{-g} g^{ij} \partial_j (\Psi\Psi^*)\Big]. \tag{3.124}$$

Using the equation of motion for the scalar $\partial_\mu(\sqrt{-g}\partial^\mu\Psi) = 0$ and the ansatz (3.52), the bulk term simplifies to

$$H_{\rm bulk} = -2\omega_R \int \sqrt{-g} dr d\mathcal{A} \Big(g^{tt}\omega_R - g^{t\phi}m_\phi - g^{t\psi}m_\psi - g^{ty}\frac{\lambda}{R}\Big)\Psi\Psi^* . \tag{3.125}$$

We now apply the decomposition into $H_{\rm bulk}$ and $H_{\rm bdy}$ separately in the inner and asymptotic regions. For this purpose, we approximate both the outer boundary of the inner region and the inner boundary of the outer region by the surface $r = (Q_1Q_5)^{\frac{1}{4}}$. Since the integral involved in $H_{\rm bulk}$ is exactly the one discussed above, it follows that the inner and asymptotic region wavefunctions give equal and opposite contributions to $H_{\rm bulk}$. We need only be concerned with the boundary terms. The only non-zero boundary terms arise from the terms with radial derivatives. We have

$$H^{\rm in}_{\rm bdy} = \frac{1}{2}\int d\mathcal{A} \Big[\sqrt{-g} g^{rr}\partial_r(\Psi\Psi^*)\Big]\Bigg|_{r=r_+}^{r=(Q_1Q_5)^{\frac{1}{4}}} = H^{\rm in,neck}_{\rm bdy} + H^{{\rm in},r=r_+}_{\rm bdy}, \tag{3.126}$$

$$H^{\rm out}_{\rm bdy} = \frac{1}{2}\int d\mathcal{A} \Big[\sqrt{-g} g^{rr}\partial_r(\Psi\Psi^*)\Big]\Bigg|_{r=(Q_1Q_5)^{\frac{1}{4}}}^{r=\infty} = H^{{\rm out},r=\infty}_{\rm bdy} + H^{\rm out,neck}_{\rm bdy}. \tag{3.127}$$

We observe that

$$H^{\rm in,neck}_{\rm bdy} = -H^{\rm out,neck}_{\rm bdy}. \tag{3.128}$$

Let us now estimate the various boundary terms. Firstly, for $H^{{\rm in},r=r_+}_{\rm bdy}$, counting powers of ρ we see that as $\rho \to 0$,

$$\sqrt{-g} g^{rr}\partial_r(\Psi\Psi^*) = \sqrt{-g}\left[g^{\rho\rho}\left(\frac{dr}{d\rho}\right)\partial_\rho(\Psi\Psi^*)\right] \sim \rho^2\partial_\rho(\Psi\Psi^*) \sim \rho^{2k|\zeta|+1}, \tag{3.129}$$

which vanishes at $\rho = 0$ (i.e. at $r = r_+$) and so we have $H^{{\rm in},r=r_+}_{\rm bdy} = 0$.

Next, for $H^{{\rm out},r=\infty}_{\rm bdy}$ we observe that $\Psi\Psi^*$ falls off exponentially with exponent (3.110) in the $r \to \infty$ limit. Therefore, in the limit $r \to \infty$ it also vanishes.

Since we have observed in (3.128) that the neck terms are equal and opposite, it is not necessary to evaluate them to conclude that the contribution to the energy from the asymptotic region and the inner region are equal and opposite. Nevertheless, out of interest we now observe that these terms are parametrically subleading with respect to the contributions from H_{bulk}.

At the neck, we have $\rho \sim \epsilon^{-1}$, so for $H^{\text{in,neck}}_{\text{bdy}}$ we find the parametric dependence

$$\begin{aligned} H^{\text{in,neck}}_{\text{bdy}} &\sim R\sqrt{-g}\left[g^{\rho\rho}\left(\frac{dr}{d\rho}\right)\partial_\rho(\Psi\Psi^*)\right]\Bigg|_{\rho=1/\epsilon} \\ &\sim R\,(Q_1Q_5)^{\frac{3}{4}}\cdot\frac{\rho^2}{(Q_1Q_5)^{\frac{1}{2}}}\cdot\frac{\rho}{(Q_1Q_5)^{\frac{1}{4}}}\frac{Q_1Q_5}{R^2}\cdot\partial_\rho\rho^{-2l-4}\Bigg|_{\rho=1/\epsilon} \sim (Q_1Q_5)^{\frac{3}{4}}\epsilon^{2l+3}\,, \end{aligned} \tag{3.130}$$

and therefore $H^{\text{in,neck}}_{\text{bdy}}$ is subleading with respect to $H^{\text{in}}_{\text{bulk}}$.

Again it is not necessary to separately estimate $H^{\text{out,neck}}_{\text{bdy}}$, however it is straightforward to observe that as a result of the matching of solutions at the neck, the asymptotic region wavefunction also behaves as ρ^{-l-2} in the neck, and with the same coefficient as the inner solution, giving precisely (3.130).

To summarize, we have seen explicitly that the inner and asymptotic region wavefunctions give equal and opposite contributions to the conserved angular momenta, linear momentum along y and energy of the scalar field. Since the inner part of the wavefunction carries negative energy with respect to the Killing vector ∂_t, it has its main support in the ergoregion. One can also see this fact explicitly by plotting a selection of examples. Thus we see explicitly in this setup the physical picture of ergoregion emission as pair creation.

3.4 Discussion

In this chapter we have proposed the holographic description of the general family of orbifolded JMaRT solutions, with orbifolding parameter k. The $k > 1$ states are of significant physical interest since states with larger k are closer to typical states than states with smaller k. We have proposed that the dual CFT states are the general set of R-R and NS-NS states obtained by fractional spectral flow in both left- and right-moving sectors from the twisted NS-NS vacuum $|0_k\rangle_{\text{NS}}$. We reviewed the fact that the orbifolded JMaRT solutions are completely smooth when the integer parameters m, n, and k have no common divisors, and presented a full analysis of the orbifold singularities which arise depending on the common divisors between these parameters.

To support our proposed identification, we matched the minimal scalar emission spectrum and emission rate between gravity and CFT. On the gravity side, this involved solving the wave equation on the general orbifolded solution, generalizing previous studies [117,120]. On the CFT side, our results were obtained via a straightforward generalization of the results of [122].

We also investigated the physical picture of ergoregion emission as pair creation, generalizing the results of [119] to include three non-zero charges, two non-zero angular momenta, the orbifolding parameter k, and the most general form of the probe scalar wavefunction. We showed that radiation from the general orbifolded JMaRT solutions can be split into two distinct parts, one escaping to infinity and the other remaining deep inside the AdS region. Since the inner part of the wavefunction carries negative energy with respect to the Killing vector ∂_t which generates time translations at spatial infinity, it has its main support in the ergoregion.

The states we have studied are non-BPS, and there is no known non-renormalization theorem protecting the quantities we have studied. Thus the fact that the orbifold CFT and gravity calculations agree exactly is quite non-trivial and better than might have been naively expected of the orbifold CFT. Naturally, the agreement observed in the $k = 1$ solutions was reason for optimism on this point. The fact that our proposed dual states are related to BPS states by fractional spectral flow may perhaps be the feature which enables this non-trivial agreement.

It would be interesting to study string theory in the subset of these backgrounds that have orbifold singularities. String theory on orbifolds of $AdS_3 \times S^3$ has previously been studied in [137, 138]. In the presence of orbifold singularities, twisted sectors of closed strings typically give rise to light (or tachyonic) degrees of freedom that are not taken into account by supergravity [142]. Furthermore, non-supersymmetric orbifolds are expected to decay to a region of smooth spacetime together with an expanding pulse of excitations [145,146] (see also [147,148]). If such a mechanism is present here, one can ask whether it interacts with the pair creation mechanism; for example one might imagine that the pair creation excitation that remains deep in the cap might interact with the orbifold and/or its decay products.

Indeed one might wonder whether such additional modes could affect the matching of emission frequencies and rates between the supergravity and CFT for the solutions with orbifold singularities. We did not find any such discrepancy; the calculations agree exactly between gravity and CFT regardless of the presence or absence of orbifold singularities. This strongly suggests that the ergoregion emission spectrum and rates are unaffected by such light degrees of freedom. It would be interesting to investigate this physics in more detail in the future.

Chapter 4

Geroch group description of black holes

In this chapter we consider black holes of five-dimensional vacuum gravity and four-dimensional Einstein-Maxwell theory and study them from the Geroch group perspective. We restrict our attention to three examples: (*i*) dyonic Kaluza-Klein black hole [149, 150], (*ii*) dyonic Kerr-Newman black hole, and (*iii*) five-dimensional doubly spinning Myers-Perry black hole [151]. Using these three examples we exhibit the construction of Geroch group matrices. We obtain Geroch group $SL(3,\mathbb{R})$ matrices for the Myers-Perry and Kaluza-Klein black holes and an $SU(2,1)$ matrix for the Kerr-Newman black hole. Along the way, we also present certain non-trivial relations between the Geroch group matrices and the corresponding charge matrices.

The motivation for studying these issues is manifold. Apart from identifying the precise Geroch group matrices for certain black holes, the examples worked out in this chapter teach us more about the inverse scattering method recently proposed in [6, 152]. The method proposed there is based on the Geroch group and it requires one to factorize Geroch group matrices in a certain way. In this chapter we factorize the matrices for the examples mentioned in the previous paragraph. Our present study brings in two new elements: (*i*) we extend the factorization algorithm developed there to incorporate five-dimensional asymptotically flat boundary conditions, (*ii*) we present a fairly non-trivial example involving the group SU(2, 1) of the general factorization algorithm presented there.

The rest of the chapter is organized as follows. In section 4.1 we start with a brief review of dimensional reduction to two dimensions, focusing on details that are most relevant for the rest of the chapter. In section 4.2 we present a simple and quite general recipe for computing the Geroch group matrix for a spacetime specified through a three-dimensional coset representative. In section 4.3 we present certain general results on the Geroch group matrices and in section 4.4 we present explicit examples for the black holes mentioned above. We close with a summary and a brief discussion of open problems in section 4.5. Certain technical details regarding $SL(3,\mathbb{R})$ and SU(2, 1) coset models are given in appendix B.1. The appendix is an important part of the chapter.

4.1 Preliminaries: dimensional reduction to two dimensions

In this section we present a brief review of dimensional reduction to two dimensions. We closely follow the notation and discussion of [5, 6, 78, 152].

We perform dimensional reduction of a higher-dimensional gravity theory to two dimensions in two steps. In the first step we reduce the theory to three-dimensions and in the second step we reduce it from three to two dimensions. We work with gravity matter systems that have some global symmetry G and some local symmetry K in three dimensions. K is a maximal subgroup of G. A general element k of the subgroup K satisfies $k^\sharp k = 1$, where hash ($\sharp$) is the anti-involution that defines the coset G/K. Let $V(x)$ be a coset representative of G/K. We use x to collectively denote the three coordinates of the three-dimensional space. The symmetries act on $V(x)$ as

$$V(x) \to k(x)V(x)g, \tag{4.1}$$

with a global $g \in \mathrm{G}$ and a local $k \in \mathrm{K}$. A more convenient object to work with is, see, e.g. [153],

$$M(x) = V^{\sharp}(x)V(x), \tag{4.2}$$

with symmetries acting on $M(x)$ as[1]

$$M(x) \to g^{\sharp}M(x)g. \tag{4.3}$$

We next consider dimensional reduction over a spacelike Killing vector to two dimensions. In order to do so we write the three-dimensional metric as

$$ds_3^2 = f^2(d\rho^2 + dz^2) + \rho^2 d\varphi^2. \tag{4.4}$$

These coordinates are called the Weyl canonical coordinates. The Killing vector ∂_φ allows us to reduce the theory from three to two dimensions. The function f multiplying the flat two-dimensional base metric $(d\rho^2 + dz^2)$ is called the conformal factor. The resulting two-dimensional gravitational system upon dimensional reduction along φ direction is integrable, meaning that there exist a Lax pair whose compatibility condition is exactly the equations of the two-dimensional gravitational system. The quantity that one solves for in the Lax equations depends on a spectral parameter. There are several Lax formulations that one can write for the two-dimensional gravitational system of interest. In this chapter we will exclusively work with the Breitenlohner-Maison (BM) Lax pair [5, 78]. It takes the following form in the notation of [6, 152]

$$\partial_m \mathcal{V}\mathcal{V}^{-1} = Q_m + \frac{1-t^2}{1+t^2}P_m - \frac{2t}{1+t^2}\epsilon_{mn}P^n. \tag{4.5}$$

Here (i) we use the notation $x^m = (\rho, z)$ and from now onwards use x to collectively denote the two-dimensional coordinates, (ii) the Lax equations require us to consider the

[1]Following standard references, see e.g., [153], we use the notation $\mathrm{G/K}$ instead of $\mathrm{K\backslash G}$ even though we define the coset element $V(x)$ using a left action of K in equation (4.1).

generalization $V(x) \to \mathcal{V}(t,x)$, a quantity that depends on the spectral parameter t with the property $\mathcal{V}(0,x) = V(x)$, (iii) P_m and Q_m are respectively the symmetric and anti-symmetric parts of the Lie algebra element $\partial_m V V^{-1} = P_m + Q_m$, $P_m^\sharp = P_m$ and $Q_m^\sharp = -Q_m$.

The integrability condition for equations (4.5) is equivalent to the equations of the motion of the two-dimensional gravitational system if and only if the spectral parameter satisfies certain spacetime dependent differential equation. That differential equation can be integrated to give

$$t_\pm(w,x) = \frac{1}{\rho}\left[(z-w) \pm \sqrt{(z-w)^2+\rho^2}\right] = -\frac{1}{t_\mp}(w,x). \tag{4.6}$$

The parameter w is an integration constant and we will refer it to as the spacetime independent spectral parameter. Equation (4.6) defines a two-sheeted Riemann surface over the two-dimensional base space. We take the positive sign in (4.6) as the physical sheet. Whenever we write t we mean t_+.

The anti-involution extends to functions $\mathcal{V}(t,x)$ as

$$(\mathcal{V}(t,x))^\sharp = \mathcal{V}^\sharp\left(-\frac{1}{t}, x\right). \tag{4.7}$$

Similar to $M(x) = V^\sharp(x)V(x)$, we can construct the so-called monodromy matrix,

$$\mathcal{M}(t,x) = \mathcal{V}^\sharp\left(-\frac{1}{t}, x\right)\mathcal{V}(t,x). \tag{4.8}$$

A priori it appears that the matrix $\mathcal{M}(t,x)$ is spacetime dependent, however, remarkably, using the Lax equations, one can show that $\mathcal{M}(t,x)$ is spacetime *independent* [5, 78]:

$$\mathcal{M}(t,x) = \mathcal{M}(w). \tag{4.9}$$

It only depends on the spacetime independent spectral parameter w. We call the monodromy matrix $\mathcal{M}(w)$ the Geroch group matrix corresponding to the spacetime configuration described by $V(x)$. Thus, the Geroch group allows one to associate a spacetime independent matrix to a spacetime configuration that effectively depends on only two coordinates.

4.2 Relation between $M(x)$ and $\mathcal{M}(w)$

The discussion of the previous section in principle allows one to associate a Geroch group matrix $\mathcal{M}(w)$ to an arbitrary spacetime configuration described by $V(x)$. However, in order to do that one must first solve for $\mathcal{V}(t,x)$ via the Lax equation (4.5). This step may not be always easy. Fortunately, one can arrive at a simple and quite general relation between the matrices $M(x)$ and $\mathcal{M}(w)$. This relation allows one to construct $\mathcal{M}(w)$ rather directly from $M(x)$. In the following we first present this relation and then present a derivation of it.

Consider the two-dimensional space spanned by the canonical coordinates (ρ, z). In the literature this space is sometimes known as the factor space. In reference [154] Hollands and Yazadjiev studied the global structure of the factor space. They showed that for spacetimes containing non-extremal horizons, the corresponding factor space is a manifold possessing a connected boundary with corners. The boundary is at $\rho = 0$ and consists of a union of intervals. The intervals either correspond to the horizon(s) or to the fixed points of the rotational Killing vectors. The corners are the points where two adjacent intervals meet. We consider the cases where we can draw a semicircle of sufficiently large radius R in the (ρ, z) half-plane, such that all corners are inside this semicircle. With these assumptions the relation between $M(x)$ and $\mathcal{M}(w)$ is simply

$$M(\rho = 0, z = w \;\text{ with }\; z < -R) = \mathcal{M}(w). \tag{4.10}$$

In this rest of this section we present a derivation of equation (4.10) following [5].

Let us start by noting that the spacetime independent spectral parameter w in general can take complex values. However, in order to relate to the discussion of the previous paragraph, in particular for the replacement $z = w$ in equation (4.10) to make sense, we must take it to be real. It turns out that the discussion below is better presented by taking w to be complex to start with and taking the limit $\textbf{Im}(w) \to 0$ towards the end.

The functions $t_\pm$ defined via equation (4.6) considered as functions of complex w have two branch points at $\rho = \pm\textbf{Im}(w), z = \textbf{Re}(w)$. At these branch points

$$t_\pm\Big|_{\rho=\textbf{Im}(w),\, z=\textbf{Re}(w)} = -i \qquad\qquad t_\pm\Big|_{\rho=-\textbf{Im}(w),\, z=\textbf{Re}(w)} = +i. \tag{4.11}$$

Note in particular that at the branch points $t_\pm$ take the same values and are consistently related by $t_\pm \to -\frac{1}{t_\mp}$ relation.

As mentioned above, for most of the consideration we take t to mean t_+, i.e., when we write $\mathcal{V}(t,\rho,z)$ we mean $\mathcal{V}(t_+,\rho,z)$. However, for the discussion below we need to be more careful about the two-sheets of the Riemann surface defined by (4.6), so we introduce one more notation

$$\mathcal{V}_\pm(w,\rho,z) = \mathcal{V}(t_\pm(w,\rho,z),\rho,z). \tag{4.12}$$

Let us now concentrate on the region $\rho \to 0$ and $z < -R$. In this region $t_+ \to 0$ and $t_- \to \infty$, as a result the Lax equations (4.5) in this region simplify to

$$\partial\mathcal{V}_+\mathcal{V}_+^{-1} = \partial V V^{-1}, \qquad\qquad \partial\mathcal{V}_-\mathcal{V}_-^{-1} = -(\partial V V^{-1})^\sharp. \tag{4.13}$$

These equations have simple solutions with the required property for $\mathcal{V}_+$,

$$\mathcal{V}_+(w,0,z) = V(0,z), \tag{4.14}$$

$$\mathcal{V}_-(w,0,z) = (V^\sharp(0,z))^{-1}C(w), \tag{4.15}$$

for some constant matrix $C(w)$. Since $t_\pm$ have the same values at the branch points, it follows that the functions $\mathcal{V}(t_\pm(w,\rho,z),\rho,z)$ also have the same values at the branch points, i.e.,

$$\mathcal{V}_+(w,\rho,z)\Big|_{\rho=\mathbf{Im}(w),\, z=\mathbf{Re}(w),} = \mathcal{V}_-(w,\rho,z)\Big|_{\rho=\mathbf{Im}(w),\, z=\mathbf{Re}(w)}. \tag{4.16}$$

In the limit $\mathbf{Im}(w) \to 0$, this implies

$$\mathcal{V}_+(w,0,w) = \mathcal{V}_-(w,0,w). \tag{4.17}$$

Using relations (4.14) and (4.15) in (4.17) we thus have

$$V(0,w) = (V^\sharp(0,w))^{-1}C(w). \tag{4.18}$$

Therefore,

$$\begin{aligned} C(w) &= V^\sharp(0,w)V(0,w) && (4.19)\\ &= M(0,w). && (4.20)\end{aligned}$$

Hence it follows that

$$\begin{aligned} \mathcal{M}(w) &= \mathcal{V}_-^\sharp(w,0,z)\mathcal{V}_+(w,0,z), && (4.21)\\ &= \left((V^\sharp(0,z))^{-1}M(0,w)\right)^\sharp V(0,z), && (4.22)\\ &= M(0,w). && (4.23)\end{aligned}$$

This is precisely equation (4.10). To summarise, one can calculate the Geroch group matrix corresponding to an axisymmetric stationary space-time configuration by simply evaluating the matrix $M(x)$ in canonical coordinates at $\rho = 0$ and $z = w$ with $z < -R$. This is the recipe we use in the later sections to study Geroch group description of black holes.

4.3 Geroch group matrices: general considerations

In reference [6] Riemann-Hilbert factorization for SL(2) Geroch Group matrices was studied. This was later generalized to other groups, in particular to the case of SO(4,4) relevant for the so-called STU supergravity, in reference [152]. In both these studies attention was focused on four-dimensional asymptotically flat boundary conditions. In this chapter, among other things, we generalize those studies to incorporate five-dimensional asymptotically flat boundary conditions. These boundary conditions bring in some minor changes to the factorization algorithm developed in [6, 152]. For simplicity, in this section we restrict our attention to SL(3,$\mathbb{R}$) — hidden symmetry group of vacuum five-dimensional gravity.

4.3.1 Boundary conditions

In an interesting paper [155] Giusto and Saxena pointed out that if dimensional reduction of five-dimensional Minkowski space is done over appropriately chosen Killing vectors then the asymptotic limit of the coset matrix $M(x)$ is a constant matrix Y. The Y matrix is different from the identity matrix. They also identified an SO(2,1) subgroup of SL(3) that leaves the constant matrix Y invariant. It follows that all five-dimensional asymptotically flat solutions can be dimensionally reduced to three dimensions in a manner that asymptotically $M(x)$ is the constant matrix Y. Using these inputs, in this chapter we explore SL(3) Geroch group matrices and their factorization, where they asymptote to the constant matrix Y different from the identity. As in [6, 152] we restrict our attention to the so-called soliton sector. A general such matrix is of the form

$$\mathcal{M}(w) = Y + \sum_{k=1}^{N} \frac{A_k}{w - w_k}, \qquad A_k = \alpha_k a_k a_k^{\sharp}. \tag{4.24}$$

In particular, we allow for only simple poles in w, and we take the rank of the residues at these poles to be one. The residue matrices are $(\sharp)$−symmetric: $A_k^{\sharp} = A_k$. We expect that this choice includes several solutions of physical interest. As we will see in the following, it certainly includes the rotating Myers-Perry black hole.

The ($\sharp$)−operation on vectors a_k is defined as $a_k^\sharp = a_k^T \eta$, where η is the quadratic form preserved by the denominator SO(2,1) subgroup of the coset SL(3)/SO(2,1). In the following we focus our attention to the case when the dimensional reduction from five to three dimensions is done first over a spacelike direction and then over a timelike direction. In that case it follows from equation (B.11) of appendix B.1 that

$$\eta = \mathrm{diag}\{1, -1, 1\}. \tag{4.25}$$

Furthermore, we restrict ourselves to the cases where the inverse of $\mathcal{M}(w)$ also has poles at the same locations as $\mathcal{M}(w)$ with residues of rank-one. We parameterize this matrix as

$$\mathcal{M}(w)^{-1} = Y^{-1} - \sum_{k=1}^{N} \frac{B_k}{w - w_k}, \qquad B_k = \beta_k \eta b_k b_k^T. \tag{4.26}$$

For later convenience we have put minus signs in front of the residues and we have put the η matrix in the residues on the left hand side. B_k matrices are also ($\sharp$)−symmetric: $B_k^\sharp = B_k$.

To find the explicit form of the matrix Y we follow the steps of Giusto and Saxena. For five-dimensional Minkowski space in coordinates

$$ds^2 = -dt^2 + dr^2 + r^2(d\theta^2 + \sin^2\theta d\phi^2 + \cos^2\theta d\psi^2), \tag{4.27}$$

we define new coordinates

$$\phi_+ = \ell(\psi + \phi), \tag{4.28}$$

$$\phi_- = (\psi - \phi), \tag{4.29}$$

where ℓ is some arbitrary length scale. Upon Kaluza-Klein reduction first along ϕ_+ and then along t the resulting matrix $M(x)$ takes the form

$$M(x) = \begin{pmatrix} \frac{4\ell^2}{r^2} & 1 & 0 \\ -1 & 0 & 0 \\ 0 & 0 & 1 \end{pmatrix}, \tag{4.30}$$

and the three-dimensional base metric takes the form

$$ds_3^2 = \frac{r^2}{4\ell^2}\left(dr^2 + r^2 d\theta^2 + r^2 \sin^2\theta \cos^2\theta d\phi_-^2\right). \tag{4.31}$$

Clearly, the matrix $M(x)$ asymptote to a constant matrix

$$M(x) = Y + O\left(\frac{1}{r^2}\right), \qquad \text{with} \qquad Y = \begin{pmatrix} 0 & 1 & 0 \\ -1 & 0 & 0 \\ 0 & 0 & 1 \end{pmatrix}. \tag{4.32}$$

The Y matrix is symmetric under generalized transposition $Y^\sharp = Y$.

In the rest of this section we briefly present the changes Y matrix brings in to the factorization algorithm of [6, 152]. Having specified the ansatz for $\mathcal{M}(w)$ and $\mathcal{M}^{-1}(w)$, we express $\frac{1}{w-w_k}$ in terms of the spacetime dependent spectral parameter t:

$$\frac{1}{w - w_k} = \nu_k\left(\frac{t_k}{t - t_k} + \frac{1}{1 + t t_k}\right), \qquad \text{where} \qquad \nu_k = -\frac{2t_k}{\rho\left(1 + t_k^2\right)}, \tag{4.33}$$

and where the poles t_k are determined by equation (4.6) evaluated at $w = w_k$ with the plus sign, $t_k = t_+(w = w_k)$. We wish to factorize $\mathcal{M}(w)$ as

$$\mathcal{M}(w) = A_-^\sharp(t,x) M(x) A_+(t,x), \tag{4.34}$$

with $A_-(t,x) = A_+\left(-\frac{1}{t}, x\right)$ and $M^\sharp(x) = M(x)$. We make an ansatz for $A_+(t)$ and $A_+^{-1}(t)$

$$A_+(t) = \mathbf{I} - \sum_{k=1}^{N} \frac{t c_k a_k^T \eta}{1 + t t_k}, \tag{4.35}$$

$$A_+^{-1}(t) = \mathbf{I} + \sum_{k=1}^{N} \frac{t \eta b_k d_k^T}{1 + t t_k}. \tag{4.36}$$

and study the pole structure of the various matrix products to determine the vectors c_k and d_k. This part of the analysis proceeds exactly as in [6, 152], so we do not repeat it here. We present the results as a recipe.

The vectors a_k and b_k must satisfy $a_k^T \eta b_k = 0$ for all k. The vectors c_k and d_k are determined from a_k and b_k by the matrix equations

$$c\Gamma = \eta b \tag{4.37}$$

$$\Gamma d = \eta a \tag{4.38}$$

where the matrix Γ_{kl} is

$$\Gamma_{kl} = \begin{cases} \frac{\gamma_k}{t_k} & \text{for} \quad k = l \\ \frac{1}{t_k - t_l} a_k^T b_l & \text{for} \quad k \neq l. \end{cases} \tag{4.39}$$

The parameters γ_k appearing in the Γ-matrix are determined by solving the equations

$$a_k^T \eta \mathcal{A}^k = \gamma_k \nu_k \beta_k b_k^T \qquad \text{and} \qquad \mathcal{A}_k \eta b_k = \gamma_k \alpha_k \nu_k a_k, \tag{4.40}$$

with the definitions

$$\mathcal{A}^k = \left[\mathcal{M}^{-1}(t,x) + \frac{\nu_k \eta \beta_k b_k b_k^T}{1 + t t_k}\right]_{t=-\frac{1}{t_k}}, \qquad \mathcal{A}_k = \left[\mathcal{M}(t,x) - \frac{\nu_k \alpha_k a_k a_k^T \eta}{1 + t t_k}\right]_{t=-\frac{1}{t_k}}. \tag{4.41}$$

Now taking the limit $w \to \infty$ in (4.34) we find $Y = M(x)A_+(\infty, x)$, i.e,

$$M(x) = YA_+^{-1}(\infty, x) = Y + Yt_k^{-1}\eta b_k(\Gamma^{-1})_{kl}a_l^T\eta. \tag{4.42}$$

4.3.2 Two-soliton matrices

So far we have only presented the general form of $\mathcal{M}(w)$ and $\mathcal{M}(w)^{-1}$ matrices. For arbitrary choices of the residue vectors a_k, b_k and the parameters α_k, β_k, these matrices do not belong to the group SL(3). The idea of using parameters α_k and β_k is that by tuning them appropriately, various coset constraints can be imposed. In the case when there are only two poles in $\mathcal{M}(w)$, it is relatively straightforward to take the coset constraints into account [77].

Let us choose the location of these poles to be $w_1 = +c$ and $w_2 = -c$. Let us take the components of the residue vectors a_1 and a_2 to be arbitrary. We introduce the notation $a = (a_1 \;\; a_2)$ where a_1 and a_2 are put as column vectors in a 3×2 matrix a. Next consider the 2×2 matrix

$$\xi = a^T\eta Y^{-1}a = \begin{pmatrix} a_1^T\eta Y^{-1}a_1 & a_1^T\eta Y^{-1}a_2 \\ a_2^T\eta Y^{-1}a_1 & a_2^T\eta Y^{-1}a_2 \end{pmatrix}. \tag{4.43}$$

We note that since Y is symmetric under generalized transposition, the matrix ηY^{-1} is symmetric under the usual matrix transposition

$$(\eta Y^{-1})^T = \eta Y^{-1}. \tag{4.44}$$

As a result the matrix ξ defined in equation (4.43) is a symmetric matrix. This crucial property allows us to choose $\alpha_1, \alpha_2, \beta_1, \beta_2$ and b_1, b_2 vectors in such a way that all coset constraints are satisfied:

$$\alpha_1 = \frac{2c}{\det \xi}\xi_{22}, \qquad \alpha_2 = -\frac{2c}{\det \xi}\xi_{11}, \tag{4.45}$$

$$\beta_1 = -\frac{1}{\det \xi}\alpha_1, \qquad \beta_2 = -\frac{1}{\det \xi}\alpha_2, \tag{4.46}$$

and

$$b = (\det \xi)\eta Y^{-1} a \xi^{-1} \epsilon, \qquad \epsilon = \begin{pmatrix} 0 & -1 \\ 1 & 0 \end{pmatrix}. \tag{4.47}$$

By construction b is a 3×2 matrix whose columns are b_1 and b_2 vectors respectively. Of course there is an ambiguity in the normalization of these vectors. We have made a convenient choice in writing the above equations. Note that

$$a^T b = (\det \xi)\epsilon. \tag{4.48}$$

4.4 Geroch group matrices for black holes: examples

In this section we give explicit expressions for Geroch group matrices for a class of black hole examples. This section should be read in conjunction with appendix B.1.

4.4.1 Dyonic Kaluza-Klein

Our first example is the dyonic Kaluza-Klein black hole [149, 150]. The Kaluza-Klein black hole is conveniently written in terms of four parameters q, p, m, a. These parameters respectively correspond to electric and magnetic Kaluza-Klein charges, mass, and angular momentum. For the discussion below we use exactly the form of the solution as given in reference [156] (in appendix A.1), except we use a instead of α ($a_{\text{here}} = \alpha_{\text{there}}$) and x instead of the polar angle θ on the two-sphere. The two are simply related by $x = \cos\theta$.

Using those expressions we construct three-dimensional scalars and from there the matrix $M(x)$. Expressions for the scalars and matrix $M(x)$ are somewhat lengthy, but after certain amount of manipulations, can be written in the following simpler form

$$M(x) = g^{\sharp} M_{\text{Kerr}}(x) g, \tag{4.49}$$

where

$$g = \frac{1}{2\sqrt{2}m} \begin{pmatrix} \sqrt{\frac{p(p+2m)(q+2m)}{p+q}} & \sqrt{(p-2m)(q+2m)} & -\sqrt{\frac{q(p-2m)(q-2m)}{p+q}} \\ 2\sqrt{\frac{q(p^2-4m^2)}{p+q}} & \sqrt{2pq} & -2\sqrt{\frac{p(q^2-4m^2)}{p+q}} \\ -\sqrt{\frac{p(p-2m)(q-2m)}{p+q}} & -\sqrt{(q-2m)(p+2m)} & \sqrt{\frac{p(p+2m)(q+2m)}{p+q}} \end{pmatrix}, \tag{4.50}$$

with $g^{\sharp} = g^{-1}$, and where $M_{\text{Kerr}}(x)$ is the matrix $M(x)$ for the Kerr solution,

$$M_{\text{Kerr}}(x) = \begin{pmatrix} 1 + \frac{2mr}{r^2-2mr+a^2x^2} & 0 & -\frac{2amx}{r^2-2mr+a^2x^2} \\ 0 & 1 & 0 \\ -\frac{2amx}{r^2-2mr+a^2x^2} & 0 & 1 + \frac{2m(2m-r)}{r^2-2mr+a^2x^2} \end{pmatrix}. \tag{4.51}$$

The first thing to note from the above expressions is the fact that the matrix $M(x)$ in equation (4.49) for the rotating dyonic black hole is written as an action of an appropriate group element on the corresponding matrix for the Kerr solution $M_{\text{Kerr}}(x)$. In fact, this is how the dyonic Kaluza-Klein black holes were constructed in the first place [149, 150]. Expression for the group element g in terms of Lie algebra generators (B.12) belonging to the denominator subgroup SO(2,1) is as follows

$$g = \exp(-\gamma k_3) \cdot \exp(-\beta k_1) \cdot \exp(\alpha k_2). \tag{4.52}$$

In this group element the generator (αk_2) generates KK magnetic charge and the generator $(-\beta k_1)$ generates KK electric charge. The generator $(-\gamma k_3)$ generates the four-dimensional Lorentzian NUT charge. The necessity of acting with the generator $(-\gamma k_3)$ lies in the fact that the group element $\exp(-\beta k_1) \cdot \exp(\alpha k_2)$ in addition to generating KK electric and magnetic charges also generates a four-dimensional NUT charge. The final NUT charge can be cancelled by appropriately tuning these parameters. To achieve this cancellation, we first use the relation

$$\tan 2\gamma = \tanh\alpha \sinh\beta, \tag{4.53}$$

and then the following somewhat unwieldy relations to write the group element in the form (4.50)

$$\cos\gamma = \frac{\sqrt{p+2m}\sqrt{q+2m}}{\sqrt{2}\sqrt{pq+4m^2}}, \qquad \coth\beta = \sqrt{\frac{q}{p}}\sqrt{\frac{pq+4m^2}{q^2-4m^2}}. \tag{4.54}$$

In order to obtain the Geroch group matrix corresponding to the above matrix $M(x)$ we need to introduce the canonical coordinates. Examining the determinant of the metric components on the Killing directions we get the canonical coordinates,

$$\rho^2 = (r^2 + a^2 - 2mr)(1 - x^2), \qquad z = (r - m)x. \tag{4.55}$$

Using these relations we can in principle write the matrix $M(x)$ in the canonical form, however, it is easier to first introduce the prolate spherical coordinates [157]

$$c^2(u^2-1)(1-v^2) = (r^2 + a^2 - 2mr)(1 - x^2), \quad cuv = (r - m)x, \quad c = \sqrt{m^2 - a^2}. \tag{4.56}$$

These relations can be solved to give $u = \frac{1}{c}(r - m), v = x$. The transformation from the prolate spherical coordinates (u, v) to the canonical coordinates is

$$u = \frac{\sqrt{\rho^2 + (z + c)^2} + \sqrt{\rho^2 + (z - c)^2}}{2c}, \qquad v = \frac{\sqrt{\rho^2 + (z + c)^2} - \sqrt{\rho^2 + (z - c)^2}}{2c}. \tag{4.57}$$

Given these expressions it is easy to see that the limit $\rho \to 0$ and taking z near $-\infty$ amounts to the replacement $u \to -\frac{z}{c}$ and $v \to -1$, equivalently $r \to -z + m$ and $x \to -1$. Making these replacements in the matrix $M(x)$ we find the monodromy matrix $\mathcal{M}(w)$. It takes the form

$$\mathcal{M}(w) = \mathbf{I} + \frac{A_1}{w-c} + \frac{A_2}{w+c}, \tag{4.58}$$

where $A_1 = \alpha_1 a_1 a_1^\sharp$, $A_2 = \alpha_2 a_2 a_2^\sharp$. The vectors a_1 and a_2 for the dyonic black hole are

$$a_1 = g^\sharp a_1^{\text{Kerr}}, \qquad a_1^{\text{Kerr}} = \{\zeta, 0, 1\}, \tag{4.59}$$

$$a_2 = g^\sharp a_2^{\text{Kerr}}, \qquad a_2^{\text{Kerr}} = \{1, 0, \zeta\}, \tag{4.60}$$

and the parameters α_1 and α_2 are

$$\alpha_1 = \frac{2c(1+\zeta^2)}{(1-\zeta^2)^2}, \qquad \alpha_2 = -\frac{2c(1+\zeta^2)}{(1-\zeta^2)^2}. \tag{4.61}$$

where $\zeta = \frac{m-c}{a}$. The $a \to 0$ limit is perfectly smooth: in this limit $c \to m$ and $\zeta \to 0$.

The Riemann-Hilbert factorization of the monodromy matrix (4.58) give the dyonic Kaluza-Klein black hole, as expected. This factorization is similar to the examples considered in [6, 152], so we skip the details.

We now write some relations between the vectors obtained above, the charge matrix for KK black hole, and the monodromy matrix. We concentrate on the Kerr black hole — for the dyonic KK black hole the corresponding relations are simply obtained by conjugation with g. The charge matrix $\mathcal{Q}$ for a four-dimensional asymptotically flat configuration is defined as [69]:

$$M(x) = \mathbf{I} - \frac{\mathcal{Q}}{r} + O\left(\frac{1}{r^2}\right). \tag{4.62}$$

In our normalization we have

$$\mathcal{Q} = -2mh_2, \tag{4.63}$$

where h_2 is the Cartan generator defined in (B.7). The charge matrix (4.63) satisfies the characteristic equation

$$\mathcal{Q}^3 - \frac{1}{2}\text{Tr}(\mathcal{Q}^2)\mathcal{Q} = 0, \tag{4.64}$$

with $\mathrm{Tr}(Q^2) = 8m^2$. The asymptotic form of the matrix $\mathcal{M}(w)$ is also determined by the charge matrix

$$\mathcal{M}(w) = \mathbf{I} + \frac{Q}{w} + O\left(\frac{1}{w^2}\right). \tag{4.65}$$

Hence, it follows that

$$Q = \sum_{i=1}^{2} \alpha_i a_i^{\mathrm{Kerr}} (a_i^{\mathrm{Kerr}})^{\sharp}. \tag{4.66}$$

We want to emphasize that relation (4.66) is in fact quite general. For the present case only two poles are present in the Geroch group matrix so the sum in (4.66) runs over only two values of the indices. When the Geroch group matrix has N poles, the charge matrix is simply the sum of the residues at the poles.

The charge matrix as defined above does not capture information about the angular momentum of the spacetime. To encode that we can introduce one more matrix (see also [158] for a related construction)[2]

$$\mathcal{A} = 2a(e_3 - e_3^{\sharp}), \tag{4.67}$$

where a is the Kerr rotation parameter and e_3 is one of the raising generators defined in (B.7). This matrix allows us to write some useful relations. Firstly, we observe that it anticommutes with the charge matrix,

$$\{Q, \mathcal{A}\} = 0. \tag{4.68}$$

Secondly, using this matrix we can write yet another characteristic equation that captures rotation properties also

$$(Q + \mathcal{A})^3 - \frac{1}{2}\mathrm{Tr}\left((Q + \mathcal{A})^2\right)(Q + \mathcal{A}) = 0, \tag{4.69}$$

with $\mathrm{Tr}\left((Q + \mathcal{A})^2\right) = 8(m^2 - a^2)$. Finally, we can write the full Geroch matrix solely in

[2]We thank Guillaume Bossard for discussions on these ideas.

terms of the Q and $\mathcal{A}$ matrices

$$\mathcal{M}(w) = \mathbf{I} + \frac{1}{w^2 - c^2}\left(wQ + \frac{1}{2}Q^2 - \frac{1}{4}[Q, \mathcal{A}]\right). \tag{4.70}$$

Note that although the matrix $\mathcal{A}$ belongs to the invariant $\mathfrak{so}(2,1)$ subalgebra, only the commutator $[Q, \mathcal{A}]$, which belongs to the complement of $\mathfrak{so}(2,1)$ in $\mathfrak{sl}(3,\mathbb{R})$ enters the Geroch group matrix (4.70).

4.4.2 Dyonic Kerr-Newman

In this section we explore dyonic Kerr-Newman black hole as a solution of four-dimensional Einstein-Maxwell theory from the Geroch group perspective. It is well known that the symmetry group of the dimensionally reduced Einstein-Maxwell theory is SU(2,1) [159]. For the case of the timelike reduction to three-dimensions the relevant coset is

$$\frac{\mathrm{SU}(2,1)}{\mathrm{SL}(2,\mathbb{R}) \times \mathrm{U}(1)}. \tag{4.71}$$

A detailed construction of the coset model is presented in appendix B.1.2.

The metric and vector for dyonic Kerr-Newman black hole are given in Boyer-Lindquist coordinates as

$$\begin{aligned} ds^2 &= -\frac{\Delta - a^2 \sin^2\theta}{\Sigma} dt^2 - 2a\left(\frac{r^2 + a^2 - \Delta}{\Sigma}\right)\sin^2\theta dt d\phi + \frac{\Sigma}{\Delta}dr^2 + \Sigma d\theta^2 \\ &\quad + \left(\frac{(r^2 + a^2)^2 - \Delta a^2 \sin^2\theta}{\Sigma}\right)\sin^2\theta d\phi^2 \qquad (4.72) \\ A &= \frac{1}{\Sigma}\left[-qr + ap\cos\theta\right] dt + \frac{1}{\Sigma}\left[-p\cos\theta(r^2 + a^2) + aqr\sin^2\theta\right] d\phi \qquad (4.73) \end{aligned}$$

where

$$\Sigma = r^2 + a^2 \cos^2\theta, \tag{4.74}$$

$$\Delta = r^2 + a^2 + q^2 + p^2 - 2mr. \tag{4.75}$$

The configuration is parameterized by four parameters: mass parameter m, rotation parameter a, and electric and magnetic charges q and p respectively. For computational convenience we use $x = \cos\theta$ instead of the azimuthal angle θ for the rest of the discussion. The four coset scalars take the form (for precise definition of these scalars we refer the reader to appendix B.1.2)

$$e^{\phi} = \frac{\Sigma}{\Sigma + p^2 + q^2 - 2mr}, \quad \psi = \frac{\sqrt{2}amx}{\Sigma}, \quad \chi_e = -\frac{qr - apx}{\Sigma}, \quad \chi_m = -\frac{pr + aqx}{\Sigma}, \tag{4.76}$$

and as a result the matrix $M(x)$ is

$$M(x) = \frac{1}{r^2 + a^2x^2 + p^2 + q^2 - 2mr} \times \tag{4.77}$$
$$\begin{pmatrix} r^2 + a^2x^2 & -\sqrt{2}(ip+q)(r+iax) & p^2+q^2+2iamx \\ \sqrt{2}(q-ip)(r-iax) & -p^2-q^2+r^2+a^2x^2-2mr & \sqrt{2}(q-ip)(2m-r+iax) \\ p^2+q^2-2iamx & \sqrt{2}(ip+q)(-2m+r+iax) & (r-2m)^2+a^2x^2 \end{pmatrix}.$$

It is not difficult to verify that this matrix belongs to the coset (4.71). For this, we need to check that the matrix belongs to the group SU(2, 1) and that it is symmetric under the appropriate generalized transposition. The SU(2, 1) property and the generalized transposition are respectively defined in (B.26) and (B.30) in the appendix. Indeed, both the conditions are satisfied.

Once again, we use relation (4.10) to find the Geroch group matrix. For this we first need to determine the canonical coordinates. By examining the determinant of the metric components on the Killing directions we get the canonical coordinates,

$$\rho^2 = \Delta(1 - x^2), \qquad z = (r - m)x. \tag{4.78}$$

Using these relations one can in principle write the matrix $M(x)$ in the canonical coordinates, however, as before, it is useful to first write the matrix in the prolate spherical coordinates

$$u = \frac{1}{c}(r - m), \qquad v = x, \qquad c = \sqrt{m^2 - a^2 - p^2 - q^2}, \tag{4.79}$$

and then convert to the canonical coordinates. After doing the appropriate replacements in $M(x)$ we find

$$\mathcal{M}(w) = \frac{1}{(w^2 - c^2)} \times \tag{4.80}$$
$$\begin{pmatrix} a^2 + (m-w)^2 & -\sqrt{2}(p-iq)(a+i(m-w)) & p^2+q^2-2iam \\ \sqrt{2}(p+iq)(a-i(m-w)) & a^2-m^2-p^2-q^2+w^2 & -\sqrt{2}(p+iq)(a+i(m+w)) \\ p^2+q^2+2iam & \sqrt{2}(p-iq)(a-i(m+w)) & a^2+(m+w)^2 \end{pmatrix}.$$

This spacetime independent matrix is sufficient to determine the full Kerr-Newman configuration. Since the Riemann-Hilbert factorization for this example is a little different from the examples previously discussed in the literature, we present certain details.

To write expressions in a less cumbersome manner we need to introduce some additional notation. We parameterize charges as

$$m = \mu\cosh 2\beta, \qquad q = \mu\sinh 2\beta\cos b, \qquad p = \mu\sinh 2\beta\sin b, \tag{4.81}$$

and choose vectors a_1 and a_2 as

$$a_1 = g a_1^{\text{Kerr}}, \qquad a_1^{\text{Kerr}} = \left\{-\frac{ia}{c+\mu}, 0, 1\right\}, \tag{4.82}$$
$$a_2 = g a_2^{\text{Kerr}}, \qquad a_2^{\text{Kerr}} = \left\{1, 0, \frac{ia}{c+\mu}\right\}, \tag{4.83}$$

where

$$g = e^{\frac{ib}{3}} \begin{pmatrix} c_\beta^2 & \sqrt{2} s_\beta c_\beta & s_\beta^2 \\ \sqrt{2} e^{-ib} s_\beta c_\beta & e^{-ib}(2c_\beta^2 - 1) & \sqrt{2} e^{-ib} s_\beta c_\beta \\ s_\beta^2 & \sqrt{2} s_\beta c_\beta & c_\beta^2 \end{pmatrix}. \tag{4.84}$$

In terms of these vectors, the matrix $\mathcal{M}(w)$ in equation (4.80) can be written in a more recognizable form

$$\mathcal{M}(w) = \mathbf{I} + \frac{A_1}{w - c} + \frac{A_2}{w + c}, \tag{4.85}$$

with

$$A_k = \alpha_k a_k a_k^\sharp = \alpha_k a_k a_k^\dagger \eta, \tag{4.86}$$

and

$$\alpha_1 = \mu\left(1 + \frac{\mu}{c}\right), \qquad \alpha_2 = -\mu\left(1 + \frac{\mu}{c}\right). \tag{4.87}$$

The inverse matrix is parameterized as[3]

$$\mathcal{M}(w)^{-1} = \kappa^{-1} \mathcal{M}^\dagger(w) \kappa = \mathbf{I} - \frac{B_1}{w - c} - \frac{B_2}{w + c}, \tag{4.88}$$

with

$$B_k = (-\alpha_k)(\kappa \eta a_k)(\kappa \eta a_k)^\sharp. \tag{4.89}$$

We note that $\kappa^{-1} = \kappa$ and $\kappa\eta = \eta\kappa$. Now all expressions are in the notation of [152] and the factorization proceeds exactly as discussed there. Following those steps we recover the coset matrix of equation (4.77).

In this case one can also construct an $\mathcal{A}$ matrix that anticommutes with the charge matrix Q and satisfies (4.69) and (4.70).

[3] The matrix κ defines the SU(2, 1) property, see equation (B.26).

4.4.3 Five-dimensional Myers-Perry

The metric components of the doubly rotating Myers-Perry (MP) black hole in our conventions are

$$g_{rr} = \frac{\Sigma r^2}{(r^2+l_1^2)(r^2+l_2^2)-2mr^2}, \qquad g_{xx} = \frac{\Sigma}{1-x^2}, \tag{4.90}$$

$$g_{tt} = -\frac{\Sigma-2m}{\Sigma}, \qquad g_{\psi\phi} = \frac{2ml_1l_2x^2(1-x^2)}{\Sigma}, \tag{4.91}$$

$$g_{t\phi} = -\frac{2ml_1(1-x^2)}{\Sigma}, \qquad g_{t\psi} = -\frac{2ml_2x^2}{\Sigma}, \tag{4.92}$$

$$g_{\phi\phi} = \frac{1-x^2}{\Sigma}\left((r^2+l_1^2)\Sigma+2ml_1^2(1-x^2)\right), \qquad g_{\psi\psi} = \frac{x^2}{\Sigma}\left((r^2+l_2^2)\Sigma+2ml_2^2x^2\right), \tag{4.93}$$

where

$$\Sigma = r^2+l_1^2x^2+l_2^2(1-x^2). \tag{4.94}$$

As in the previous examples, for computational convenience we use $x = \cos\theta$ instead of the polar angle θ. Variables m, l_1, and l_2 are the mass and the two rotation parameters respectively.

For reasons mentioned in section 4.3.1 we define

$$\phi_+ = \ell(\psi+\phi), \tag{4.95}$$

$$\phi_- = (\psi-\phi), \tag{4.96}$$

and perform Kaluza-Klein reduction first along ϕ_+ and then along the t direction. The resulting scalars are somewhat cumbersome. Appropriately choosing the axionic shifts for the scalars χ_1, χ_2, χ_3 we indeed find that the resulting matrix $M(r,x)$ has the asymptotic behaviour

$$M(r,x) = Y + O\left(\frac{1}{r^2}\right), \tag{4.97}$$

where Y is the constant matrix (4.32). In order to construct the monodromy matrix $\mathcal{M}(w)$ from $M(r,x)$ we first need to change coordinates to the canonical coordinates (ρ,z) and then take the limit $\rho \to 0$ and take z near $-\infty$ and finally replace z with w.

The relation between the coordinates used above and the canonical coordinates is [157]

$$\rho = rx\sqrt{\Delta(1-x^2)}, \qquad z = \frac{1}{2}r^2\left(1 - \frac{2m - l_1^2 - l_2^2}{2r^2}\right)(2x^2-1), \tag{4.98}$$

where Δ is

$$\Delta = r^2\left(1 + \frac{l_1^2}{r^2}\right)\left(1 + \frac{l_2^2}{r^2}\right) - 2m. \tag{4.99}$$

In practice, performing this change of coordinates is not easy. It is easier to first introduce the prolate spherical coordinates (u, v) and then change to the canonical coordinates. The prolate spherical coordinates are defined via

$$\alpha^2(u^2-1)(1-v^2) = r^2x^2\Delta(1-x^2), \quad \alpha uv = \frac{1}{2}r^2\left(1 - \frac{2m - l_1^2 - l_2^2}{2r^2}\right)(2x^2-1), \tag{4.100}$$

or equivalently

$$u = \frac{1}{4\alpha}(2r^2 + l_1^2 + l_2^2 - 2m), \quad v = 2x^2 - 1, \quad \alpha = \frac{1}{4}\sqrt{(2m - l_1^2 - l_2^2)^2 - 4l_1^2l_2^2}. \tag{4.101}$$

The transformation from the prolate spherical coordinates to the canonical coordinates is

$$u = \frac{\sqrt{\rho^2 + (z+\alpha)^2} + \sqrt{\rho^2 + (z-\alpha)^2}}{2\alpha}, \quad v = \frac{\sqrt{\rho^2 + (z+\alpha)^2} - \sqrt{\rho^2 + (z-\alpha)^2}}{2\alpha}. \tag{4.102}$$

Given these expressions it is easy to see that the limit $\rho \to 0$ and taking z near $-\infty$ amounts to the replacement $u \to -\frac{z}{\alpha}$ and $v \to -1$, equivalently $r^2 \to -2z - \frac{1}{2}(l_1^2 + l_2^2 - 2m)$ and $x \to 0$.

Making these replacements in the matrix $M(r, x)$ we find the monodromy matrix $\mathcal{M}(w)$. It takes the form

$$\mathcal{M}(w) = Y + \frac{A_1}{w - \alpha} + \frac{A_2}{w + \alpha}, \tag{4.103}$$

where $A_1 = \alpha_1 a_1 a_1^T \eta$, $A_2 = \alpha_2 a_2 a_2^T \eta$, and $\eta = \text{diag}\{1, -1, 1\}$. In particular, the Myers-

Perry monodromy matrix has two poles at locations $w = \pm\alpha$ and the residues at these poles are of rank one. Clearly there is an ambiguity in the choice of the a vectors and the α parameters. We choose these quantities such that they have smooth limits when either of the rotation parameters l_1 or l_2 go to zero. An explicit form of the a vectors and the parameters α's is as follows

$$a_1 = \left\{-\frac{\ell\left(4\alpha + l_1^2 - l_2^2 - 2m\right)}{2l_2 m}, \frac{4\alpha + (l_1+l_2)(l_1+3l_2) - 2m}{8\ell l_2}, 1\right\}, \tag{4.104}$$

$$a_2 = \left\{\frac{\ell\left(4\alpha - l_1^2 + l_2^2 + 2m\right)}{2\sqrt{2}m}, \frac{-4\alpha + (l_1+l_2)(l_1+3l_2) - 2m}{8\sqrt{2}\ell}, \frac{l_2}{\sqrt{2}}\right\}, \tag{4.105}$$

$$\alpha_1 = \frac{m\left(l_1^4 - 4\alpha l_1^2 - 2l_1^2\left(l_2^2+2m\right) + 4\alpha l_2^2 + \left(l_2^2 - 2m\right)^2 + 8\alpha m\right)}{2\left((l_1-l_2)^2 - 2m\right)\left((l_1+l_2)^2 - 2m\right)}, \tag{4.106}$$

$$\alpha_2 = \frac{m\left(l_1^4 + 4\alpha l_1^2 - 2l_1^2\left(l_2^2+2m\right) - 4\alpha l_2^2 + \left(l_2^2 - 2m\right)^2 - 8\alpha m\right)}{l_2^2\left((l_1-l_2)^2 - 2m\right)\left((l_1+l_2)^2 - 2m\right)}. \tag{4.107}$$

In the limit $l_1 \to 0$ these expressions simplify to

$$\alpha_1 = \frac{2m^2}{2m - l_2^2}, \qquad a_1 = \left\{\frac{\ell l_2}{m}, \frac{l_2}{4\ell}, 1\right\}, \tag{4.108}$$

$$\alpha_2 = -\frac{2m}{2m - l_2^2}, \qquad a_2 = \left\{\sqrt{2}\ell, \frac{l_2^2 - m}{2\sqrt{2}\ell}, \frac{l_2}{\sqrt{2}}\right\}. \tag{4.109}$$

Additionally, in the limit $l_2 \to 0$ whereupon we obtain Schwarzschild black hole, these expressions further simplify to

$$\alpha_1 = m, \qquad a_1 = \{0, 0, 1\}, \tag{4.110}$$

$$\alpha_2 = -1, \qquad a_2 = \left\{\sqrt{2}\ell, -\frac{m}{2\sqrt{2}\ell}, 0\right\}. \tag{4.111}$$

These last expressions are especially informative. Since α_1 is equal to m and the vector a_1 is simply a constant, in the limit $m \to 0$ the residue of the pole $w = +\alpha$ vanishes, i.e., the pole $w = +\alpha$ disappears. Whereas the residue of the pole $w = -\alpha$ does not vanish in the same limit. In fact in this limit the pole location α also goes to zero. This limit corresponds to five-dimensional Minkowski space. The monodromy matrix simplifies to

$$\mathcal{M}(w) = Y + \frac{\alpha_2 a_2 a_2^T \eta}{w}, \tag{4.112}$$

with $\alpha_2 = -1$ and $a_2 = \left\{\sqrt{2}\ell, 0, 0\right\}$. Thus, from the Geroch group point of view five-dimensional Minkowski space has a non-trivial monodromy matrix. Its asymptotic limit is the constant matrix Y. It also has a pole at $w = 0$ with residue of rank one. The residue depends on the parameter ℓ introduced via equation (4.95) and as such it can take any non-zero value.

The Riemann-Hilbert factorization of the monodromy matrix (4.103) gives the double spinning Myers-Perry solution, as expected. Details of this factorization are also very similar to the examples considered in [6, 152]. The only difference is that one needs to take into account the Y matrix via equation (4.42).

We end this section by observing some properties of the monodromy matrix (4.103) in relation to the charge matrix for the Myers-Perry spacetime.

The concept of charge matrix for the five-dimensional boundary conditions was introduced in [160]. In the present context it is computed as follows. First we define

$$D = \begin{pmatrix} \frac{1}{\sqrt{2}} & \frac{1}{\sqrt{2}} & 0 \\ \frac{1}{\sqrt{2}} & -\frac{1}{\sqrt{2}} & 0 \\ 0 & 0 & 1 \end{pmatrix}, \tag{4.113}$$

with the property that

$$D^\sharp D = Y. \tag{4.114}$$

Next we conjugate $M(r, x)$ with D^{-1}. This operation has the effect that the matrix

$$(D^\sharp)^{-1} M(r, x) D^{-1} \tag{4.115}$$

asymptote to identity matrix. Then, the charge matrix is defined by the coefficient of r^{-2} term in the asymptotic expansion near infinity

$$(D^\sharp)^{-1} M(r,x) D^{-1} = \mathbf{I} - \frac{2\mathcal{Q}}{r^2} + O\left(\frac{1}{r^4}\right). \tag{4.116}$$

The charge matrix obtained in this way satisfies the characteristic equation

$$\mathcal{Q}^3 - \frac{1}{2}\mathrm{Tr}(\mathcal{Q}^2)\mathcal{Q} = 0. \tag{4.117}$$

It does not capture information about both angular momentum l_1 and l_2 of the MP spacetime. To encode that we can introduce one more matrix

$$\mathcal{A} = a_1(e_1 - e_1^\sharp) + a_2(e_2 - e_2^\sharp) + a_3(e_3 - e_3^\sharp), \tag{4.118}$$

with coefficients

$$a_1 = -\frac{m - 4\ell^2}{4\sqrt{2}\ell}(l_1 - l_2), \quad a_2 = -\frac{1}{2}(l_1 + l_2)(l_1 - l_2), \quad a_3 = -\frac{m + 4\ell^2}{4\sqrt{2}\ell}(l_1 - l_2), \tag{4.119}$$

where e_1, e_2, e_3 are the raising generators defined in (B.7). This matrix allows us to write relations similar to the ones written above for dyonic KK black hole. Firstly, we observe that it anticommutes with the charge matrix,

$$\{\mathcal{Q}, \mathcal{A}\} = 0. \tag{4.120}$$

Secondly, using this matrix we can write yet another characteristic equation that captures rotation properties as well,

$$(\mathcal{Q} + \mathcal{A})^3 - \frac{1}{2}\mathrm{Tr}\left((\mathcal{Q} + \mathcal{A})^2\right)(\mathcal{Q} + \mathcal{A}) = 0, \tag{4.121}$$

with $\mathrm{Tr}\left((\mathcal{Q} + \mathcal{A})^2\right) = 8\alpha^2$. Finally, we can write the full Geroch matrix solely in terms of

$\mathcal{Q}$, $\mathcal{A}$, and D matrices

$$\mathcal{M}(w) = Y + \frac{1}{w^2 - \alpha^2} D^\sharp \left(w\mathcal{Q} + \frac{1}{2}\mathcal{Q}^2 - \frac{1}{4}[\mathcal{Q}, \mathcal{A}] \right) D. \tag{4.122}$$

4.5 Summary and open problems

In this chapter we have analysed Geroch group description of black holes. We presented a general relation, equation (4.10), between the three-dimensional coset matrix $M(x)$ and the Geroch group matrix $\mathcal{M}(w)$. Using this simple relation we constructed Geroch group matrices for dyonic Kaluza-Klein black hole, five-dimensional Myers-Perry black hole, and for Kerr-Newman black hole. Along the way, we presented some non-trivial relations between the Geroch group matrices and charge matrices. We also incorporated five-dimensional asymptotically flat boundary conditions in the factorization algorithm of [6, 152].

There are several ways in which our study can be extended. Perhaps the simplest such extension will be to work out similar details for the Einstein-Maxwell dilaton-axion model (EMDA) that has the hidden symmetry group $\mathrm{Sp}(4, \mathbb{R})$. Equally interesting is the case of bosonic sector of the $N = 2$ supergravity with one vector multiplet with prepotential $F = -iX_0X_1$. This theory has the hidden symmetry group $\mathrm{SU}(2, 2)$. In both these cases we do not expect to meet any surprises. We expect that a straightforward extension of the above discussion will be applicable.

Chapter 5

Smooth non-extremal D1-D5-P solutions as charged gravitational instantons

It is natural to hope that understanding the known non-extremal microstates [3, 51, 52, 56, 58, 161, 162] from various possible perspectives will shed light on how to go about constructing more general non-extremal microstates. Drawing movitation from properties of the supersymmetric solutions, one such study was performed in reference [50] for the solutions found by Jejjala, Madden, Ross, and Titchener (JMaRT) [3]. They found that upon dimensional reduction from 6d to 5d, the 5d solution features locally non-supersymmetric orbifold singularities. Upon further reduction to 4d, they found that the two singularities are connected by a conical singularity. The presence of the conical singularity does not allow for an unambiguous association of brane charges to the two centers. This led the authors to conclude that the picture of "half-BPS atoms" making up the multiple centers of supersymmetric microstates does not extent to the non-supersymmetric ones in any easy way. One must consider more general kinds of basic building blocks.

In this chapter we add a new dimension to this discussion. We show that the JMaRT solution can also be thought of as a charged version of Euclidean five-dimensional Myers-Perry instanton trivially lifted to six dimensions by the addition of a flat timelike direction. Gravitational instantons in four-dimensions have received much attention under the Euclidean Gravity paradigm, though their higher-dimensional cousins are not so well explored. For the cases where these objects have been explored, their classification is presented in terms of turning points of various degenerating Killing vectors [163]; more precisely in terms of the so-called rod structure [154, 157, 164]. Since for the non-supersymmetric microstates only spacelike Killing vectors degenerate, it is natural to expect that non-supersymmetric microstates are closely related to gravitational instantons.

For the construction of the multi-center supersymmetric solutions this connection is the key element [39, 40]. In these constructions the four-dimensional base space is taken to be multi-center Gibbons-Hawking instanton. For non-extremal microstates such a link has also been explored, though not yet in a fully systematic way. For example, the first generalisation [51] of the JMaRT solution was constructed by adding appropriate charges to the so-called Kerr-Taub-Bolt instanton. Similar ideas, in different guises, were also used in references [56, 58, 59, 165]. More recently, these and a related circle of ideas have led to the construction of the first example of non-extremal multi-bubble microstate geometries [162].

It had been anticipated that the JMaRT solution has a close connection to gravitational instantons (see e.g. comments in [51, 59]), though it has never been made precise. A connection was established in reference [57] where it was highlighted that the JMaRT metric can be related to the Myers-Perry instanton metric via a simple analytic continuation. In this chapter we extend and simplify that construction. There are several differences: we consider both angular momentum and all three charges, whereas reference [57] only dealt with the case of two-charges and a single rotation. We work with the well developed Belinski-Zakharov inverse scattering method [79–81, 166], as opposed to the Breitenlohner-Maison method [5, 6, 152, 167] used in [57]. Moreover, for adding charges we do reductions over the standard angular coordinates ψ and ϕ as opposed to linear combinations of these coordinates as was done there. We use timelike reduction to go from 4d to 3d, as opposed to [57] where the timelike reduction was used to go from 6d to 5d. These points considerably simplify the calculations and make the full construction more accessible.

The rest of the chapter is organised as follows. In section 5.1 we gather our main ideas relegating all detailed calculations to the appendices. In section 5.1.1 we present the Myers-Perry instanton metric. In section 5.1.2 we perform a specific $SO(4,4)$ transformation — a Weyl reflection — on the matrix of scalars for the Myers-Perry instanton. This Weyl reflection allows us to match the final solution rather directly to the JMaRT parameterisation upon adding charges. In section 5.1.3 we perform the charging transformations on the Weyl reflected Myers-Perry instanton matrix. The corresponding six-dimensional fields match on to the over-rotating Cvetič-Youm metric.

We present in detail the inverse scattering construction of the Myers-Perry instanton metric in appendix C.1. Certain details on the construction of the $SO(4,4)$ matrix and the action of the Weyl reflection on three-dimensional scalars are provided in appendix C.2. Details on the construction of the six-dimensional fields are provided in appendix C.3. A discussion on the rod structure of the Cvetič-Youm metric is presented in appendix C.4. The black hole and the fuzzball cases are analysed separately.

We end with a brief discussion in section 5.2.

5.1 JMaRT as charged Myers-Perry instanton

The JMaRT solutions presented in Ref. [3] were originally obtained by starting with a large family of metrics and determining special choices of parameters that rendered the geometries smooth and horizonless. Specifically, the starting point was the general five-dimensional non-extremal solutions, derived by Cvetič and Youm [132], carringy two angular momenta and three independent U(1) charges, in addition to a mass parameter M. These metrics are solutions to five-dimensional supergravity theory obtained from ten-dimensional type IIB supergravity upon compactification on $T^4 \times S^1$. While the compact T^4 part of the metric does not play a significant role in the JMaRT construction, the S^1 direction is crucial for the smoothness analysis. Therefore, the metric and matter fields are most conveniently considered as six-dimensional quantities. Our goal is to demonstrate that the JMaRT solutions can be generated in an alternative and more direct way.

5.1.1 Myers-Perry instanton

The five-dimensional Myers-Perry instanton metric can be expressed as

$$\begin{aligned} ds^2_{5d} &= dy^2 + \frac{M}{\Sigma}\left[dy + a_1 \sin^2\theta\, d\phi + a_2 \cos^2\theta\, d\psi\right]^2 \\ &\quad + (r^2 - a_1^2)\sin^2\theta\, d\phi^2 + (r^2 - a_2^2)\cos^2\theta\, d\psi^2 + \frac{\Sigma}{\Delta} dr^2 + \Sigma\, d\theta^2, \end{aligned} \tag{5.1}$$

where

$$\Sigma = r^2 - a_1^2 \cos^2\theta - a_2^2 \sin^2\theta, \qquad \Delta = r^2\left(1 - \frac{a_1^2}{r^2}\right)\left(1 - \frac{a_2^2}{r^2}\right) + M. \tag{5.2}$$

This is a vacuum solution of Euclidean gravity possessing three commuting Killing vector fields, namely $\partial_y, \partial_\phi$ and ∂_ψ, and is parametrised by the three numbers M, a_1 and a_2. We obtain a Lorentzian metric by trivially lifting to six-dimensions through the addition of a flat time direction,

$$ds^2_{6d} = -\, dt^2 + ds^2_{5d}. \tag{5.3}$$

The line element (5.1) can be easily obtained by the following analytic continuation on the Myers-Perry metric as given in Ref. [157]:

$$
\begin{aligned}
a_1 &\to -ia_1, \\
a_2 &\to -ia_2, \\
t &\to +iy, \\
M &\to -M.
\end{aligned}
\tag{5.4}
$$

A standard Euclidean version of the Myers-Perry solution would not include the analytic continuation on the mass parameter, $M \to -M$ [1]. While this raises questions about the regularity of such geometries, we are not concerned with the smoothness properties of this metric *per se*. In section 5.1.3 below, we will add charges on top of this metric and it is the smoothness properties of the final charged metric that we will be interested in. The same approach was taken in other references, see e.g., [51, 56].

Inverse scattering construction

The 3-parameter family of solutions (5.1) can also be constructively generated from five dimensional Euclidean Schwarzschild metric by applying the Belinski-Zakharov (BZ) inverse scattering method. This procedure is detailed in appendix C.1 and parallels the derivation of the 5D Myers-Perry metric from Schwarzschild metric in Lorenztian gravity [166]. One of the key points that is borne out by this construction is that the parameters must obey

$$M < (a_1 - a_2)^2. \tag{5.5}$$

This bound arises in the JMaRT solutions as a condition ensuring that the smooth geometries are horizonless [3].

[1]Nevertheless, with a slight abuse of language we will continue to call metric (5.1) — and its six-dimensional uplift (5.3) — the Myers-Perry instanton.

As is well known for the Lorentzian Myers-Perry metric, the inverse scattering procedure is not unique. The same is true for the Euclidean metric. In appendix C.1 we describe one such way of generating the Euclidean solution. A brief summary is as follows. Let us recall that stationary axi-symmetric solutions of vacuum Einstein equations in five-dimensions can be expressed in canonical coordinates in the form [157]

$$ds^2 = G_{ab}(\rho, z)\, dx^a dx^b + e^{2\nu(\rho,z)}(d\rho^2 + dz^2)\,, \qquad \text{with} \quad \det G = \rho^2\,. \tag{5.6}$$

Note that the determinant of the Killing matrix G_{ab} is positive, since we are working in Euclidean gravity. In canonical coordinates the vacuum Einstein equations yield a decoupled set of equations for the Killing metric G_{ab}. These equations can be equivalently formulated as a system of first order differential equations (the Lax pair) for the so-called generating matrix. One 'dresses' the generating matrix of the seed solution appropriately to obtain a new solution.

We follow the procedure of Ref. [166]. We first remove a soliton and an anti-soliton with 'trivial' BZ vectors from the five dimensional Euclidean Schwarzschild metric, and then add the same soliton and the anti-soliton with 'nontrivial' BZ vectors. Changing the co-ordinates from canonical to more standard radial coordinates, and choosing convenient names for the parameters added through the BZ vectors, we obtain the metric (5.1) together with the bound (5.5). A step-by-step description of the procedure is presented in appendix C.1.

Shifted coordinates

For the ensuing discussion the following coordinates are more useful to work with. These coordinates allow to match rather directly the charged version of the Myers-Perry instanton to the over-rotating Cvetič-Youm metric. The coordinate transformation is

$$r^2 \longrightarrow r^2 + a_1^2 + a_2^2 - M, \tag{5.7}$$

$$\theta \longrightarrow \frac{\pi}{2} - \theta. \tag{5.8}$$

Along with these coordinate shifts, we also interchange coordinates ϕ and ψ and names of the rotation parameters a_1 and a_2:

$$\phi \longleftrightarrow \psi, \tag{5.9}$$

$$a_1 \longleftrightarrow a_2. \tag{5.10}$$

The resulting metric reads

$$\begin{aligned} ds^2_{6d} = & - dt^2 + dy^2 + \frac{M}{\tilde{\Sigma}} \left[dy + a_1 \sin^2\theta \, d\phi + a_2 \cos^2\theta \, d\psi \right]^2 \\ & + (r^2 + a_2^2 - M) \sin^2\theta \, d\phi^2 + (r^2 + a_1^2 - M) \cos^2\theta \, d\psi^2 + \frac{\tilde{\Sigma}}{\tilde{\Delta}} dr^2 + \tilde{\Sigma} \, d\theta^2, \end{aligned} \tag{5.11}$$

where

$$\tilde{\Sigma} = r^2 + a_1^2 \sin^2\theta + a_2^2 \cos^2\theta - M, \tag{5.12}$$

$$\tilde{\Delta} = r^2 \left(1 + \frac{a_1^2}{r^2}\right)\left(1 + \frac{a_2^2}{r^2}\right) - M. \tag{5.13}$$

5.1.2 Dimensional reduction to 3d and Weyl reflection

As our next step we will apply a solution generating technique based on three-dimensional duality symmetries on the Myers-Perry instanton metric (5.11). Thus, we begin by dimensionally reducing down to three dimensions.

The six-dimensional truncation of IIB theory on T^4 that we work with is

$$\mathbb{L}_6 = R_6 \star_6 1 - \frac{1}{2} \star_6 d\Phi \wedge d\Phi - \frac{1}{2} e^{\mathrm{sq}2\Phi} \star_6 F_{[3]} \wedge F_{[3]}, \tag{5.14}$$

where the field strength $F_{[3]} = dC_{[2]}$ comes from the Ramond-Ramond sector of the ten-dimensional IIB theory. The six-dimensional metric (5.11) is viewed as a solution of theory (5.14), specifically a solution with trivial dilaton Φ and two-form field $C_{[2]}$.

Three-dimensional dualities

Upon dimensional reduction a large number of gravity and supergravity theories become gravity coupled to form-fields and non-linear sigma models. Such non-linear sigma models are maps from a lower-dimensional base space to a target space. The target space is generally a coset G/K. The group G is the group of global isometries of the target space. The group K is the isotropy subgroup of the target space – a subgroup of G. The symmetry group G of a sigma model can be used to generate new solutions of the higher-dimensional gravity theory by applying a group transformation to a coset representative of a seed solution.

These techniques become particularly powerful when the reduction is performed down to three dimensions. In three dimensions all higher dimensional form fields can be dualized to scalars. As a result the symmetry groups become significantly enhanced, and one has at ones disposal a rich solution generating technique. Further richness comes from changing the details of the dimensional reduction. For example, by changing the order of the timelike reduction within the whole sequence of reductions, one can change the denominator subgroup.

These techniques have been presented at several places in the literature, see e.g., [65]; we will not review it here. We refer the reader to appendix C.2 for some more details and notation. The key quantity in this method to work with is a matrix $\mathcal{M}$ that encodes all three-dimensional scalars. These are obtained by performing a sequence of Kaluza-Klein reductions down to 3d, together with the dualisation of the one-forms that are left over. The matrix $\mathcal{M}$ belongs to the coset G/K.

For the theory (5.14) the coset model is

$$\frac{\mathrm{SO}(4,4)}{\mathrm{SO}(2,2)\times\mathrm{SO}(2,2)}, \tag{5.15}$$

where the embedding of the denominator subgroup in the numerator group depends on the details of the dimensional reduction. The specific ordering of the Kaluza-Klein reductions we adopted was over y, ϕ, and t, respectively. Group transformations with elements belonging to the denominator subgroup act as

$$\mathcal{M}\to g^{-1}\,\mathcal{M}\,g, \qquad \text{for} \qquad g\ \in\ \mathrm{SO}(2,2)\times\mathrm{SO}(2,2). \tag{5.16}$$

Thus, from the metric (5.11) we construct the SO(4,4) matrix $\mathcal{M}$, roughly by exponentiating the various group generators — each generator being weighted by one of the 3d scalars — and multiplying them all together. The group SO(4,4) has dimension 28. The Cartan subalgebra is spanned by four generators, denoted H_Λ, with $\Lambda = 0,\ldots,3$. The remaining 24 generators are broken into 'positive' ($E_\Lambda, E_{q_\Lambda}, E_{p^\Lambda}$) and 'negative' ($F_\Lambda, F_{q_\Lambda}, F_{p^\Lambda}$) elements and the number of available 3d scalars (sixteen) matches the number of Cartan plus positive generators. More details are given in appendix C.2. We adopted the same basis for the $\mathfrak{so}(4,4)$ algebra as the one defined in Refs. [8, 70].

Weyl reflection

On the resulting matrix $\mathcal{M}$ we act with the following group element

$$g_w = \exp\left[i\frac{\pi}{2}K_{q_2}\right]\exp\left[i\frac{\pi}{2}K_{q_3}\right], \tag{5.17}$$

as

$$\mathcal{M}_w = g_w^{-1} \mathcal{M} g_w. \tag{5.18}$$

Here, we have defined $K_{q_\Lambda} := E_{q_\Lambda} - {E_{q_\Lambda}}^\sharp$, where the symbol $^\sharp$ denotes the generalised transpose [see appendix C.2 below Eq. (C.33)]. Although complex numbers appear in definition (5.17), it can be checked by direct inspection that the resulting matrix is real and indeed belongs to the denominator $\mathrm{SO}(2,2) \times \mathrm{SO}(2,2)$ subgroup of the numerator $\mathrm{SO}(4,4)$ group. We follow the $\mathfrak{so}(4,4)$ Lie algebra conventions of [8, 70].

In the numerator $\mathrm{SO}(4,4)$, g_w is a Weyl reflection. Of particular interest is the action of this transformation on the Euclidean gravity truncation to which the metric (5.11) belongs. As is discussed in detail in appendix C.2, its action changes the truncation from Euclidean five-dimensional vacuum gravity to Lorentzian five-dimensional vacuum gravity. The bound (5.5) on the parameters does not change. The resulting matrix $\mathcal{M}_w$ can be thought of as describing 'over-rotating' Lorentzian Myers-Perry metric. This needs to be contrasted with the inverse scattering construction of the Lorentzian Myers-Perry metric, e.g., as presented in [166], where the bound (5.5) cannot be fulfilled with real pole positions in the dressing transformations. A very similar transformation was used in [57]. However, details are not identical.

Of course, one could have taken directly, as a starting point, the 'over-rotating' Myers-Perry solution and then charge it up as we will do next. But by following this longer route we emphasise that the JMaRT smooth solutions can be systematically constructed from gravitational instantons.

5.1.3 Charging transformations and 6d fields

On the resulting matrix $\mathcal{M}_w$ we act with a charging transformation that adds three electric charges. We choose names for the charging parameters so that the final answer conforms to the JMaRT notation. The charging transformation is

$$g_{\mathrm{c}} = \exp\left[\delta_p K_{q_1}\right] \exp\left[-\delta_1 K_{q_2}\right] \exp\left[\delta_5 K_{q_3}\right], \tag{5.19}$$

acting as

$$\mathcal{M}_{\text{final}} = g_c^{-1} \mathcal{M}_w g_c. \tag{5.20}$$

We read scalars from the matrix $\mathcal{M}_{\text{final}}$ and build the metric, dilaton, and the C-field in six-dimensions. We find an answer identical to the fields given in reference [3]. Certain details on the construction of the six-dimensional fields are provided in appendix C.3. For completeness, and for use in appendices, we write the final fields here. The six-dimensional Einstein frame metric reads

$$\begin{aligned} ds^2_{6d} \;=\; & -\frac{f}{\sqrt{\tilde{H}_1\tilde{H}_5}}(dt^2 - dy^2) + \frac{M}{\sqrt{\tilde{H}_1\tilde{H}_5}}(s_p dy - c_p dt)^2 \\ & + \sqrt{\tilde{H}_1\tilde{H}_5}\left(\frac{r^2 dr^2}{(r^2+a_1^2)(r^2+a_2^2) - Mr^2} + d\theta^2\right) \\ & + \left(\sqrt{\tilde{H}_1\tilde{H}_5} - (a_2^2 - a_1^2)\frac{(\tilde{H}_1 + \tilde{H}_5 - f)\cos^2\theta}{\sqrt{\tilde{H}_1\tilde{H}_5}}\right)\cos^2\theta d\psi^2 \\ & + \left(\sqrt{\tilde{H}_1\tilde{H}_5} + (a_2^2 - a_1^2)\frac{(\tilde{H}_1 + \tilde{H}_5 - f)\sin^2\theta}{\sqrt{\tilde{H}_1\tilde{H}_5}}\right)\sin^2\theta d\phi^2 \\ & + \frac{M}{\sqrt{\tilde{H}_1\tilde{H}_5}}(a_1\cos^2\theta d\psi + a_2\sin^2\theta d\phi)^2 \\ & + \frac{2M\cos^2\theta}{\sqrt{\tilde{H}_1\tilde{H}_5}}[(a_1c_1c_5c_p - a_2s_1s_5s_p)dt + (a_2s_1s_5c_p - a_1c_1c_5s_p)dy]d\psi \\ & + \frac{2M\sin^2\theta}{\sqrt{\tilde{H}_1\tilde{H}_5}}[(a_2c_1c_5c_p - a_1s_1s_5s_p)dt + (a_1s_1s_5c_p - a_2c_1c_5s_p)dy]d\phi, \end{aligned} \tag{5.21}$$

where

$$\tilde{H}_i = f + M\sinh^2\delta_i, \quad f = r^2 + a_1^2\sin^2\theta + a_2^2\cos^2\theta, \tag{5.22}$$

and $c_i = \cosh\delta_i$, $s_i = \sinh\delta_i$. The six-dimensional two-form is given by

$$
\begin{aligned}
C_2 \;=\; & -\frac{M s_1 c_1}{\tilde{H}_1} dt \wedge dy - \frac{M s_5 c_5}{\tilde{H}_1}(r^2 + a_2^2 + M s_1^2)\cos^2\theta d\psi \wedge d\phi \\
& + \frac{M\cos^2\theta}{\tilde{H}_1}\Big[(a_2 c_1 s_5 c_p - a_1 s_1 c_5 s_p)dt + (a_1 s_1 c_5 c_p - a_2 c_1 s_5 s_p)dy\Big] \wedge d\psi \\
& + \frac{M\sin^2\theta}{\tilde{H}_1}\Big[(a_1 c_1 s_5 c_p - a_2 s_1 c_5 s_p)dt + (a_2 s_1 c_5 c_p - a_1 c_1 s_5 s_p)dy\Big] \wedge d\phi,
\end{aligned} \tag{5.23}
$$

and finally the six-dimensional dilaton Φ, cf. (C.19), reads

$$
e^{2\sqrt{2}\Phi} = \frac{\tilde{H}_1}{\tilde{H}_5}. \tag{5.24}
$$

A discussion of the rod structure for this metric is presented in appendix C.4.

5.2 Conclusions

In this chapter we have presented an alternative and more direct (inverse-scattering based) construction of the over-rotating Cvetič-Youm metric. We have generalized — and at the same time simplified — the construction of [57]. Certain further restrictions on the parameters of the resulting 6d fields give rise to a discrete family of non-extremal smooth bound states of the D1-D5-P system [3].

Another objective of this work was to emphasise the idea that the over-rotating Cvetič-Youm metric can be viewed as a charged version of the Myers-Perry instanton metric. Indeed, this picture is strongly suggested by the similarities between the rod structures of the two metrics. Although the Cvetič-Youm geometry is not a vacuum solution, from the metric alone one can still define a rod structure and this was presented in appendix C.4.

More generally, one may hope that adding appropriate charges to gravitational instantons might lead to a class of non-supersymmetric fuzzballs. It will be very exciting if this circle of ideas can be pushed further to construct a class of multi-bubble non-extremal fuzzball solutions. Given the remarkable success that the inverse scattering method has had with black rings, we expect that progress should be possible on "three-center" non-extremal solutions. This may be achieved by generalising the present study by taking a (yet unknown) Euclidean black ring as the starting point for the charging transformation.

Chapter 6

Conclusion

In the first part of the thesis we studied a specific class of non supersymmetric smooth D1-D5-P supergravity bound state, known as the JMaRT solution [3]. These are asymptotically flat metrics with an inner $AdS_3 \times S^3$ region. These were originally constructed as an over rotating limit of Cvetič-Youm geometries. The general family of smooth JMaRT solutions also include orbifolds. In chapter 3 we considered certain orbifolds on JMaRT solutions with an orbifold parameter k. Using the AdS/CFT correspondence we identified the dual CFT states of the orbifolded JMaRT solutions. The orbifold appears in the JMaRT metric by demanding that the compact circle that degenerates at the origin actually degenerates with a radius kR instead of R where R is the radius of the circle at spatial infinity. We studied the action of orbifolds on the $AdS_3 \times S^3$ metric and concluded that when the three integer parameters m, n and k of the metric become mutually co-prime, the orbifold acts freely on the background and the metric becomes regular everywhere. Three more interesting cases appear in the analysis when one or more of the common divisors between the parameters become greater than unity. In that case the geometry had a conical singularity either at the poles of S^3 or all over S^3 including its poles. In the supersymmetric construction [22], there was no orbifold singularity all over S^3 due to reasons obvious from our analysis.

The dual two dimensional CFT for low energy excitations is described by the $\mathcal{N} = (4,4)$ SCFT. It is conjectured that there is a point in the CFT moduli space called the orbifold point where this SCFT is a symmetric product orbifold theory, consisting of $n_1 n_5$ symmetrized copies of a free $(4,4)$ SCFT with target space T^4 [34, 111]. Since the target manifold is a quotient space, there exist twisted sectors in the theory. The dual CFT states that describe orbifolded JMaRT solutions are constructed from fractional spectral flow both in the left and in the right sectors, applied to twisted RR ground states $|0_k\rangle_R$. Remarkably with the identification of the map between the gravity and CFT parameters we have been able to match the corresponding charges calculated from the gravity and CFT sides.

We further investigated our proposed identification since there can be several CFT states for the given conformal dimension h and $SU(2)_R$ charge m. We studied the ergoregion instability of three charge JMaRT [117] in the presence of orbifolds. We considered massless minimally coupled scalar perturbations in the background geometry and found exact matching of the emission frequency and emission rates calculated both from the gravity and CFT sides. We also established a pair creation like picture from the ergoregion of these geometries. We showed that the scalar wavefunction is of a very special form: a part of it flies off to infinity and the other part has support in the AdS region.

In chapter 3 we also considered Fermi filling of states in the CFT without holes. As a future direction it will be worthwhile to recognize the bulk duals of CFT states that have gaps in the Fermi seas. In chapter 2 we reviewed the multicenter Gibbons Hawking metrics that are smooth supersymmetric solutions in the M-theory frame. The dual CFT states for general such solutions have not been understood so far. It will be exciting to understand the holographic identification for both BPS and non BPS solutions in this class.

In chapter 4 we studied four and five dimensional black holes from two dimensional perspective. We discussed dimensional reduction from five to two dimensions over two spacelike and one timelike direction. Higher dimensional gravity theories when dimensionally reduced to two dimensions exhibit infinite dimensional symmetry at the level of the equations of motion. The infinite dimensional symmetry group is called the Geroch group. In chapter 4 we discussed five dimensional Myers-Perry and dyonic Kaluza Klein black holes and four dimensional Kerr-Newman black hole from the two dimensional Geroch group point of view. The integrability of the two dimensional equations of motion implies that one can associate a linear set of Lax equations. We worked with a Breitenlohner Maison (BM) linear system [5] that keeps the group structure manifest. For solitonic solutions, given a seed we can generate new exact solutions in the BM method just following a few algebraic steps. We discovered a direct relation between the three dimensional spacetime monodromy matrix and two dimensional constant Geroch group matrix. We explicitly constructed Geroch group matrices for five dimensional rotating Myers-Perry and Dyonic Kaluza Klein black holes and four dimensional Kerr Newman black hole. Both cases are two soliton solutions, solitons sitting at the two poles of monodromy matrix with residues of rank one. The subleading term in the asymptotic expansion of the Geroch group matrix determines the charge matrix. We presented nontrivial relations between the Geroch group matrices and the charge matrices.

Recently there have been attempts to generalize the Geroch group techniques to Einstein spaces [168]. The method captures only examples of cohomogeneity-1 spacetimes; Schwarzschild AdS and Taub-NUT AdS. In these setups, in the dimensional reduction from $4D$ to $3D$ the $SL(2,R)$ symmetry is partially broken. It would be interesting to extend the formalism to include angular momentum and understand integrability for Einstein spaces that generically depend on two coordinates.

A theory that requires new ideas is minimal supergravity in five-dimensions. This theory has hidden symmetry group to be the smallest exceptional group $G_{2(2)}$. For this set-up also, given $M(x)$ one can construct $\mathcal{M}(w)$ using (4.10). The residues at the poles will turn out to be of rank-2. Since the residues are of rank-2 one needs to separate out contributions into the $a-$ and $b-$vectors. This seems to be a non-trivial step. Moreover, since the defining relation for $G_{2(2)}$ matrices in fundamental representation is non-linear,

$$c_{abc}\mathcal{M}_{aa'}\mathcal{M}_{bb'}\mathcal{M}_{cc'} = c_{a'b'c'},$$

with c_{abc} the $\mathfrak{g}_{2(2)}$ invariant three-form, most likely certain details of the factorization algorithm as presented in [152] need to be adjusted (see also related comments in [169]). We do hope that working out examples of Geroch group matrices using (4.10), as we have done in chapter 4, will shed some light on those issues as well.

For practical calculations involving more complicated solutions such as black rings and two-centered black holes we need to consider cases where Geroch group matrices may not be asymptotically constant. For example, for a neutral rotating Emparan-Reall black ring [170] it is most manageable to do dimensional reduction first along the S^1 direction, and then along the time direction. The matrix $M(x)$ obtained in this way does not asymptote to a constant matrix at spatial infinity, and for the same reason the matrix $\mathcal{M}(w)|_{w\to\infty}$ also does not approach a constant. In fact, as we saw in chapter 4 the matrix $\mathcal{M}(w)$ has a pole at $w = \infty$. The factorization algorithm developed in [6, 152] does not incorporate this feature. It will be worthwhile to extend the previously developed factorization algorithms to allow for such a possibility. This will be a natural arena for describing black rings and related set-ups from the Geroch group point of view.

In chapter 5 we viewed the three charge doubly rotating JMaRT solution as a charged Myers-Perry instanton. Gravitational instantons are smooth euclidean solutions of vacuum Einstein's equations with or without a cosmoloical constant. They are well understood in four dimensions in the Euclidean gravity paradigm, however their higher dimensional cousins are not so well studied. We presented a Belinsky-Zakharov [79] inverse scattering construction for the five dimensional Myers Perry (MP) instanton starting from a five dimensional Euclidean Schwarzschild metric. The BZ method uses a dressing technique for a given seed solution to generate new solutions and is best applicable for generating solutions in four and five dimensional vacuum gravity. In the next step we dimensionally uplifted the five dimensional MP instanton to six dimensions by adding a flat timelike direction to it. We performed dimensional reduction from six to three dimensions over two spacelike and one timelike direction. The resultant three dimensional Lagrangian had $SO(4,4)$ global symmetry. We then performed $SO(4,4)$ charging transformation on the three dimensional coset matrix of the MP solution to generate D1, D5 and P charges and constructed a new coset matrix for JMaRT. We finally uplifted the solution to six dimensions and constructed the JMaRT metric in six dimensions. We also constructed the two form RR field C_2 in six dimensions and studied the rod structure for the over rotating Cvetič-Youm metrics. Our work was a generalisation and simplification of the construction presented earlier in [57].

The primary goal of the fuzzball program is to understand the microscopic description of blackholes. The initial studies focussed exclusively on BPS (supersymmetric) and near BPS geometries and were successful in extracting universal features of black hole microstates. In the BPS class, scaling solutions, multicenter bubbling geometries and families of superstratum solutions have been constructed by Bena,Warner, DeBoer, Shigemori, Russo, Giusto and others (for references look at chapter 2). Genuinely Non-BPS smooth solutions involve more computational complexity, and till date only a handful of non-extremal solutions have been constructed. The first non-supersymmetric black hole microstate solutions to be discovered were the solutions found by Jejjala, Madden, Ross and Titchener (often abbreviated to JMaRT) [3]. For other studies of non-supersymmetric black hole microstate solutions, see chapter 2. In our work [4] we extended the studies to genuinely non-supersymmetric fuzzball geometries by considering various orbifolds of JMaRT and analysing their microscopic descriptions. However, these non-supersymmetric solutions are still solutions in supergravity theories. Nevertheless, the non-supersymmetric fuzzball geometries are ideal testing grounds for many ideas that may lead to a deeper insight into the understanding of generic microstates for Schwarzchild and Kerr black holes and eventually astrophysical black holes as well.

In this thesis, we have mostly looked at single center black holes and related solutions from group theory perspective. It will be interesting to develop the requisite mathematical techniques to understand Geroch group description of multi-center black holes. This investigation can help us discover new classes of non-extremal multi-center black holes in supergravity theories and possibly new classes of non-extremal fuzzballs. Connecting our work to a recent construction by Bena, Bossard, Katmadas and Turton [162] will be an immediate direction to pursue.

Appendix A

Appendices for Chapter 3

A.1 Solving the wave equation via matched asymptotic expansion

In this appendix we solve the wave equation in a matched asymptotic expansion analysis. We obtain the instability frequencies and also fix the normalization of the wavefunction in the asymptotic region given its form in the inner region.

We define the following regions of the geometry, in which we set up the matched asymptotic expansion. In Section 3.1.2 we specified that when studying AdS/CFT on the JMaRT solutions, one works in the regime of parameters

$$\epsilon = \frac{(Q_1 Q_5)^{\frac{1}{4}}}{R} \ll 1. \tag{A.1}$$

In terms of the dimensionless radial variable x defined in Eq. (3.57), we define the 'inner region' to be the range $0 \leq x \ll \epsilon^{-2}$; to be more specific, let us introduce another parameter $\delta \ll 1$ and define the inner region to be given by[1]

$$0 \leq x \lesssim \delta \frac{1}{\epsilon^2}\,. \tag{A.2}$$

We then define the 'asymptotic region' to be given by the range

$$x \gtrsim \frac{1}{\delta}\frac{1}{\epsilon^2}\,. \tag{A.3}$$

The inner and asymptotic regions do not overlap. We will match solutions in the 'neck' region $x \sim \frac{1}{\epsilon^2}$, or more specifically

$$\delta \frac{1}{\epsilon^2} \lesssim x \lesssim \frac{1}{\delta}\frac{1}{\epsilon^2} \tag{A.4}$$

where solutions to the radial wave equation are power law in x [133]. Solutions from the inner and asymptotic regions match on to these power law solutions from the two sides.[2]

Inner region

In the inner region one can neglect $\kappa^2 x$ relative to the other terms, and so the radial wave equation (3.58) simplifies to

$$4\partial_x\left[x\left(x+\frac{1}{k^2}\right)\partial_x h\right] + \left(1-\nu^2+\frac{\xi^2}{x+k^{-2}}-\frac{\zeta^2}{x}\right)h = 0. \tag{A.5}$$

Demanding regularity at the origin we get the solution for this equation

$$h = \left(x+\frac{1}{k^2}\right)^{\frac{k\xi}{2}} x^{\frac{k|\zeta|}{2}} \left[{}_2F_1(a,b,c,-k^2x)\right], \tag{A.6}$$

[1]While one must consider ϵ to be exponentially small in order to get a large AdS inner region (see for example the discussion in [112]), here δ is simply a bookkeeping device. The important point is that the inner and asymptotic regions do not overlap, and must be matched onto the neck region.

[2]Note that the regions involved in the present matched asymptotic expansion analysis are different to those employed, e.g., in [112].

where

$$a = \frac{1}{2}(1 + \nu + k|\zeta| + k\xi), \qquad b = \frac{1}{2}(1 - \nu + k|\zeta| + k\xi), \qquad c = 1 + k|\zeta|. \tag{A.7}$$

In writing this solution we have chosen to normalize the wavefunction (A.6) by setting its overall normalization constant to unity. The behaviour of the inner solution near $x \to 0$ is simply $h \sim k^{-k\xi} x^{\frac{k|\zeta|}{2}}$, and its expansion for large x is

$$\begin{aligned} h \quad \simeq \quad & \Gamma(1 + k|\zeta|)\Big[\frac{k^{-1-\nu-k|\zeta|-k\xi}\Gamma(-\nu)}{\Gamma\left(\frac{1}{2}(1 - \nu + k|\zeta| + k\xi)\right)\Gamma\left(\frac{1}{2}(1 - \nu + k|\zeta| - k\xi)\right)} x^{-\frac{\nu+1}{2}} \\ & + \frac{k^{-1+\nu-k|\zeta|-k\xi}\Gamma(\nu)}{\Gamma\left(\frac{1}{2}(1 + \nu + k|\zeta| + k\xi)\right)\Gamma\left(\frac{1}{2}(1 + \nu + k|\zeta| - k\xi)\right)} x^{\frac{\nu-1}{2}}\Big]. \end{aligned} \tag{A.8}$$

We will match this onto the power law behaviour in the neck region below.

Asymptotic region

In the asymptotic region, one can neglect $\frac{\xi^2}{x+k^{-2}} - \frac{\zeta^2}{x}$ relative to the other terms, and so the radial wave equation simplifies to

$$\partial_x^2(xh) + \left[\frac{\kappa^2}{4x} + \frac{1 - \nu^2}{4x^2}\right](xh) = 0. \tag{A.9}$$

The most general solution to this equation is a linear combination of Bessel functions

$$h = \frac{1}{\sqrt{x}}\left[C_1 J_\nu(\kappa\sqrt{x}) + C_2 J_{-\nu}(\kappa\sqrt{x})\right]. \tag{A.10}$$

For $\kappa\sqrt{x} \ll 1$, its behaviour is

$$h \sim \frac{C_1}{\Gamma(1 + \nu)}\left(\frac{\kappa}{2}\right)^\nu x^{\frac{\nu-1}{2}} + \frac{C_2}{\Gamma(1 - \nu)}\left(\frac{\kappa}{2}\right)^{-\nu} x^{-\frac{\nu+1}{2}}, \tag{A.11}$$

and its large $\kappa\sqrt{x}$ behaviour is

$$h \sim \frac{1}{x^{\frac{3}{4}}}\frac{1}{\sqrt{2\pi\kappa}}\left[e^{i\kappa\sqrt{x}}e^{-i\frac{\pi}{4}}(C_1 e^{-i\nu\frac{\pi}{2}} + C_2 e^{i\nu\frac{\pi}{2}}) + e^{-i\kappa\sqrt{x}}e^{i\frac{\pi}{4}}(C_1 e^{i\nu\frac{\pi}{2}} + C_2 e^{-i\nu\frac{\pi}{2}})\right]. \quad (A.12)$$

Neck region

In the neck region, both $\kappa^2 x$ and $\frac{\xi^2}{x+k^{-2}} - \frac{\zeta^2}{x}$ can be neglected, and the wave equation approximates to

$$\partial_x^2(xh) + \left[\frac{1-\nu^2}{4x^2}\right](xh) = 0. \quad (A.13)$$

The general solution is

$$h = A\, x^{\frac{\nu-1}{2}} + B\, x^{-\frac{\nu+1}{2}}. \quad (A.14)$$

Matching the solutions

We can now match the solutions at each end of the neck region, and thereby patch together the three matching regions.

We are interested in instability of the geometry where there are no incoming waves, yet we have outgoing waves carrying energy and other charges to infinity. The requirement of no incoming waves gives the relation

$$C_1 + C_2 e^{-i\nu\pi} = 0. \quad (A.15)$$

Matching the two asymptotic expansions (A.8) and (A.11) to the solutions in the neck region, we obtain

$$-\,e^{-i\pi\nu}\frac{\Gamma(1-\nu)}{\Gamma(1+\nu)}\left(\frac{\kappa}{2k}\right)^{2\nu} = \frac{\Gamma(\nu)}{\Gamma(-\nu)}\frac{\Gamma\left(\frac{1}{2}(1-\nu+k|\zeta|+k\xi)\right)\Gamma\left(\frac{1}{2}(1-\nu+k|\zeta|-k\xi)\right)}{\Gamma\left(\frac{1}{2}(1+\nu+k|\zeta|+k\xi)\right)\Gamma\left(\frac{1}{2}(1+\nu+k|\zeta|-k\xi)\right)}. \quad (A.16)$$

The emission frequencies are given by the solutions to this transcendental equation.

Instability frequencies

Let us now analyze equation (A.16). Recall that we work in the large R limit, $\epsilon \ll 1$. In this limit, taking $\omega \sim 1/R$ and $\lambda \sim 1$, one finds $\kappa^2 \sim \epsilon^4$, as can be seen from Eqs. (B.26), (3.34), and (3.22). Therefore the LHS of equation (A.16) is parametrically small. The RHS is parametrically small when one of the Γ functions in the denominator is parametrically close to developing a pole. To leading order, the values of the parameters will be those which give poles. Let us set[3]

$$\frac{1}{2}(1+\nu+k|\zeta|+k\xi) \simeq -N, \tag{A.17}$$

with N a non-negative integer. From equations (3.62) and (3.63) we see that in the large R limit $\varrho \to 1$ and $\vartheta \sim \epsilon^2$. Hence to leading order one obtains

$$\xi \simeq \omega R - m_\phi \frac{n}{k} + m_\psi \frac{m}{k}, \tag{A.18}$$

$$\nu \simeq l+1. \tag{A.19}$$

Replacing these relations in equation (A.17) gives the leading order instability frequencies. To leading order, the instability frequencies are real; we define ω_R to be the real part of ω, thus obtaining

$$\omega_R \simeq \frac{1}{kR}\Big(-l - m_\psi m + m_\phi n - \big|-k\lambda - m_\psi n + m_\phi m\big| - 2(N+1)\Big). \tag{A.20}$$

At next-to-leading order, we will obtain the leading imaginary part of ω. To do this, we replace $N \to N + \delta N$ and eliminate ξ in favour of N. From equation (3.67) we have $\delta\xi = R\delta\omega$, which upon using (A.17) gives the change in ω due to shifting N to be

$$\delta\omega = -\frac{2}{kR}\delta N\,. \tag{A.21}$$

[3]Taking parameters for which the other Gamma function in the denominator of (A.16) develops a pole leads to an exponentially decaying mode, rather than an exponentially growing mode.

There are also contributions to the subleading part of ω from corrections to ν and ξ at order ϵ^2, however these affect only the real part of ω. Therefore, denoting by ω_I the imaginary part of ω, to leading order in ϵ we have

$$\omega_I \simeq -\frac{2}{kR}\mathrm{Im}(\delta N). \tag{A.22}$$

The small deformation δN controls the pole of the divergent Γ function. We assume that $\delta N \ll \epsilon$, so that to leading order in ϵ it can be neglected in the argument of all the other Γ functions. In what follows we shall verify the consistency of this assumption. The residue at the pole of the Γ function is given by

$$\Gamma(-N-\delta N) = \frac{(-1)^{N+1}}{N!}\frac{1}{\delta N}. \tag{A.23}$$

Using the relations

$$\Gamma(n+1+x) = xn![x]_n\Gamma(x), \qquad \Gamma(-n-x) = \frac{\Gamma(-x)}{(-1)^n n![x]_n}, \tag{A.24}$$

where $[x]_n = \prod_{i=1}^{n}\left(1+\frac{x}{i}\right)$, we obtain

$$\delta N = -e^{-i\pi\nu}\left(\frac{\nu\Gamma(-\nu)}{\Gamma(\nu)}\right)\left(\frac{\kappa}{2k}\right)^{2\nu}[\nu]_N[\nu]_{N+k|\zeta|}. \tag{A.25}$$

For p and q integers, we have $[p]_q = {}^{p+q}C_p = \binom{p+q}{p}$.

The identity

$$\Gamma(\nu)\Gamma(-\nu) = \frac{-\pi}{\nu\sin(\pi\nu)} \tag{A.26}$$

allows us to extract $\mathrm{Im}(\delta N)$. From (A.25) we obtain

$$\omega_I \simeq \frac{2}{kR}\frac{\pi}{\Gamma(\nu)^2}\left(\frac{\kappa}{2k}\right)^{2\nu}[\nu]_N[\nu]_{N+k|\zeta|}\,. \tag{A.27}$$

Recalling that $\nu = l + 1 + O(\epsilon^2)$, we observe that $\mathrm{Im}(\delta N) \sim \epsilon^{4l+4}$, and that $\mathrm{Re}(\delta N) \sim \epsilon^{4l+2}$, which demonstrates the consistency of our approach. Then to leading order the imaginary part of the frequency is

$$\omega_I \simeq \frac{1}{kR}\frac{\pi}{2^{2l+1}(l!)^2}\left[\left(\omega^2 - \frac{\lambda^2}{R^2}\right)\frac{Q_1 Q_5}{k^2 R^2}\right]^{l+1}\binom{N+l+1}{l+1}\binom{N+k|\zeta|+l+1}{l+1}. \tag{A.28}$$

A.2 Details of pair creation calculation

A.2.1 Normalization of the asymptotic region wavefunction

In this appendix we fix the normalization of the asymptotic region wavefunction, for use in Section 3.3.

Using the asymptotic region wavefunction (A.12) together with the requirement of only outgoing waves (A.15), we obtain

$$h_{\mathrm{out}}(x) = C_2 \frac{1}{\sqrt{2\pi\kappa}}\frac{1}{x^{\frac{3}{4}}} e^{i\kappa\sqrt{x}} e^{-i\frac{\pi}{4}}\left(e^{i\frac{\pi\nu}{2}} - e^{-i\frac{3\pi\nu}{2}}\right), \tag{A.29}$$

and thus

$$h_{\mathrm{out}}(x) h^*_{\mathrm{out}}(x) = |C_2|^2 \frac{2}{\pi|\kappa|}\frac{1}{x^{\frac{3}{2}}} e^{i(\kappa-\kappa^*)\sqrt{x}}\sin^2(\pi\nu). \tag{A.30}$$

Matching the two asymptotic expansions – (A.11) and (A.8) – say by comparing coefficients of $x^{\frac{\nu-1}{2}}$, we get an equation that determines C_2,

$$\frac{k^{-1+\nu-k|\zeta|-k\xi}\Gamma(1+k|\zeta|)\Gamma(\nu)}{\Gamma\left(\frac{1}{2}(1+\nu+k|\zeta|+k\xi)\right)\Gamma\left(\frac{1}{2}(1+\nu+k|\zeta|-k\xi)\right)} = (-C_2 e^{-i\pi\nu})\frac{1}{\Gamma(1+\nu)}\left(\frac{\kappa}{2}\right)^{\nu}. \tag{A.31}$$

To find the real and imaginary frequencies we matched the solution using

$$\Gamma\left(\frac{1}{2}(1+\nu+k|\zeta|+k\xi)\right) = \Gamma(-N-\delta N) = \frac{(-1)^{N+1}}{N!\delta N}. \tag{A.32}$$

Replacing this expression in (A.31) we get

$$\frac{k^{2N+2\nu}\Gamma(1+k|\zeta|)\Gamma(\nu)}{\Gamma(N+\nu+1+k|\zeta|)}(-1)^{N+1}N!\delta N=(-C_2e^{-i\pi\nu})\frac{1}{\Gamma(1+\nu)}\left(\frac{\kappa}{2}\right)^{\nu}. \tag{A.33}$$

Taking modulus of the above relation allows us to extract $|C_2|^2$. We get,

$$\frac{k^{4N+4\nu}\Gamma(1+k|\zeta|)^2\Gamma(\nu)^2\Gamma(N+1)^2}{\Gamma(N+\nu+1+k|\zeta|)^2}(\delta N)(\delta N)^*=|C_2|^2\frac{1}{\Gamma(1+\nu)^2}\left(\frac{|\kappa|}{2}\right)^{2\nu}. \tag{A.34}$$

We now use (A.25), and working to leading order in ϵ, we approximate $|\kappa|^2\simeq\kappa^2$. For use in the main text, it is convenient to extract one power of ω_I using (A.27). We thus obtain

$$|C_2|^2\sin^2(\pi\nu)=\frac{\pi}{2}k^{4N+2\nu}(kR)\omega_I\,\frac{\Gamma(1+k|\zeta|)^2\,\Gamma(N+1)\,\Gamma(N+\nu+1)}{\Gamma(N+\nu+1+k|\zeta|)\,\Gamma(N+1+k|\zeta|)}. \tag{A.35}$$

A.2.2 A hypergeometric function identity

Identity: For positive γ and for arbitrary positive integers N and l,

$$\begin{aligned}&\int_0^\infty d\rho\rho^{2\gamma+1}(1+\rho^2)^{-2N-l-3-\gamma}({}_2F_1(-N,-N-l-1,1+\gamma,-\rho^2))^2\\&=\frac{1}{2(2N+\gamma+l+2)}\frac{\Gamma(1+\gamma)^2\,\Gamma(N+1)\,\Gamma(N+l+2)}{\Gamma(N+\gamma+l+2)\,\Gamma(N+\gamma+1)}.\end{aligned} \tag{A.36}$$

Proof: A proof of the above identity can be given by relating hypergeometric functions in the integral to Jacobi polynomials. From identity 8.962.1 (third line) of Gradshteyn and Ryzhik [171], page 999, we have

$$P_N^{(\gamma,l+1)}(y)=\frac{\Gamma(N+1+\gamma)}{\Gamma(N+1)\Gamma(1+\gamma)}\left(\frac{1+y}{2}\right)^N{}_2F_1\left(-N,-N-l-1,1+\gamma,\frac{y-1}{y+1}\right). \tag{A.37}$$

Defining

$$\frac{y-1}{y+1}=-\rho^2, \tag{A.38}$$

the integral can be converted into

$$\frac{1}{2^{\gamma+l+3}}\left(\frac{\Gamma(N+1)\Gamma(1+\gamma)}{\Gamma(N+1+\gamma)}\right)^2\int_{-1}^{1}dy(1-y)^{\gamma}(1+y)^{l+1}\left(P_N^{(\gamma,l+1)}(y)\right)^2, \tag{A.39}$$

which simply gives the right hand side of (A.36) upon using identity 7.391.1 (second line) on page 806 of [171].

A.3 Conventions

In this appendix we record our conventions and their relation to those of Ref. [122], which we use to obtain Eq. (3.93) of the main text.

Our conventions are that

$$\text{left-moving} \quad \leftrightarrow \quad \text{holomorphic} \quad \leftrightarrow \quad \text{positive } P_y, \tag{A.40}$$

where P_y is momentum along y. So the holomorphic coordinate in the CFT is related to the null coordinate $v = (t - y)$ in the spacetime.

Our map between CFT and gravity SU(2) quantum numbers is given in (3.88),

$$m_\psi \;=\; -(m+\bar{m}), \qquad m_\phi \;=\; (m-\bar{m}). \tag{A.41}$$

Let us compare our conventions to those of Avery-Chowdhury [122], whose quantities we denote with a superscript AC. In that paper, the anti-holomorphic coordinate corresponds to positive y. Therefore we interchange L and R in mapping between the two papers, so the spectral flow parameters are

$$\alpha \;=\; \bar{\alpha}^{AC}, \qquad \bar{\alpha} \;=\; \alpha^{AC}. \tag{A.42}$$

Next, the parameter controlling the twist is

$$\kappa^{AC} \;=\; k\,. \tag{A.43}$$

In the conventions of [122], the emission of a scalar with gravity quantum numbers $(l, m_\psi^{AC}, m_\phi^{AC})$ corresponds to the CFT vertex

$$\mathcal{V}_{l,-m_\psi^{AC},-m_\phi^{AC}} \tag{A.44}$$

where

$$-m_\psi^{AC} \;=\; l - k^{AC} - \bar{k}^{AC}\,, \qquad -m_\phi^{AC} \;=\; k^{AC} - \bar{k}^{AC}\,. \tag{A.45}$$

In addition, similarly to our conventions we have the relation

$$m_\psi^{AC} \;=\; -(m^{AC} + \bar{m}^{AC})\,, \qquad m_\phi^{AC} \;=\; m^{AC} - \bar{m}^{AC}\,. \tag{A.46}$$

Since L and R are interchanged between the two papers, we have

$$m_L \;=\; \bar{m}^{AC}\,, \quad m_R \;=\; m^{AC} \quad \Rightarrow \quad m_\psi \;=\; m_\psi^{AC}\,, \quad m_\phi \;=\; -\,m_\phi^{AC}\,. \tag{A.47}$$

Therefore we obtain

$$k^{AC} \;=\; \frac{1}{2}\Big(l + m_\psi + m_\phi\Big)\,, \qquad \bar{k}^{AC} \;=\; \frac{1}{2}\Big(l + m_\psi - m_\phi\Big)\,. \tag{A.48}$$

Using these relations in Eq. (10.3) of [122], we arrive at (3.93).

Appendix B

Appendix for Chapter 4

B.1 Coset models

In this appendix we present construction of relevant coset models. The discussion below is fairly standard, to set up our notation for the main text we present certain details.

B.1.1 SL(3, $\mathbb{R}$)/SO(2,1)

Let us start with a discussion of SL(3, $\mathbb{R}$)/SO(2,1) coset relevant for five-dimensional vacuum gravity. The Lagrangian for vacuum gravity is $\mathcal{L}_5 = R_5 \star 1$. We perform KK reduction to three dimensions using the ansatz [153]

$$ds_5^2 = e^{\frac{1}{\sqrt{3}}\phi_1+\phi_2} ds_3^2 + \epsilon_2 e^{\frac{\phi_1}{\sqrt{3}}-\phi_2} \left(dz_4 + \mathcal{A}^2_{(1)}\right)^2 + \epsilon_1 e^{-\frac{2\phi_1}{\sqrt{3}}} \left(dz_5 + \chi_1 dz_4 + \mathcal{A}^1_{(1)}\right)^2, \quad \text{(B.1)}$$

where reduction is first done along z_5 and then along z_4. Here ϵ_1 and ϵ_2 take values ± 1, they respectively denote the signature of the first and second direction over which reduction from five to three dimensions is performed. We will take one of them to be -1 and the other $+1$.

The reduced three-dimensional Lagrangian in terms of the fields appearing in (B.1) is

$$\begin{aligned}\mathcal{L}_3 &= R_3 \star 1 - \frac{1}{2} \star d\vec{\phi} \wedge d\vec{\phi} - \frac{1}{2}\epsilon_1\epsilon_2 e^{-\sqrt{3}\phi_1+\phi_2} \star \mathcal{F}_{(1)} \wedge \mathcal{F}_{(1)} \\ &\quad -\frac{1}{2}\epsilon_1 e^{-\sqrt{3}\phi_1-\phi_2} \star \mathcal{F}^1_{(2)} \wedge \mathcal{F}^1_{(2)} - \frac{1}{2}\epsilon_2 e^{-2\phi_2} \star \mathcal{F}^2_{(2)} \wedge \mathcal{F}^2_{(2)},\end{aligned} \tag{B.2}$$

where

$$\mathcal{F}_{(1)} = d\chi_1, \qquad \mathcal{F}^1_{(2)} = d\mathcal{A}^1_{(1)} + \mathcal{A}^2_{(1)} \wedge d\chi_1, \qquad \mathcal{F}^2_{(2)} = d\mathcal{A}^2_{(1)}, \tag{B.3}$$

are the field strengths for χ_1, $\mathcal{A}^1_{(1)}$, and $\mathcal{A}^2_{(1)}$ respectively. Adding the Lagrange multiplier terms

$$-\chi_2 d(\mathcal{F}^1_{(2)} - \mathcal{A}^2_{(1)} \wedge d\chi_1) - \chi_3 d\mathcal{F}^2_{(2)}, \tag{B.4}$$

and eliminating $\mathcal{F}^1_{(2)}$ and $\mathcal{F}^2_{(2)}$ we obtain the duality relations

$$\epsilon_1 e^{-\sqrt{3}\phi_1-\phi_2} \star \mathcal{F}^1_{(2)} = d\chi_2, \qquad \epsilon_2 e^{-2\phi_2} \star \mathcal{F}^2_{(2)} = d\chi_3 - \chi_1 d\chi_2. \tag{B.5}$$

In terms of the dualized variables the reduced three-dimensional Lagrangian becomes

$$\begin{aligned}\mathcal{L} &= R \star 1 - \frac{1}{2} \star d\vec{\phi} \wedge d\vec{\phi} - \frac{1}{2}\epsilon_1\epsilon_2 e^{-\sqrt{3}\phi_1+\phi_2} \star d\chi_1 \wedge d\chi_1 - \frac{1}{2}\epsilon_2 e^{\sqrt{3}\phi_1+\phi_2} \star d\chi_2 \wedge d\chi_2 \\ &\quad -\frac{1}{2}\epsilon_1 e^{2\phi_2} \star (d\chi_3 - \chi_1 d\chi_2) \wedge (d\chi_3 - \chi_1 d\chi_2).\end{aligned} \tag{B.6}$$

To obtain Lagrangian (B.6) from a coset construction we choose the basis for the fundamental representation of SL(3) where the Cartan-Weyl generators take the form,

$$h_1 = \frac{1}{\sqrt{3}}\begin{pmatrix} 1 & 0 & 0 \\ 0 & -2 & 0 \\ 0 & 0 & 1 \end{pmatrix}, \quad h_2 = \begin{pmatrix} 1 & 0 & 0 \\ 0 & 0 & 0 \\ 0 & 0 & -1 \end{pmatrix}, \quad e_1 = \begin{pmatrix} 0 & 0 & 0 \\ 0 & 0 & 1 \\ 0 & 0 & 0 \end{pmatrix}, \quad e_2 = \begin{pmatrix} 0 & 1 & 0 \\ 0 & 0 & 0 \\ 0 & 0 & 0 \end{pmatrix}, \tag{B.7}$$

and $e_3 = [e_2, e_1]$. The lowering generators are simply $f_i = e_i^T$. In this basis the positive roots are

$$\alpha_1 = (-\sqrt{3}, 1), \qquad \alpha_2 = (\sqrt{3}, 1), \qquad \alpha_3 = \alpha_1 + \alpha_2 = (0, 2), \tag{B.8}$$

and the negative roots are $-\alpha_1, -\alpha_2, -\alpha_3$.

We are interested in dimensional reduction of five-dimensional vacuum gravity over one timelike and one spacelike Killing direction. Since a timelike direction is involved, the standard Chevalley involution that expresses the symmetry between positive and negative roots does not define the coset of interest. The pertinent involution is,

$$\tau(h_1) = -h_1, \quad \tau(h_2) = -h_2, \quad \tau(e_1) = -\epsilon_1\epsilon_2 f_1, \quad \tau(e_2) = -\epsilon_2 f_2, \quad \tau(e_3) = -\epsilon_1 f_3, \tag{B.9}$$

where $\epsilon_{1,2} = \pm 1$. When $\epsilon_1 = \epsilon_2 = +1$ we get back the Chevalley involution. The involution (B.9) defines the generalized transposition

$$x^\sharp = -\tau(x), \quad \forall \quad x \in \mathfrak{sl}(3, \mathbb{R}), \tag{B.10}$$

that can be implemented as matrix multiplication via

$$x^\sharp = \eta x^T \eta, \qquad \text{where} \qquad \eta = \mathrm{diag}(1, \epsilon_2, \epsilon_1). \tag{B.11}$$

We note that $\eta^T = \eta^{-1} = \eta$. The Lie algebra generators that are invariant under the involution are

$$k_1 = e_1 - e_1^\sharp, \qquad k_2 = e_2 - e_2^\sharp, \qquad k_3 = e_3 - e_3^\sharp. \tag{B.12}$$

For the case $\epsilon_1 = -1, \epsilon_2 = +1$ or $\epsilon_1 = +1, \epsilon_2 = -1$ these generators form an $\mathfrak{so}(2, 1)$ Lie algebra.

The three-dimensional scalar Lagrangian (B.6) can be parameterized by the SL(3, $\mathbb{R}$)/SO(2,1) coset representative

$$\mathcal{V} = e^{\frac{1}{2}\phi_1 h_1} e^{\frac{1}{2}\phi_2 h_2} e^{\chi_1 e_1} e^{\chi_2 e_2} e^{\chi_3 e_3}. \tag{B.13}$$

From the coset representative we construct $M = \mathcal{V}^\sharp \mathcal{V}$. The three-dimensional Lagrangian can then be written as

$$\mathcal{L}'_3 = R \star 1 - \frac{1}{4}\mathrm{tr}(\star(M^{-1}dM) \wedge (M^{-1}dM)). \tag{B.14}$$

This form of the Lagrangian makes it manifestly invariant under SL(3, $\mathbb{R}$).

B.1.2 SU(2, 1)/(SL(2, $\mathbb{R}$) × U(1))

Let us start by performing timelike Kaluza-Klein reduction from four to three dimensions of the four-dimensional Einstein-Maxwell theory. In our conventions the Lagrangian is

$$\mathcal{L} = R \star 1 - 2 \star F \wedge F, \tag{B.15}$$

where $F = dA$. We reduce it to three-dimensions using the ansatz

$$ds_4^2 = -e^{-\phi}(dt + \omega)^2 + e^{\phi} ds_3^2, \tag{B.16}$$

$$A = \chi_e dt + \tilde{A}. \tag{B.17}$$

All quantities on the right hand sides of equations (B.16) and (B.17) are independent of the time coordinate t. The reduced three-dimensional Lagrangian takes the form

$$\mathcal{L}_3 = R \star 1 - \frac{1}{2} \star d\phi \wedge d\phi + \frac{1}{2} e^{-2\phi} \star \mathcal{F} \wedge \mathcal{F} - 2e^{-\phi} \star \tilde{F} \wedge \tilde{F} + 2e^{\phi} \star d\chi_e \wedge d\chi_e, \tag{B.18}$$

where

$$\mathcal{F} = d\omega, \qquad \tilde{F} = d\tilde{A} - d\chi_e \wedge \omega. \tag{B.19}$$

Adding the Lagrange multiplier terms

$$-4d\chi_m \wedge \tilde{F} - (2\chi_m d\chi_e - 2\chi_e d\chi_m + \sqrt{2}d\psi) \wedge \mathcal{F}, \tag{B.20}$$

and eliminating $\tilde{F}$ and $\mathcal{F}$ we obtain the duality relations

$$\tilde{F} = -e^{\phi} \star d\chi_m, \tag{B.21}$$

$$\mathcal{F} = e^{2\phi} \star (2\chi_m d\chi_e - 2\chi_e d\chi_m + \sqrt{2}d\psi). \tag{B.22}$$

The dualized Lagrangian then takes the form

$$\begin{aligned} \mathcal{L}_3' = \; & R \star 1 - \frac{1}{2} \star d\phi \wedge d\phi + 2e^{\phi}(\star d\chi_e \wedge d\chi_e + \star d\chi_m \wedge d\chi_m) \\ & -e^{2\phi} \star (d\psi + \sqrt{2}\chi_m d\chi_e - \sqrt{2}\chi_e d\chi_m) \wedge (d\psi + \sqrt{2}\chi_m d\chi_e - \sqrt{2}\chi_e d\chi_m). \end{aligned} \tag{B.23}$$

The Lagrange multiplier terms (B.20) are chosen in such a way that in the three-dimensional Lagrangian (B.23) the electric and magnetic scalars χ_e and χ_m appear in a symmetrical manner. In equation (B.23) there are some sign changes compared to the standard spacelike reduction: the three-dimensional Lagrangian for that case can be obtained by a "Wick rotation" of the Maxwell scalars

$$\chi_e \to -i\chi_e, \qquad \chi_m \to i\chi_m, \qquad \psi \to -\psi. \tag{B.24}$$

p The scalar part of the three-dimensional Lagrangian (B.23) can be identified with the coset $SU(2,1)/(SL(2,\mathbb{R}) \times U(1))$. We describe this construction in the rest of this appendix. For the case of the spacelike reduction the corresponding coset is

$$SU(2,1)/(SU(2) \times U(1)). \tag{B.25}$$

Naturally, the change in the denominator group has its origin in different signs for the kinetic terms in (B.23) corresponding to the timelike or spacelike reduction.

In order to describe the coset construction, let us start by recalling some basic properties of the group SU(2,1). In our conventions the group SU(2,1) is defined by the set of unit determinant (3×3) *complex* matrices g that preserve a metric κ of signature $(+, +, -)$:

$$\mathrm{SU}(2,1) = \left\{ g \in \mathrm{SL}(3,\mathbb{C}) : g^\dagger \kappa g = \kappa \right\} \qquad \text{with} \qquad \kappa = \begin{pmatrix} 0 & 0 & -1 \\ 0 & 1 & 0 \\ -1 & 0 & 0 \end{pmatrix}. \tag{B.26}$$

The associated Lie algebra is denoted as $\mathfrak{su}(2,1)$. The $\mathfrak{su}(2,1)$ Lie algebra is a non-split real form of $\mathfrak{sl}(3,\mathbb{C})$. In the basis (B.7)[1] it is described by the real span of the following linear combinations of the $\mathfrak{sl}(3,\mathbb{C})$ generators

$$\{i\sqrt{3}h_1, h_2, e_1 + e_2, f_1 + f_2, i(e_2 - e_1), i(f_2 - f_1), ie_3, if_3\}. \tag{B.27}$$

It can be readily checked using the matrix representation given above that these linear combinations of generators satisfy $x^\dagger \kappa + \kappa x = 0$. The generators $\{i\sqrt{3}h_1, h_2\}$ belong to the Cartan subalgebra of $\mathfrak{su}(2,1)$, $\{e_1 + e_2, i(e_2 - e_1), ie_3\}$ are the positive generators while $\{f_1 + f_2, i(f_2 - f_1), if_3\}$ are the negative generators. The two subalgebras that play important role in our analysis are (*i*) the maximally compact subalgebra

$$\mathfrak{su}(2) \oplus \mathfrak{u}(1) = \{x \in \mathfrak{su}(2,1) : x^\dagger = -x\}, \tag{B.28}$$

that defines the $\mathrm{SU}(2,1)/(\mathrm{SU}(2) \times \mathrm{U}(1))$ coset, and (*ii*) the maximally non-compact subalgebra

$$\mathfrak{sl}(2,\mathbb{R}) \oplus \mathfrak{u}(1) = \{x \in \mathfrak{su}(2,1) : x^\dagger = -\eta x \eta^{-1}\}, \tag{B.29}$$

where $\eta = \mathrm{diag}\{1, -1, 1\}$ that defines the $\mathrm{SU}(2,1)/(\mathrm{SL}(2,\mathbb{R}) \times \mathrm{U}(1))$ coset. Explicit linear combinations of generators that make these subalgebras manifest can be found in [172].

[1] Recall that the real span of the $\mathfrak{sl}(3,\mathbb{C})$ generators in the Cartan-Weyl basis gives the $\mathfrak{sl}(3,\mathbb{R})$ Lie algebra – the split real form of $\mathfrak{sl}(3,\mathbb{C})$.

We define generalized transposition as

$$x^\sharp := \eta x^\dagger \eta^{-1} \quad \forall \quad x \in \mathfrak{su}(2,1). \tag{B.30}$$

The three-dimensional scalar Lagrangian in equation (B.23) can be parameterized by the coset representative (see e.g. reference [172])

$$\mathcal{V} = \exp\left[\frac{1}{2}\phi h_2\right] \cdot \exp\left[\sqrt{2}\chi_e(e_1 + e_2) + \sqrt{2}\chi_m(i(e_2 - e_1)) + \sqrt{2}\psi(ie_3)\right]. \tag{B.31}$$

From the coset representative we construct

$$M = \mathcal{V}^\sharp \mathcal{V}. \tag{B.32}$$

The three-dimensional Lagrangian (B.23) can now be written as

$$\mathcal{L}'_3 = R \star 1 - \frac{1}{4}\text{tr}(\star(M^{-1}dM) \wedge (M^{-1}dM)). \tag{B.33}$$

This form of the Lagrangian makes it manifestly invariant under SU(2,1) with $M \to M' = g^\sharp M g$, where g is any SU(2,1) matrix.

Appendix C

Appendices for Chapter 5

C.1 Inverse scattering construction of the Myers-Perry instanton

In the interest of providing a complete derivation of the JMaRT solutions, we present in this Appendix all the details necessary to generate the Myers-Perry instanton from the Euclidean Schwarzschild solution using the Inverse Scattering Method (ISM). As is well known, the procedure is not uniquely determined. Below we describe, step by step, one such way of generating this solution. To set the context, and also to fix some notation, we begin by offering a very concise account of the formalism.

Overview of the procedure

Recall that solutions of the vacuum Einstein equations in $D = 5$ dimensions, $R_{\mu\nu} = 0$, that are both stationary and (doubly-)axially symmetric (thus possessing $D - 3$ commuting

Killing vector fields) can always be expressed in canonical coordinates in the form [157][1]

$$ds^2 = G_{ab}(\rho, z)\, dx^a dx^b + e^{2\nu(\rho,z)}(d\rho^2 + dz^2)\,, \qquad \text{with} \quad \det G = \rho^2\,. \tag{C.1}$$

In these coordinates the vacuum Einstein equations yield a decoupled elliptic PDE for the Killing metric G_{ab}. This can be equivalently formulated as a system of *first order linear* equations (the Lax pair) for the so-called generating matrix, which depends on an additional variable (the spectral parameter). A linear transformation on this generating matrix — in standard terminology, one refers to it getting *dressed* — takes us to a new solution of the same field equations. Under the assumption of a linear transformation that adds only simple poles in the spectral parameter complex plane (i.e. a *solitonic* transformation) the whole procedure reduces to a sequence of algebraic calculations [79–81]. The determination of the *conformal factor* $e^{2\nu}$ can be straightforwardly accomplished by a line integral once the Killing matrix is found. Nevertheless, even this can be sidestepped since the conformal factor of the new solution can be directly obtained from that of the seed solution via another simple algebraic evaluation.

Details of the ISM construction

After this lightening review of the ISM, we now move on to the construction of the 5D Euclideanized Myers-Perry geometry, closely following Pomeransky's derivation of 5D Lorentzian Myers-Perry [166]. This instanton can be connected with the zero-charge JMaRT solution by later adding a flat timelike direction [57]. The construction proceeds as follows:

1. The starting point is the diagonal metric corresponding to 5D Euclidean Schwarzschild, which is written in the form (C.1), with $G = G_0$ and $\nu = \nu_0$ (the "0" in the subscript

[1] Since we are working in the Euclidean section, the determinant of the *Killing matrix* G_{ab} is positive. For Lorentzian solutions we would have an extra minus sign on the far right hand side of (C.1).

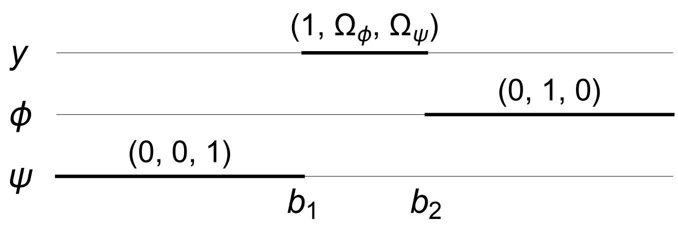

Figure C.1: Rod diagram for the 5D Euclidean Myers-Perry geometry. The direction for each rod is indicated above the corresponding segment. The rod diagram for the seed solution (Euclidean Schwarzschild) is trivially obtained by setting both "angular velocities" Ω_ϕ and Ω_ψ to zero. The points b_1 and b_2 indicate turning points where regularity of the solution has to be checked explicitly.

refers to the seed solution),

$$(G_0)_{ab} = \text{diag}\left\{\frac{\mu_1}{\mu_2}, \mu_2, \frac{\rho^2}{\mu_1}\right\}. \tag{C.2}$$

The rod diagram for such a solution is displayed in Fig. C.1 (Ω_ϕ and Ω_ψ must be set to zero). The Killing sector is parametrized by coordinates (y, ϕ, ψ) and the solitons and anti-solitons are defined, respectively, by

$$\mu_i = \sqrt{\rho^2 + (z - b_i)^2} - (z - b_i), \qquad \overline{\mu}_i = -\sqrt{\rho^2 + (z - b_i)^2} - (z - b_i). \tag{C.3}$$

They satisfy $\mu_i \overline{\mu}_i = -\rho^2$.

2. The conformal factor for this seed is algorithmically determined by following the procedure described in Ref. [173],

$$e^{2\nu_0} = k^2 \frac{\mu_2\left(\mu_1\mu_2 + \rho^2\right)}{\left(\mu_1^2 + \rho^2\right)\left(\mu_2^2 + \rho^2\right)}. \tag{C.4}$$

The multiplicative constant k can be fixed by requiring asymptotic flatness.

3. From the seed Killing matrix (C.2) we[2]:

[2]This step is necessary in $D > 4$ to ensure that the final solution satisfies the constraint $\det G = \rho^2$ in Eq. (C.1). R efer to e.g. Refs. [174–176] for concise accounts of the details of the ISM procedure.

(a) remove a soliton at $z = b_1$ with trivial BZ vector $m_0^{(1)} = (0, 0, 1)$, which amounts to dividing $G_{\psi\psi}$ by $-\rho^2/\mu_1^2$;

(b) remove an anti-soliton at $z = b_2$ with trivial BZ vector $m_0^{(2)} = (0, 1, 0)$, which amounts to dividing $G_{\phi\phi}$ by $-\mu_2^2/\rho^2$;

(c) multiply the whole matrix by a factor $-\mu_2/\mu_1$, for convenience.

The Killing matrix thus obtained is

$$(G'_0)_{ab} = \text{diag}\{-1, \overline{\mu_1}, \mu_2\} . \tag{C.5}$$

This will serve as the seed for the next solitonic transformation.

4. Now we add the (anti-)solitons that we removed previously but with nontrivial BZ vectors. Namely, we:

(a) add a soliton at $z = b_1$ with BZ vector $m_0'^{(1)} = (A_1, 0, C_1)$;

(b) add an anti-soliton at $z = b_2$ with BZ vector $m_0'^{(2)} = (A_2, B_2, 0)$.

At this stage we have obtained a new Killing matrix. Clearly, if we set $A_1 = A_2 = 0$ and $C_1 = B_2 = 1$ (and rescale to revert step 3.(c)) this just undoes the previous step and so we must retrieve the original solution. It is the presence of non vanishing coefficients A_i that mixes y (Euclidean time) and angular components. In the Lorentzian picture this would correspond to turning on angular velocities.

5. Rescale again the Killing matrix (multiply it by $-\mu_1/\mu_2$) to undo the scaling of step 3.(c). This yields a physical metric satisfying the constraint $\det G = \rho^2$. However, the orientation of the rods is non standard: the solitonic transformation performed to mix y direction and angular components simultaneously rotated the directions of the outermost rods. So an analysis of the rods' orientation must be done at this point, which we turn to next.

6. It is convenient to set $b_1 = -b_2 = -\alpha$, with $\alpha > 0$, without loss of generality[3]. A rod structure analysis reveals that:

   (a) the rightmost rod (rod 3: $\rho = 0,\ z > \alpha$) has orientation $\left(-\frac{4\alpha A_2}{B_2}, 1, \frac{4\alpha A_1 A_2}{B_2 C_1}\right)$;

   (b) the leftmost rod (rod 1: $\rho = 0,\ z < -\alpha$) has orientation $\left(-\frac{4\alpha A_1}{C_1}, \frac{4\alpha A_1 A_2}{B_2 C_1}, 1\right)$.

   As a useful check, we confirm that a trivial solitonic transformation ($A_i = 0$) does not change the direction of the rods.

7. The linear transformation $G \to \Lambda^T G \Lambda$, with

$$\Lambda = \begin{pmatrix} 1 & -4A_2C_1\alpha & -4A_1B_2\alpha \\ 0 & B_2C_1 & 4A_1A_2\alpha \\ 0 & 4A_1A_2\alpha & B_2C_1 \end{pmatrix}, \tag{C.6}$$

   brings us back to standard orientation (so that rod 1 and rod 3 are aligned with directions $(0, 0, 1)$ and $(0, 1, 0)$, respectively). In the process the finite middle rod 2 acquires direction $(1, \Omega_\phi, \Omega_\psi)$, where

$$\Omega_\phi = \frac{A_2}{C_1(4\alpha A_2^2 - B_2^2)}, \qquad \Omega_\psi = \frac{A_1}{B_2(4\alpha A_1^2 - C_1^2)}. \tag{C.7}$$

   We have thus generated the Euclidean Myers-Perry solution.

Final metric in convenient coordinates

The solution as obtained above (but not explicitly shown), written in canonical coordinates (ρ, z), is not particularly illuminating and it is desirable to express it in a more compact form. One useful system is the choice of prolate spherical coordinates (u, v), related with

[3]The metric (C.1) with G and $e^{2\nu}$ depending on z only through the combinations μ_i is invariant under simultaneous shifts of the z coordinate and the b_i parameters.

the canonical coordinates through

$$\rho = \alpha \sqrt{(u^2 - 1)(1 - v^2)}\,, \qquad z = \alpha u v\,, \tag{C.8}$$

where $u \geq 1$ and $-1 \leq v \leq 1$.

Besides changing coordinates, it is also convenient to redefine the parameters. The parameters characterising the solution are $\alpha, A_1/B_2, A_2/C_1$. The dependence of the solution only on the ratios A_1/B_2 and A_2/C_1 is a consequence of the invariance of the ISM procedure under rescalings of the BZ vectors, $m_0^{(i)} \to \lambda_i m_0^{(i)}$, with $\lambda_i \neq 0$. Following Pomeransky [166] we fix the normalisation

$$B_2^2 C_1^2 - 16\alpha^2 A_1^2 A_2^2 = 1\,, \tag{C.9}$$

which simplifies intermediate steps of the calculation. Then we define

$$M = -4\alpha\left(4\alpha A_1^2 - C_1^2\right)\left(4\alpha A_2^2 - B_2^2\right), \tag{C.10}$$

$$a_1 = 4\alpha A_2 C_1\,, \tag{C.11}$$

$$a_2 = 4\alpha A_1 B_2\,. \tag{C.12}$$

Note that α, a_1, a_2 and M are not all independent since they satisfy

$$M = a_1^2 + a_2^2 - 2\sqrt{4\alpha^2 + a_1^2 a_2^2}\,. \tag{C.13}$$

The requirement that α should be real and positive, i.e., the location of rod endpoints are as described above, implies

$$M < (a_1 - a_2)^2. \tag{C.14}$$

After applying all these transformations we obtain the Euclidean Myers-Perry solution in prolate spherical coordinates. We present the final metric in a different set of coordinates, (r, θ), closely related to the coordinates used in the Cvetič-Youm and JMaRT papers. They are related with (u, v) through

$$\alpha^2 \left(u^2 - 1\right)\left(1 - v^2\right) = \frac{r^2}{4}\Delta \sin^2(2\theta)\,, \qquad \alpha u v = \frac{r^2}{2}\left(1 - \frac{a_1^2 + a_2^2 - M}{2r^2}\right)\cos(2\theta)\,, \quad \text{(C.15)}$$

where

$$\Delta \equiv r^2\left(1 - \frac{a_1^2}{r^2}\right)\left(1 - \frac{a_2^2}{r^2}\right) + M\,. \quad \text{(C.16)}$$

It is convenient to introduce the following combination:

$$\Sigma = r^2 - a_1^2 \cos^2\theta - a_2^2 \sin^2\theta. \quad \text{(C.17)}$$

In terms of these new coordinates the metric is expressed as

$$\begin{aligned} ds^2 =& dy^2 + \frac{M}{\Sigma}\left[dy + a_1 \sin^2\theta\, d\phi + a_2 \cos^2\theta\, d\psi\right]^2 \\ &+ (r^2 - a_1^2)\sin^2\theta\, d\phi^2 + (r^2 - a_2^2)\cos^2\theta\, d\psi^2 + \frac{\Sigma}{\Delta}dr^2 + \Sigma\, d\theta^2. \end{aligned} \quad \text{(C.18)}$$

This metric is to be compared with the five-dimensional spatial part of Eq. (4.13) in Ref. [57], which corresponds to the singly spinning case. Indeed, that line element is recovered by setting $a_2 = 0$, and redefining $r \to \tilde{r}$ (note that Σ becomes equal to $\tilde{f}$ in [57].)

C.2 From 6d to 3d and back

In this appendix we present some details on 6d to 3d reduction. We follow conventions of [8]. We focus on details complementary to what is already presented in that reference.

Notation

A well known truncation of IIB supergravity on T^4 has 6D Lagrangian

$$\mathbb{L}_6 = R_6 \star_6 1 - \frac{1}{2} \star_6 d\Phi \wedge d\Phi - \frac{1}{2} e^{\sqrt{2}\Phi} \star_6 F_{[3]} \wedge F_{[3]}, \tag{C.19}$$

where the field strength $F_{[3]} = dC_{[2]}$ comes from the RR sector of the ten-dimensional IIB theory. As discussed in appendix A of [8] upon dimensional reduction on a spacelike circle the 6D theory reduces to the $U(1)^3$ supergravity in 5D. The reduction ansatz for the metric and the 3-form field strength are

$$ds_6^2 = e^{-\sqrt{\frac{3}{2}}\Psi}(dz_6 + A^1_{[1]})^2 + e^{\frac{\Psi}{\sqrt{6}}} ds_5^2, \tag{C.20}$$

$$F_{[3]} = F^{5d}_{[3]} + dA^2_{[1]} \wedge (dz_6 + A^1_{[1]}), \tag{C.21}$$

with

$$F^{(5d)}_{[3]} = dC^{(5d)}_{[2]} - dA^2_{[1]} \wedge A^1_{[1]}. \tag{C.22}$$

After dualizing $C^{(5d)}_{[2]}$ to a vector $A^3_{[1]}$ in 5D using the method of Lagrange multipliers, the triality structure of $U(1)^3$ supergravity becomes manifest.

Now we have obtained two scalars in five-dimensions, namely Ψ and Φ. We parameterise the $U(1)^3$ supergravity scalars as

$$h^1 = e^{\sqrt{\frac{2}{3}}\Psi}, \quad h^2 = e^{-\sqrt{\frac{1}{6}}\Psi - \sqrt{\frac{1}{2}}\Phi}, \quad h^3 = e^{-\sqrt{\frac{1}{6}}\Psi + \sqrt{\frac{1}{2}}\Phi}, \tag{C.23}$$

which manifestly satisfy $h^1 h^2 h^3 = 1$. Further dimensional reduction along a spacelike direction with the ansatz

$$ds_5^2 = f^2(dz_5 + \check{A}^0_{[1]})^2 + f^{-1}ds_4^2, \tag{C.24}$$

$$A^I_{[1]} = \check{A}^I_{[1]} + \chi^I(dz_5 + \check{A}^0_{[1]}), \tag{C.25}$$

gives rise to the $N = 2$ STU model in 4D. The scalars χ^I and h^I combine to form complex scalars of the STU theory $z^I = -\chi^I + ifh^I \equiv x^I + iy^I$.

Further dimensional reduction over a timelike direction gives an $\mathrm{SO}(4,4)/(\mathrm{SO}(2,2) \times \mathrm{SO}(2,2))$ coset model. The ansatz for this reduction step is

$$ds_4^2 = -e^{2U}(dt + \omega_3)^2 + e^{-2U}ds_3^2, \tag{C.26}$$

$$\check{A}^\Lambda_{[1]} = A_3^\Lambda + \zeta^\Lambda(dt + \omega_3), \tag{C.27}$$

where ω_3 and A_3^Λ are 1-forms in 3D and $\Lambda = 0, \ldots, 3$. We dualise these vectors in 3D to scalars using a similar Lagrange multiplier method as mentioned before. The duality relations are

$$-d\tilde{\zeta}_\Lambda = e^{2U}(\mathrm{Im}\,N)_{\Lambda\Sigma} \star_3 (dA_3^\Sigma + \zeta^\Sigma d\omega_3) + (\mathrm{Re}\,N)_{\Lambda\Sigma}d\zeta^\Sigma, \tag{C.28}$$

and

$$-d\sigma = 2e^{4U} \star_3 d\omega_3 - \zeta^\Lambda d\tilde{\zeta}_\Lambda + \tilde{\zeta}_\Lambda d\zeta^\Lambda, \tag{C.29}$$

where $\tilde{\zeta}_\Lambda$ and σ are pseudo-scalars dual to A_3^Λ and ω_3 respectively. The $\mathrm{Re}\,N$ and $\mathrm{Im}\,N$ are the real and imaginary parts of the period matrix N of the STU theory and they are constructed out of the χ^I's and h^I's, respectively.

Therefore, in 3D we have a total of sixteen scalars

$$\varphi^a = \{U, z^I, \bar{z}^I, \zeta^\Lambda, \tilde{\zeta}_\Lambda, \sigma\}, \tag{C.30}$$

parameterising an $SO(4,4)/(SO(2,2)\times SO(2,2))$ coset model. Further details on this set-up can be found in appendix A of [8], where conventions for the $\mathfrak{so}(4,4)$ Lie algebra are also given. The resulting 3D Lagrangian is

$$\mathbb{L}_3 = R_3 \star_3 1 - \frac{1}{2} G_{ab} \star_3 d\varphi^a \wedge d\varphi^b. \tag{C.31}$$

The whole point of the cumbersome procedure described above was to reduce the theory to such a sigma model.

If we perform the first dimensional reduction over a timelike direction and the following reductions over spacelike directions we get a different $SO(4,4)/(SO(2,2)\times SO(2,2))$ coset model. One can take other combinations as well. Such reductions are used in different contexts, see [57, 177].

The scalar coset space can be parameterised in the Iwasawa gauge by the coset element

$$\mathbb{V} = e^{-UH_0} \cdot \left(\prod_{I=1,2,3} e^{-\frac{1}{2}(\log y^I) H_I} \cdot e^{-x^I E_I} \right) \cdot e^{-\zeta^\Lambda E_{q_\Lambda} - \tilde{\zeta}_\Lambda E_{p^\Lambda}} \cdot e^{-\frac{1}{2}\sigma E_0}. \tag{C.32}$$

The matrix $\mathcal{M}$ is defined as

$$\mathcal{M} = \mathbb{V}^\sharp \mathbb{V}, \tag{C.33}$$

where $\theta^\sharp = \eta' \theta^T \eta'^{-1}$ for all $\theta \in \mathfrak{so}(4,4)$ and η' =diag$(-1,-1,1,1,-1,-1,1,1)$ is invariant under the action of the maximal subgroup $SO(2,2)\times SO(2,2)$.

Scalars and some relations from matrix $\mathcal{M}$

We define a matrix $\mathcal{N}$ that conveniently encodes all one-forms in three dimensions, $\mathcal{N} = \mathcal{M}^{-1} d\mathcal{M}$. Under group transformation the matrix $\mathcal{N}$ transforms as $\mathcal{N} \to g^{-1}\mathcal{N} g$. From this matrix one can extract duals of one forms [9] as follows,

$$\star_3 d\omega_3 = \mathcal{N}_{74}, \tag{C.34}$$

$$\star_3 dA^0_3 = \mathcal{N}_{71}, \tag{C.35}$$

$$\star_3 dA^1_3 = \mathcal{N}_{81}, \tag{C.36}$$

$$\star_3 dA^2_3 = \mathcal{N}_{76}, \tag{C.37}$$

$$\star_3 dA^3_3 = \mathcal{N}_{72}. \tag{C.38}$$

Having obtained $\star_3 d\omega_3$ one can straightforwardly integrate to construct ω_3. This procedure is emphasised in references [9,178][4] for STU supergravity. For minimal supergravity it was noted in [179], though in that set-up it did not bring much technical advantage. For STU theory this procedure indeed simplifies calculations.

The remaining three-dimensional scalars are determined directly from the matrix $\mathcal{M}$. There are many ways to extract scalars from the matrix $\mathcal{M}$. Among others, we have found the following equations useful [9]:

$$e^{4U} = \frac{1}{\mathcal{M}_{33}\mathcal{M}_{44} - \mathcal{M}^2_{34}}, \tag{C.39}$$

$$\zeta^0 = e^{4U} \left(\mathcal{M}_{31}\mathcal{M}_{34} - \mathcal{M}_{41}\mathcal{M}_{33}\right), \tag{C.40}$$

$$\zeta^1 = e^{4U} \left(\mathcal{M}_{31}\mathcal{M}_{44} - \mathcal{M}_{41}\mathcal{M}_{34}\right), \tag{C.41}$$

$$\zeta^2 = e^{4U} \left(\mathcal{M}_{64}\mathcal{M}_{33} - \mathcal{M}_{63}\mathcal{M}_{34}\right), \tag{C.42}$$

$$\zeta^3 = e^{4U} \left(\mathcal{M}_{32}\mathcal{M}_{34} - \mathcal{M}_{42}\mathcal{M}_{33}\right), \tag{C.43}$$

[4] We thank Geoffrey Compère for discussions on this point and for sharing some of his notes with us.

$$x_1 = \frac{\mathcal{M}_{34}}{\mathcal{M}_{33}}, \tag{C.44}$$
$$\frac{x_2}{y_2 y_3} = \mathcal{M}_{16} + \mathrm{e}^{4U}(\mathcal{M}_{34}\mathcal{M}_{41}\mathcal{M}_{63} + \mathcal{M}_{31}\mathcal{M}_{34}\mathcal{M}_{64} - \mathcal{M}_{31}\mathcal{M}_{44}\mathcal{M}_{63} - \mathcal{M}_{33}\mathcal{M}_{41}\mathcal{M}_{64}),$$
$$\frac{x_3}{y_2 y_3} = \mathcal{M}_{12} + \mathrm{e}^{4U}(\mathcal{M}_{31}\mathcal{M}_{32}\mathcal{M}_{44} + \mathcal{M}_{33}\mathcal{M}_{41}\mathcal{M}_{42} - \mathcal{M}_{31}\mathcal{M}_{34}\mathcal{M}_{42} - \mathcal{M}_{32}\mathcal{M}_{34}\mathcal{M}_{41}),$$

$$\frac{1}{y_2 y_3} = \mathcal{M}_{11} + \mathrm{e}^{4U}(\mathcal{M}_{33}\mathcal{M}_{41}^2 + \mathcal{M}_{44}\mathcal{M}_{31}^2 - 2\mathcal{M}_{31}\mathcal{M}_{34}\mathcal{M}_{41}), \tag{C.45}$$
$$y_1^2 = \frac{\mathrm{e}^{-4U}}{\mathcal{M}_{33}^2}, \tag{C.46}$$
$$\frac{y_3}{y_2} = \mathcal{M}_{22} - \frac{x_3^2}{y_2 y_3} + \frac{\mathcal{M}_{23}^2}{\mathcal{M}_{33}} + \mathrm{e}^{4U}\frac{(\mathcal{M}_{32}\mathcal{M}_{34} - \mathcal{M}_{33}\mathcal{M}_{42})^2}{\mathcal{M}_{33}}. \tag{C.47}$$

Details on Weyl reflection

The truncation to pure five-dimensional Lorentzian gravity corresponds to taking the six-dimensional metric of the form

$$ds_6^2 = dy^2 + ds_5^2, \tag{C.48}$$

and setting $\Phi = 0$ and $F_{[3]} = 0$. In terms of the three-dimensional coset scalars, this truncation corresponds to setting

$$x^I = 0, \qquad y^I = y, \qquad \zeta^I = 0, \qquad \tilde{\zeta}_I = 0. \tag{C.49}$$

Therefore, the 'active' fields are

$$U, \quad y, \quad \sigma, \quad \zeta^0, \quad \tilde{\zeta}_0. \tag{C.50}$$

These five fields correspond to an SL(3, $\mathbb{R}$) truncation of SO(4, 4), generated by the elements

$$H_0, \quad H_1 + H_2 + H_3, \quad E_{q_0}, \quad E_{p^0}, \quad E_0, \quad F_{q_0}, \quad F_{p^0}, \quad F_0. \tag{C.51}$$

Under conjugation (5.17), this SL(3, $\mathbb{R}$) gets mapped to another SL(3, $\mathbb{R}$) generated by,

$$H_1, \quad H_0 + H_2 + H_3, \quad F_{p^1}, \quad E_{p^0}, \quad E_1, \quad E_{p^1}, \quad F_{p^0}, \quad F_1. \tag{C.52}$$

This new SL(3, $\mathbb{R}$) corresponds to 'active' fields

$$y^1, \quad U, \quad \tilde{\zeta}_0, \quad \tilde{\zeta}_1, \quad x^1. \tag{C.53}$$

We would like to compare this to a truncation to Euclidean five-dimensional, a metric that arises as

$$ds_6^2 = -dt^2 + ds_5^2, \tag{C.54}$$

and where the six-dimensional dilaton and the three-form field are set to zero. This Euclidean gravity truncation corresponds to setting

$$y^1 = f^3 e^{-4U}, \tag{C.55}$$

$$y^2 = y^3 = e^{2U}, \tag{C.56}$$

$$\tilde{\zeta}_2 = \tilde{\zeta}_3 = 0, \tag{C.57}$$

$$\zeta^0 = \zeta^1 = \zeta^2 = \zeta^3 = 0, \tag{C.58}$$

$$x^2 = x^3 = 0, \tag{C.59}$$

$$\sigma = 0, \tag{C.60}$$

which conforms to (C.53).

Three-dimensional seed scalars

For calculational simplicity we work with coordinate $\varkappa$,

$$\varkappa := \cos\theta, \tag{C.61}$$

instead of the polar angle θ. For writing equations in the main text we use θ.

We perform a Kaluza-Klein reduction over y, ϕ, and t respectively. In three-dimensions we use the convention $\epsilon_{r\varkappa\psi} = +\sqrt{+\det g_{3\mathrm{d}}}$. The non-zero scalars in three-dimensions for the metric (5.11) are

$$
\begin{aligned}
\mathrm{e}^{4U} &= \frac{\tilde{\Gamma}}{\tilde{\Sigma}}(1-\varkappa^2), & \tilde{\zeta}_0 &= -a_1 a_2 M \frac{(1-\varkappa^2)^2}{\tilde{\Sigma}}, && \text{(C.62)}\\
\tilde{\zeta}_1 &= -a_2 M \frac{(1-\varkappa^2)}{\tilde{\Sigma}}, & x^1 &= -a_1 M \frac{(1-\varkappa^2)}{\tilde{\Sigma}+M}, && \text{(C.63)}\\
y_1 &= \frac{\sqrt{\tilde{\Sigma}\tilde{\Gamma}}}{\tilde{\Sigma}+M}\sqrt{1-\varkappa^2}, & y_2 = y_3 &= \sqrt{\frac{\tilde{\Gamma}}{\tilde{\Sigma}}}\sqrt{1-\varkappa^2}, && \text{(C.64)}
\end{aligned}
$$

where

$$\tilde{\Sigma} = r^2 + a_1^2(1-\varkappa^2) + a_2^2\varkappa^2 - M, \qquad \text{(C.65)}$$

$$\tilde{\Gamma} = (r^2 + a_2^2)\tilde{\Sigma} + M a_2^2(1-\varkappa^2). \qquad \text{(C.66)}$$

Note that Eq. (C.65) reproduces the relation (5.12) introduced earlier. The three-dimensional base metric is

$$ds_3^2 = \frac{\tilde{\Gamma}}{\tilde{\Delta}}(1-\varkappa^2)dr^2 + \tilde{\Gamma}d\varkappa^2 + \tilde{\Delta}\varkappa^2(1-\varkappa^2)d\psi^2, \qquad \text{(C.67)}$$

where $\tilde{\Delta}$ was introduced in (5.13).

Six-dimensional metric

Using scalars (C.62)–(C.64) we construct the matrix $\mathcal{M}$. We act on this matrix $\mathcal{M}$ with the Weyl reflection transformation (5.17) and then we perform the charging transformation (5.20). From the resulting matrix $\mathcal{M}$ we read all scalars (those obtained in 3d without resorting to dualisation of one-forms) and from the corresponding matrix $\mathcal{N}$ the three-dimensional one-forms. These pieces allow us to construct the 6d metric. We obtain the over-rotating Cvetič-Youm metric (5.21). In these calculations we have followed the conventions for dimensional reduction and group theory of [8]. We have adapted minus signs in the charging transformation (5.20), so that the final answer is same as the JMaRT notation.

A construction of the C-field is more tedious, which we describe next.

C.3 Construction of the C-field

In principle all the information about the C-field is also contained in the three-dimensional scalars. Though, in practice, extracting the C-field is tedious. We have proceeded in the following manner.

Overview of the procedure

An expression for six-dimensional three form $F_{[3]}$ in terms of five-dimensional fields is [8],

$$F^{(6d)}_{[3]} = -(h^3)^{-2} \star_5 dA^3_{[1]} + dA^2_{[1]} \wedge (dy + A^1_{[1]}). \tag{C.68}$$

In order to compute $F^{(6d)}_{[3]}$ we need (*i*) an explicit expression for the dilatonic scalar h^3, cf. (C.23), (*ii*) five-dimensional metric to perform the hodge star, and (*iii*) the three one-forms in five-dimensions.

The dilatonic scalar h^3 can be obtained from values of the scalars y^I from the final matrix $\mathcal{M}_{\text{final}}$. We get

$$h^3 = \left(\frac{\tilde{H}_p \tilde{H}_1}{\tilde{H}_5^2}\right)^{\frac{1}{3}}, \tag{C.69}$$

where

$$\tilde{H}_i = r^2 + a_1^2(1 - \varkappa^2) + a_2^2 \varkappa^2 + M s_i^2. \tag{C.70}$$

Five-dimensional metric

The following form of the five-dimensional metric is quite useful [50] to perform the Hodge star operation,

$$ds^2 = -F^2 f(f-M)(dt+k)^2 + F^{-1} ds^2_{\text{base}}. \tag{C.71}$$

It is obtained by dimensional reduction of the 6d dimensional metric (5.21) over the y-direction. The four-dimensional base metric in (C.71) is

$$\begin{aligned} ds^2_{\text{base}} \;=\; & \frac{r^2}{(r^2+a_1^2)(r^2+a_2^2)-Mr^2}dr^2 + \frac{d\varkappa^2}{1-\varkappa^2} \\ & + (f(f-M))^{-1}\Big\{(f(f-M)+f(a_2^2-a_1^2)(1-\varkappa^2)+Ma_1^2(1-\varkappa^2))(1-\varkappa^2)d\phi^2 \\ & + (f(f-M)+f(a_1^2-a_2^2)\varkappa^2+Ma_2^2\varkappa^2)\varkappa^2 d\psi^2 \\ & + 2Ma_1a_2(1-\varkappa^2)\varkappa^2 d\phi d\psi\Big\}. \end{aligned} \tag{C.72}$$

The one form k in (C.71) is

$$k = \left[\frac{Ms_1s_5s_p}{f}a_1 - \frac{Mc_1c_5c_p}{f-M}a_2\right](1-\varkappa^2)d\phi + \left[\frac{Ms_1s_5s_p}{f}a_2 - \frac{Mc_1c_5c_p}{f-M}a_1\right]\varkappa^2 d\psi, \tag{C.73}$$

and the functions F and f are,

$$F = (\tilde{H}_1\tilde{H}_5\tilde{H}_p)^{-1/3}, \tag{C.74}$$

$$f = r^2 + a_1^2(1-\varkappa^2) + a_2^2\varkappa^2. \tag{C.75}$$

Five-dimensional one forms

All three one-forms in five-dimensions are required for the construction of three-form field strength in six-dimensions. These one-forms (for $I = 1,2,3$), obtained using the matrices $\mathcal{M}$ and $\mathcal{N}$, are

$$A^I = A^I_\psi d\psi + A^I_t dt + A^I_\phi d\phi, \tag{C.76}$$

where

$$A^1_t = -\frac{M s_p c_p}{\tilde{H}_p}, \qquad A^2_t = +\frac{M s_1 c_1}{\tilde{H}_1}, \qquad A^3_t = -\frac{M s_5 c_5}{\tilde{H}_5}, \tag{C.77}$$

and

$$A^1_\phi = \frac{M(a_1 c_p s_1 s_5 - a_2 s_p c_1 c_5)(1-\varkappa^2)}{\tilde{H}_p} \qquad A^1_\psi = \frac{M(a_2 c_p s_1 s_5 - a_1 s_p c_1 c_5)\varkappa^2}{\tilde{H}_p} \tag{C.78}$$

$$A^2_\phi = -\frac{M(a_1 s_p c_1 s_5 - a_2 c_p s_1 c_5)(1-\varkappa^2)}{\tilde{H}_1} \qquad A^2_\psi = -\frac{M(a_2 s_p c_1 s_5 - a_1 c_p s_1 c_5)\varkappa^2}{\tilde{H}_1} \tag{C.79}$$

$$A^3_\phi = \frac{M(a_1 s_p s_1 c_5 - a_2 c_p c_1 s_5)(1-\varkappa^2)}{\tilde{H}_5} \qquad A^3_\psi = \frac{M(a_2 s_p s_1 c_5 - a_1 c_p c_1 s_5)\varkappa^2}{\tilde{H}_5}. \tag{C.80}$$

Some of our signs are different from those of reference [50], but this is simply because some of our conventions are different[5] and our calculations are organised differently.

Final answer

Given these expressions it is straightforward, if somewhat tedious, to implement (C.68). We find in six-dimensions $F_{[3]}$ field has 12 independent components. The first six, coming from the first term in (C.68), $-(h^3)^{-2} \star_5 dA^3_{[1]}$, are

$$F_{r\phi t}, F_{r\phi\psi}, F_{rt\psi}, F_{\varkappa\phi t}, F_{\varkappa\phi\psi}, F_{\varkappa t\psi}, \tag{C.81}$$

and the next six coming from the second term, $dA^2_{[1]} \wedge (dy + A^1_{[1]})$, are

$$F_{r\phi y}, F_{rty}, F_{r\psi y}, F_{\varkappa\phi y}, F_{\varkappa ty}, F_{\varkappa\psi y}. \tag{C.82}$$

[5]Note that we use the convention $\epsilon_{r\varkappa\psi} = +\sqrt{+\det g_{3\mathrm{d}}}$, where $\varkappa = \cos\theta$.

From the resulting F-field a C-field can be constructed by appropriate integrations. An answer is

$$C_2 = C_{ty}\, dt\wedge dy + C_{t\phi}\, dt\wedge d\phi + C_{t\psi}\, dt\wedge d\psi + C_{y\phi}\, dy\wedge d\phi + C_{\psi\phi}\, d\psi\wedge d\phi + C_{y\psi}\, dy\wedge d\psi, \quad \text{(C.83)}$$

where

$$\begin{aligned} C_{ty} &= +\frac{M s_1 c_1}{\tilde{H}_1}, & C_{\psi\phi} &= +\frac{M}{\tilde{H}_1} s_5 c_5 \left(r^2 + a_2^2 + M s_1^2\right)\varkappa^2, \\ C_{t\psi} &= -\frac{M}{\tilde{H}_1}\left(a_2 s_5 c_1 c_p - a_1 c_5 s_1 s_p\right)\varkappa^2, & C_{t\phi} &= -\frac{M}{\tilde{H}_1}\left(a_1 s_5 c_1 c_p - a_2 c_5 s_1 s_p\right)(1-\varkappa^2), \\ C_{y\psi} &= -\frac{M}{\tilde{H}_1}\left(a_1 c_5 s_1 c_p - a_2 s_5 c_1 s_p\right)\varkappa^2, & C_{y\phi} &= -\frac{M}{\tilde{H}_1}\left(a_2 c_5 s_1 c_p - a_1 s_5 c_1 s_p\right)(1-\varkappa^2). \end{aligned} \quad \text{(C.84)}$$

These expressions match the corresponding expressions in [3] upto an over-all minus sign (which is convention dependent). In the main text, cf. (5.23), we have flipped the over-all minus sign, and have employed the polar angle θ instead of $\varkappa$.

C.4 Rod structure of the Cvetič-Youm metric

Our goal here is to understand the rod structures of the Cvetič-Youm metric, in particular the two cases (*i*) black hole and (*ii*) fuzzball.

We recall that solutions of the vacuum Einstein equations in d dimensions with $d-2$ commuting Killing vector fields are classified according to their rod structure: the rods correspond to line sources for a generalised Poisson equation that determines the Killing metric (see appendix C.1). In coordinates adapted to the isometries the metric depends explicitly only on two variables, the canonical coordinates (ρ, z), and the rods are located at $\rho = 0$. They are physically interpreted as the set of spacetime points where some Killing vector — the associated rod direction — degenerates. In particular if the rod is spacelike and extends to $z = \pm\infty$ this indicates an axis of rotation. If the rod is finite and timelike

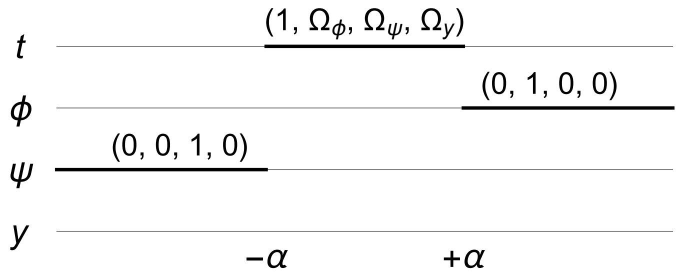

Figure C.2: Rod diagram for the Cvetič-Youm black hole. The direction for each rod is indicated above the corresponding segment.

(spacelike) it signals an event horizon (Kaluza-Klein bubble). We refer to [157, 164] for further details.

The above description of rod structures applies only in vacuum, *a priori*. Consequently, there is no guarantee that the Cvetič-Youm solution is amenable to such a treatment when the charges δ_p, δ_1 and δ_5 are non vanishing. However, we will now see that the rod structure can also be defined for this class of metrics. Since for the JMaRT fuzzball, the y direction shrinks to zero size in the interior of the spacetime, the analysis of the rod structure is best done in six dimensions. Our starting point is the metric (5.21). For this discussion the order of the Killing coordinates we use is (t, ϕ, ψ, y).

Case 1: Black Holes

The Cvetič-Youm metric describes black holes when $M > (a_1 + a_2)^2$. To analyze the rod structure it is convenient to introduce the prolate spherical coordinates (u, v) and the canonical coordinates (ρ, z). In the present case the coordinate transformation relating the radial coordinates (r, θ) used in metric (5.21) to the prolate spherical coordinates (u, v) is

$$r^2 = \frac{1}{2}\left(M + 4u\alpha - a_1^2 - a_2^2\right), \tag{C.85}$$

$$\cos^2\theta = \frac{1}{2}(1 - v), \tag{C.86}$$

where

$$\alpha = \frac{1}{4}\sqrt{M-(a_1+a_2)^2}\sqrt{M-(a_1-a_2)^2}. \tag{C.87}$$

We take $a_1 \geq a_2 \geq 0$. Thus $\alpha > 0$. The canonical coordinates (ρ, z) are related to the prolate coordinates as

$$u = \frac{\sqrt{\rho^2+(z+\alpha)^2}+\sqrt{\rho^2+(z-\alpha)^2}}{2\alpha}, \tag{C.88}$$

$$v = \frac{\sqrt{\rho^2+(z+\alpha)^2}-\sqrt{\rho^2+(z-\alpha)^2}}{2\alpha}. \tag{C.89}$$

Note that Eqs. (C.85-C.86) and (C.87) above are the inverses of (C.15) and (C.13), respectively, upon implementation of the shift transformation (5.7–5.8). This makes $r^2\Delta \to r^2\tilde{\Delta}$, $\cos(2\theta) \to -\cos(2\theta)$ and consequently $(u, v) \to (u, -v)$. This implies $(\rho, z) \to (\rho, -z)$ according to Eqs. (C.8), which are just the inverses of Eqs. (C.88–C.89).

The first rod $\rho = 0, z \in (-\infty, -\alpha)$ corresponds to the degeneration of the ψ circle at $\theta = \pi/2$, i.e., its rod vector is $(0, 0, 1, 0)$. The second rod $\rho = 0, z \in (-\alpha, \alpha)$ corresponds to the horizon with rod vector $(1, \Omega_\phi, \Omega_\psi, \Omega_y)$. The Killing vector that degenerates at the horizon is

$$\xi = \frac{\partial}{\partial t} + \Omega_\phi\frac{\partial}{\partial\phi} + \Omega_\psi\frac{\partial}{\partial\psi} + \Omega_y\frac{\partial}{\partial y}. \tag{C.90}$$

Explicit expressions for Ω_ϕ, Ω_ψ, and Ω_y are (see also [133]),

$$\Omega_\phi = +\frac{1}{\gamma}\left[\frac{a_1-a_2}{\sqrt{M-(a_1-a_2)^2}} - \frac{a_1+a_2}{\sqrt{M-(a_1+a_2)^2}}\right], \tag{C.91}$$

$$\Omega_\psi = -\frac{1}{\gamma}\left[\frac{a_1-a_2}{\sqrt{M-(a_1-a_2)^2}} + \frac{a_1+a_2}{\sqrt{M-(a_1+a_2)^2}}\right], \tag{C.92}$$

$$\Omega_y = \frac{M}{\gamma}\left[\frac{c_1c_5s_p - s_1s_5c_p}{\sqrt{M-(a_1-a_2)^2}} + \frac{c_1c_5s_p + s_1s_5c_p}{\sqrt{M-(a_1+a_2)^2}}\right],$$

where

$$\gamma = M\left[\frac{c_1c_5c_p - s_1s_5s_p}{\sqrt{M-(a_1-a_2)^2}} + \frac{c_1c_5c_p + s_1s_5s_p}{\sqrt{M-(a_1+a_2)^2}}\right]. \tag{C.93}$$

The third rod $\rho = 0, z \in (\alpha, \infty)$ corresponds to the degeneration of the ϕ circle at $\theta = 0$,

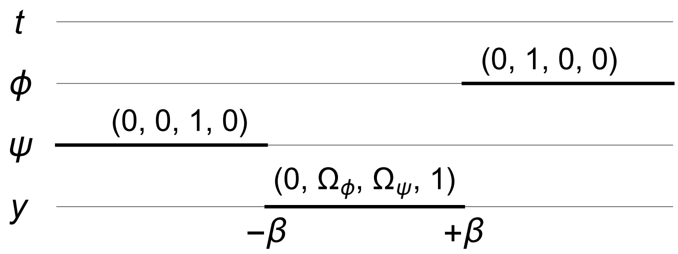

Figure C.3: Rod diagram for the JMaRT fuzzball. The direction for each rod is indicated above the corresponding segment.

i.e., its rod vector is $(0,1,0,0)$. The rod diagram is shown in figure C.2.

Case 2: Fuzzballs

For the smooth solitonic fuzzball solutions we have $(a_1-a_2)^2 > M$. The end points of the rod on the z-axis are at $\pm\beta$ where

$$\beta = \frac{1}{4}\sqrt{(a_1+a_2)^2-M}\,\sqrt{(a_1-a_2)^2-M}. \tag{C.94}$$

Note that $\beta > 0$. We introduce the prolate and the canonical coordinates exactly in the same manner as in the black hole case. The radial coordinates (r,θ) used in metric (5.21) are related to the prolate spherical coordinates (u,v) via

$$r^2 = \frac{1}{2}\left(M+4u\beta-a_1^2-a_2^2\right), \tag{C.95}$$

$$\cos^2\theta = \frac{1}{2}(1-v), \tag{C.96}$$

and the canonical coordinates (ρ,z) are related to the prolate coordinates as

$$u = \frac{\sqrt{\rho^2+(z+\beta)^2}+\sqrt{\rho^2+(z-\beta)^2}}{2\beta}, \tag{C.97}$$

$$v = \frac{\sqrt{\rho^2+(z+\beta)^2}-\sqrt{\rho^2+(z-\beta)^2}}{2\beta}. \tag{C.98}$$

As in the black hole case, the first rod $z \in (-\infty, -\beta)$ corresponds to the degeneration of the ψ circle at $\theta = \pi/2$, i.e., its rod vector is $(0, 0, 1, 0)$. The third rod $z \in (\beta, \infty)$ corresponds the degeneration of the ϕ circle at $\theta = 0$, i.e., its rod vector is $(0, 1, 0, 0)$. The second rod $\rho = 0, z \in (-\beta, \beta)$ corresponds to the degeneration of the y direction. The determinant of the (4×4) Killing matrix over coordinates (t, ϕ, ψ, y) vanishes at $\rho = 0$, which in terms of the original radial coordinate translates into

$$r^2 = r_+^2 := \frac{M + 4\beta - a_1^2 - a_2^2}{2}. \tag{C.99}$$

The fuzzball construction [3] further requires that the determinant of the (3×3) Killing matrix over purely spatial directions (ϕ, ψ, y) vanishes at $\rho = 0, z \in (-\beta, \beta)$, i.e., at $r = r_+$. So, we consider $t = \text{const}$ slice along with $r = r_+$. The determinant of the (3×3) Killing matrix vanishes for

$$M = a_1^2 + a_2^2 - a_1 a_2 \frac{(s_1^2 s_5^2 s_p^2 + c_1^2 c_5^2 c_p^2)}{s_1 s_5 s_p c_1 c_5 c_p}. \tag{C.100}$$

Substituting this value of M in (C.99) we get,

$$r_+^2 = -a_1 a_2 \frac{s_1 s_5 s_p}{c_1 c_5 c_p}. \tag{C.101}$$

The Killing vector that degenerates at the second rod $\rho = 0, z \in (-\beta, \beta)$ is

$$\xi = \frac{\partial}{\partial y} + \Omega_\phi \frac{\partial}{\partial \phi} + \Omega_\psi \frac{\partial}{\partial \psi}, \tag{C.102}$$

with

$$\Omega_\phi = \frac{s_p c_p}{a_2 c_1 c_5 c_p - a_1 s_1 s_5 s_p}, \qquad \Omega_\psi = \frac{s_p c_p}{a_1 c_1 c_5 c_p - a_2 s_1 s_5 s_p}. \tag{C.103}$$

The rod diagram is shown in figure C.3.

Bibliography

[1] O. Lunin and S. D. Mathur, "AdS / CFT duality and the black hole information paradox," *Nucl. Phys.* **B623** (2002) 342–394, arXiv:hep-th/0109154 [hep-th].

[2] I. Bena, J. de Boer, M. Shigemori, and N. P. Warner, "Double, Double Supertube Bubble," *JHEP* **10** (2011) 116, arXiv:1107.2650 [hep-th].

[3] V. Jejjala, O. Madden, S. F. Ross, and G. Titchener, "Non-supersymmetric smooth geometries and D1-D5-P bound states," *Phys. Rev.* **D71** (2005) 124030, arXiv:hep-th/0504181 [hep-th].

[4] B. Chakrabarty, D. Turton, and A. Virmani, "Holographic description of non-supersymmetric orbifolded D1-D5-P solutions," *JHEP* **11** (2015) 063, arXiv:1508.01231 [hep-th].

[5] P. Breitenlohner and D. Maison, "On the Geroch Group," *Ann. Inst. H. Poincare Phys. Theor.* **46** (1987) 215.

[6] D. Katsimpouri, A. Kleinschmidt, and A. Virmani, "Inverse Scattering and the Geroch Group," *JHEP* **02** (2013) 011, arXiv:1211.3044 [hep-th].

[7] M. C. Camara, G. L. Cardoso, T. Mohaupt, and S. Nampuri, "A Riemann-Hilbert approach to rotating attractors," arXiv:1703.10366 [hep-th].

[8] A. Virmani, "Subtracted Geometry From Harrison Transformations," *JHEP* **07** (2012) 086, arXiv:1203.5088 [hep-th].

[9] D. D. K. Chow and G. Compere, "Black holes in N=8 supergravity from SO(4,4) hidden symmetries," *Phys. Rev.* **D90** no. 2, (2014) 025029, arXiv:1404.2602 [hep-th].

[10] B. Chakrabarty and A. Virmani, "Geroch Group Description of Black Holes," *JHEP* **11** (2014) 068, arXiv:1408.0875 [hep-th].

[11] S. Giusto and S. D. Mathur, "Geometry of D1-D5-P bound states," *Nucl. Phys.* **B729** (2005) 203–220, arXiv:hep-th/0409067 [hep-th].

[12] B. Chakrabarty, J. V. Rocha, and A. Virmani, "Smooth non-extremal D1-D5-P solutions as charged gravitational instantons," *JHEP* **08** (2016) 027, arXiv:1603.06799 [hep-th].

[13] **Virgo, LIGO Scientific** Collaboration, B. P. Abbott *et al.*, "Observation of Gravitational Waves from a Binary Black Hole Merger," *Phys. Rev. Lett.* **116** no. 6, (2016) 061102, arXiv:1602.03837 [gr-qc].

[14] S. W. Hawking, "Particle Creation by Black Holes," *Commun. Math. Phys.* **43** (1975) 199–220. [,167(1975)].

[15] J. D. Bekenstein, "Black holes and entropy," *Phys. Rev.* **D7** (1973) 2333–2346.

[16] J. M. Bardeen, B. Carter, and S. W. Hawking, "The Four laws of black hole mechanics," *Commun. Math. Phys.* **31** (1973) 161–170.

[17] T. Jacobson, *Introductory lectures on Black hole Thermodynamics*. http://www.physics.umd.edu/grt/taj/776b/lectures.pdf.

[18] R. M. Wald, "The thermodynamics of black holes," *Living Rev. Rel.* **4** (2001) 6, arXiv:gr-qc/9912119 [gr-qc].

[19] J. M. Maldacena, "The Large N limit of superconformal field theories and supergravity," *Int. J. Theor. Phys.* **38** (1999) 1113–1133, arXiv:hep-th/9711200 [hep-th]. [Adv. Theor. Math. Phys.2,231(1998)].

[20] E. Witten, "Anti-de Sitter space and holography," *Adv. Theor. Math. Phys.* **2** (1998) 253–291, arXiv:hep-th/9802150 [hep-th].

[21] O. Aharony, S. S. Gubser, J. M. Maldacena, H. Ooguri, and Y. Oz, "Large N field theories, string theory and gravity," *Phys. Rept.* **323** (2000) 183–386, arXiv:hep-th/9905111 [hep-th].

[22] S. Giusto, O. Lunin, S. D. Mathur, and D. Turton, "D1-D5-P microstates at the cap," *JHEP* **02** (2013) 050, arXiv:1211.0306 [hep-th].

[23] S. D. Mathur, "The Information paradox: A Pedagogical introduction," *Class. Quant. Grav.* **26** (2009) 224001, arXiv:0909.1038 [hep-th].

[24] O. Lunin and S. D. Mathur, "Statistical interpretation of Bekenstein entropy for systems with a stretched horizon," *Phys. Rev. Lett.* **88** (2002) 211303, arXiv:hep-th/0202072 [hep-th].

[25] S. D. Mathur, "What prevents gravitational collapse in string theory?," *Int. J. Mod. Phys.* **D25** no. 12, (2016) 1644018, arXiv:1609.05222 [hep-th].

[26] S. Mathur, "Black holes in String theory,". http://www.physics.ohio-state.edu/~mathur/gian/bhdrivershortentropy.pdf.

[27] E. Witten and D. I. Olive, "Supersymmetry Algebras That Include Topological Charges," *Phys. Lett.* **B78** (1978) 97–101.

[28] K. Becker, M. Becker, and J. Schwarz, *String Theory and M-Theory: A Modern Introduction*. Cambridge University Press, 2006. https://books.google.co.in/books?id=WgUkSTJWQacC.

[29] A. Sen, "Extremal black holes and elementary string states," *Mod. Phys. Lett.* **A10** (1995) 2081–2094, arXiv:hep-th/9504147 [hep-th].

[30] C. G. Callan, J. M. Maldacena, and A. W. Peet, "Extremal black holes as fundamental strings," *Nucl. Phys.* **B475** (1996) 645–678, arXiv:hep-th/9510134 [hep-th].

[31] A. Dabholkar, J. P. Gauntlett, J. A. Harvey, and D. Waldram, "Strings as solitons and black holes as strings," *Nucl. Phys.* **B474** (1996) 85–121, arXiv:hep-th/9511053 [hep-th].

[32] O. Lunin, J. M. Maldacena, and L. Maoz, "Gravity solutions for the D1-D5 system with angular momentum," arXiv:hep-th/0212210 [hep-th].

[33] V. S. Rychkov, "D1-D5 black hole microstate counting from supergravity," *JHEP* **01** (2006) 063, arXiv:hep-th/0512053 [hep-th].

[34] A. Strominger and C. Vafa, "Microscopic origin of the Bekenstein-Hawking entropy," *Phys. Lett.* **B379** (1996) 99–104, arXiv:hep-th/9601029 [hep-th].

[35] H. Elvang, R. Emparan, D. Mateos, and H. S. Reall, "Supersymmetric black rings and three-charge supertubes," *Phys. Rev.* **D71** (2005) 024033, arXiv:hep-th/0408120 [hep-th].

[36] I. Bena and N. P. Warner, "One ring to rule them all ... and in the darkness bind them?," *Adv. Theor. Math. Phys.* **9** no. 5, (2005) 667–701, arXiv:hep-th/0408106 [hep-th].

[37] J. P. Gauntlett, J. B. Gutowski, C. M. Hull, S. Pakis, and H. S. Reall, "All supersymmetric solutions of minimal supergravity in five- dimensions," *Class. Quant. Grav.* **20** (2003) 4587–4634, arXiv:hep-th/0209114 [hep-th].

[38] S. Giusto and S. D. Mathur, "Geometry of D1-D5-P bound states," *Nucl. Phys.* **B729** (2005) 203–220, arXiv:hep-th/0409067 [hep-th].

[39] I. Bena and N. P. Warner, "Bubbling supertubes and foaming black holes," *Phys. Rev.* **D74** (2006) 066001, arXiv:hep-th/0505166 [hep-th].

[40] P. Berglund, E. G. Gimon, and T. S. Levi, "Supergravity microstates for BPS black holes and black rings," *JHEP* **06** (2006) 007, arXiv:hep-th/0505167 [hep-th].

[41] I. L. R. Bena, *Black Holes, Black Rings and their Microstates*. PhD thesis, UCSB, 2009. http://ipht.cea.fr/Docspht//search/article.php?IDA=9690.

[42] G. W. Gibbons and N. P. Warner, "Global structure of five-dimensional fuzzballs," *Class. Quant. Grav.* **31** (2014) 025016, arXiv:1305.0957 [hep-th].

[43] V. Balasubramanian, E. G. Gimon, and T. S. Levi, "Four Dimensional Black Hole Microstates: From D-branes to Spacetime Foam," *JHEP* **01** (2008) 056, arXiv:hep-th/0606118 [hep-th].

[44] I. Bena, C.-W. Wang, and N. P. Warner, "Plumbing the Abyss: Black ring microstates," *JHEP* **07** (2008) 019, arXiv:0706.3786 [hep-th].

[45] I. Bena, N. Bobev, S. Giusto, C. Ruef, and N. P. Warner, "An Infinite-Dimensional Family of Black-Hole Microstate Geometries," *JHEP* **03** (2011) 022, arXiv:1006.3497 [hep-th]. [Erratum: JHEP04,059(2011)].

[46] I. Bena, S. Giusto, R. Russo, M. Shigemori, and N. P. Warner, "Habemus Superstratum! A constructive proof of the existence of superstrata," *JHEP* **05** (2015) 110, arXiv:1503.01463 [hep-th].

[47] K. Goldstein and S. Katmadas, "Almost BPS black holes," *JHEP* **05** (2009) 058, arXiv:0812.4183 [hep-th].

[48] I. Bena, S. Giusto, C. Ruef, and N. P. Warner, "Multi-Center non-BPS Black Holes: the Solution," *JHEP* **11** (2009) 032, arXiv:0908.2121 [hep-th].

[49] I. Bena, G. Dall'Agata, S. Giusto, C. Ruef, and N. P. Warner, "Non-BPS Black Rings and Black Holes in Taub-NUT," *JHEP* **06** (2009) 015, arXiv:0902.4526 [hep-th].

[50] E. G. Gimon, T. S. Levi, and S. F. Ross, "Geometry of non-supersymmetric three-charge bound states," *JHEP* **08** (2007) 055, arXiv:0705.1238 [hep-th].

[51] S. Giusto, S. F. Ross, and A. Saxena, "Non-supersymmetric microstates of the D1-D5-KK system," *JHEP* **12** (2007) 065, arXiv:0708.3845 [hep-th].

[52] J. H. Al-Alawi and S. F. Ross, "Spectral Flow of the Non-Supersymmetric Microstates of the D1-D5-KK System," *JHEP* **10** (2009) 082, arXiv:0908.0417 [hep-th].

[53] I. Bena, A. Puhm, and B. Vercnocke, "Metastable Supertubes and non-extremal Black Hole Microstates," *JHEP* **04** (2012) 100, arXiv:1109.5180 [hep-th].

[54] I. Bena, A. Puhm, and B. Vercnocke, "Non-extremal Black Hole Microstates: Fuzzballs of Fire or Fuzzballs of Fuzz ?," *JHEP* **12** (2012) 014, arXiv:1208.3468 [hep-th].

[55] S. D. Mathur and D. Turton, "Oscillating supertubes and neutral rotating black hole microstates," *JHEP* **04** (2014) 072, arXiv:1310.1354 [hep-th].

[56] S. Banerjee, B. D. Chowdhury, B. Vercnocke, and A. Virmani, "Non-supersymmetric Microstates of the MSW System," *JHEP* **05** (2014) 011, arXiv:1402.4212 [hep-th].

[57] D. Katsimpouri, A. Kleinschmidt, and A. Virmani, "An Inverse Scattering Construction of the JMaRT Fuzzball," *JHEP* **12** (2014) 070, arXiv:1409.6471 [hep-th].

[58] G. Bossard and S. Katmadas, "A bubbling bolt," *JHEP* **07** (2014) 118, arXiv:1405.4325 [hep-th].

[59] G. Bossard and S. Katmadas, "Floating JMaRT," *JHEP* **04** (2015) 067, arXiv:1412.5217 [hep-th].

[60] P. de Lange, D. R. Mayerson, and B. Vercnocke, "Structure of Six-Dimensional Microstate Geometries," *JHEP* **09** (2015) 075, arXiv:1504.07987 [hep-th].

[61] J. C. Breckenridge, R. C. Myers, A. W. Peet, and C. Vafa, "D-branes and spinning black holes," *Phys. Lett.* **B391** (1997) 93–98, arXiv:hep-th/9602065 [hep-th].

[62] J. R. David, G. Mandal, and S. R. Wadia, "Microscopic formulation of black holes in string theory," *Phys. Rept.* **369** (2002) 549–686, arXiv:hep-th/0203048 [hep-th].

[63] B. Julia, "APPLICATION OF SUPERGRAVITY TO GRAVITATION THEORY," in *International School of Cosmology and Gravitation: 8th Course: Unified Field Theories of More than Four Dimensions, Including Exact Solutions Erice, Italy, May 20-June 1, 1982*, pp. 215–235. 1982.

[64] P. Breitenlohner, D. Maison, and G. W. Gibbons, "Four-Dimensional Black Holes from Kaluza-Klein Theories," *Commun. Math. Phys.* **120** (1988) 295.

[65] D. Youm, "Black holes and solitons in string theory," *Phys. Rept.* **316** (1999) 1–232, arXiv:hep-th/9710046 [hep-th].

[66] D. D. K. Chow and G. Compere, "Seed for general rotating non-extremal black holes of $\mathcal{N} = 8$ supergravity," *Class. Quant. Grav.* **31** (2014) 022001, arXiv:1310.1925 [hep-th].

[67] S. Tomizawa, Y. Yasui, and A. Ishibashi, "Uniqueness theorem for charged rotating black holes in five-dimensional minimal supergravity," *Phys. Rev.* **D79** (2009) 124023, arXiv:0901.4724 [hep-th].

[68] S. Hollands, "Black hole uniqueness theorems and new thermodynamic identities in eleven dimensional supergravity," *Class. Quant. Grav.* **29** (2012) 205009, arXiv:1204.3421 [gr-qc].

[69] G. Bossard, H. Nicolai, and K. S. Stelle, "Universal BPS structure of stationary supergravity solutions," *JHEP* **07** (2009) 003, arXiv:0902.4438 [hep-th].

[70] G. Bossard, Y. Michel, and B. Pioline, "Extremal black holes, nilpotent orbits and the true fake superpotential," *JHEP* **01** (2010) 038, arXiv:0908.1742 [hep-th].

[71] G. Bossard and C. Ruef, "Interacting non-BPS black holes," *Gen. Rel. Grav.* **44** (2012) 21–66, arXiv:1106.5806 [hep-th].

[72] G. Bossard, "Octonionic black holes," *JHEP* **05** (2012) 113, arXiv:1203.0530 [hep-th].

[73] R. P. Geroch, "A Method for generating solutions of Einstein's equations," *J. Math. Phys.* **12** (1971) 918–924.

[74] R. P. Geroch, "A Method for generating new solutions of Einstein's equation. 2," *J. Math. Phys.* **13** (1972) 394–404.

[75] B. Julia, "INFINITE LIE ALGEBRAS IN PHYSICS," in *Unified field theories and beyond*, pp. 23–41. 1981.

[76] B. Julia, "GROUP DISINTEGRATIONS," *Conf. Proc.* **C8006162** (1980) 331–350.

[77] P. Breitenlohner and D. Maison, "Solitons in Kaluza Klein theories," *unpublished notes* **June** (1986) .

[78] H. Nicolai, "Two-dimensional gravities and supergravities as integrable system," *Lect. Notes Phys.* **396** (1991) 231–273.

[79] V. A. Belinsky and V. E. Zakharov, "Integration of the Einstein Equations by the Inverse Scattering Problem Technique and the Calculation of the Exact Soliton Solutions," *Sov. Phys. JETP* **48** (1978) 985–994. [Zh. Eksp. Teor. Fiz.75,1953(1978)].

[80] V. A. Belinsky and V. E. Sakharov, "Stationary Gravitational Solitons with Axial Symmetry," *Sov. Phys. JETP* **50** (1979) 1–9. [Zh. Eksp. Teor. Fiz.77,3(1979)].

[81] V. Belinski and E. Verdaguer, *Gravitational Solitons*. Cambridge Monographs on Mathem. Cambridge University Press, 2001. https://books.google.co.in/books?id=bUfCqIYrc8IC.

[82] I. Bakas, "0(2,2) transformations and the string Geroch group," *Nucl. Phys.* **B428** (1994) 374–398, arXiv:hep-th/9402016 [hep-th].

[83] A. Sen, "Duality symmetry group of two-dimensional heterotic string theory," *Nucl. Phys.* **B447** (1995) 62–84, arXiv:hep-th/9503057 [hep-th].

[84] I. Bakas, "Solitons of axion - dilaton gravity," *Phys. Rev.* **D54** (1996) 6424–6434, arXiv:hep-th/9605043 [hep-th].

[85] A. K. Das, J. Maharana, and A. Melikyan, "Duality, monodromy and integrability of two-dimensional string effective action," *Phys. Rev.* **D65** (2002) 126001, arXiv:hep-th/0203144 [hep-th].

[86] J. Ehlers, "Transformations of static exterior solutions of Einstein's gravitational field equations into differential solutions by means of conformal mappings," *Les theories physiques de la gravitation, CNRS* (1959) .

[87] R. A. Matzner and C. W. Misner, "Gravitational Field Equations for Sources with Axial Symmetry and Angular Momentum," *Phys. Rev.* **154** (1967) 1229–1232.

[88] H. Nicolai and A. Nagar, "Infinite-dimensional symmetries in gravity,," *In *Ciufolini, I. (ed.) et al.: Gravitational waves** 243–267.

[89] D. Katsimpouri, *Integrability in two dimensional gravity*. PhD thesis, Humboldt University, Berlin, 2015. http://edoc.hu-berlin.de/dissertationen/katsimpouri-despoina-2015-06-12/PDF/katsimpouri.pdf.

[90] V. Kac, *Infinite Dimensional Lie Algebras: An Introduction*. Progress in Mathematics. Birkhäuser Boston, 2013. https://books.google.co.in/books?id=ifHiBwAAQBAJ.

[91] S. W. Hawking, "Breakdown of Predictability in Gravitational Collapse," *Phys. Rev.* **D14** (1976) 2460–2473.

[92] S. D. Mathur, "The Fuzzball proposal for black holes: An Elementary review," *Fortsch. Phys.* **53** (2005) 793–827, arXiv:hep-th/0502050 [hep-th].

[93] K. Skenderis and M. Taylor, "The fuzzball proposal for black holes," *Phys. Rept.* **467** (2008) 117–171, arXiv:0804.0552 [hep-th].

[94] V. Balasubramanian, J. de Boer, S. El-Showk, and I. Messamah, "Black Holes as Effective Geometries," *Class. Quant. Grav.* **25** (2008) 214004, arXiv:0811.0263 [hep-th].

[95] B. D. Chowdhury and A. Virmani, "Modave Lectures on Fuzzballs and Emission from the D1-D5 System," in *5th Modave Summer School in Mathematical Physics Modave, Belgium, August 17-21, 2009*. 2010. arXiv:1001.1444 [hep-th]. https://inspirehep.net/record/842481/files/arXiv:1001.1444.pdf.

[96] S. D. Mathur, "Black Holes and Beyond," *Annals Phys.* **327** (2012) 2760–2793, arXiv:1205.0776 [hep-th].

[97] I. Bena and N. P. Warner, "Resolving the Structure of Black Holes: Philosophizing with a Hammer," arXiv:1311.4538 [hep-th].

[98] S. Giusto, S. D. Mathur, and A. Saxena, “Dual geometries for a set of 3-charge microstates,” *Nucl. Phys.* **B701** (2004) 357–379, arXiv:hep-th/0405017 [hep-th].

[99] O. Lunin, “Adding momentum to D-1 - D-5 system,” *JHEP* **04** (2004) 054, arXiv:hep-th/0404006 [hep-th].

[100] S. Giusto, S. D. Mathur, and A. Saxena, “3-charge geometries and their CFT duals,” *Nucl. Phys.* **B710** (2005) 425–463, arXiv:hep-th/0406103 [hep-th].

[101] I. Bena, C.-W. Wang, and N. P. Warner, “Mergers and typical black hole microstates,” *JHEP* **11** (2006) 042, arXiv:hep-th/0608217 [hep-th].

[102] S. Giusto, R. Russo, and D. Turton, “New D1-D5-P geometries from string amplitudes,” *JHEP* **11** (2011) 062, arXiv:1108.6331 [hep-th].

[103] S. Giusto and R. Russo, “Perturbative superstrata,” *Nucl. Phys.* **B869** (2013) 164–188, arXiv:1211.1957 [hep-th].

[104] S. Giusto, L. Martucci, M. Petrini, and R. Russo, “6D microstate geometries from 10D structures,” *Nucl. Phys.* **B876** (2013) 509–555, arXiv:1306.1745 [hep-th].

[105] B. E. Niehoff, O. Vasilakis, and N. P. Warner, “Multi-Superthreads and Supersheets,” *JHEP* **04** (2013) 046, arXiv:1203.1348 [hep-th].

[106] B. E. Niehoff and N. P. Warner, “Doubly-Fluctuating BPS Solutions in Six Dimensions,” *JHEP* **10** (2013) 137, arXiv:1303.5449 [hep-th].

[107] S. S. Gubser, I. R. Klebanov, and A. M. Polyakov, “Gauge theory correlators from noncritical string theory,” *Phys. Lett.* **B428** (1998) 105–114, arXiv:hep-th/9802109 [hep-th].

[108] S. Giusto, E. Moscato, and R. Russo, “AdS_3 holography for 1/4 and 1/8 BPS geometries,” *JHEP* **11** (2015) 004, arXiv:1507.00945 [hep-th].

[109] K. Skenderis and M. Taylor, "Fuzzball solutions and D1-D5 microstates," *Phys. Rev. Lett.* **98** (2007) 071601, arXiv:hep-th/0609154 [hep-th].

[110] I. Kanitscheider, K. Skenderis, and M. Taylor, "Holographic anatomy of fuzzballs," *JHEP* **04** (2007) 023, arXiv:hep-th/0611171 [hep-th].

[111] C. Vafa, "Gas of d-branes and Hagedorn density of BPS states," *Nucl. Phys.* **B463** (1996) 415–419, arXiv:hep-th/9511088 [hep-th].

[112] S. D. Mathur and D. Turton, "Microstates at the boundary of AdS," *JHEP* **05** (2012) 014, arXiv:1112.6413 [hep-th].

[113] S. D. Mathur and D. Turton, "Momentum-carrying waves on D1-D5 microstate geometries," *Nucl. Phys.* **B862** (2012) 764–780, arXiv:1202.6421 [hep-th].

[114] O. Lunin, S. D. Mathur, and D. Turton, "Adding momentum to supersymmetric geometries," *Nucl. Phys.* **B868** (2013) 383–415, arXiv:1208.1770 [hep-th].

[115] V. Balasubramanian, J. de Boer, E. Keski-Vakkuri, and S. F. Ross, "Supersymmetric conical defects: Towards a string theoretic description of black hole formation," *Phys. Rev.* **D64** (2001) 064011, arXiv:hep-th/0011217 [hep-th].

[116] J. M. Maldacena and L. Maoz, "Desingularization by rotation," *JHEP* **12** (2002) 055, arXiv:hep-th/0012025 [hep-th].

[117] V. Cardoso, O. J. C. Dias, J. L. Hovdebo, and R. C. Myers, "Instability of non-supersymmetric smooth geometries," *Phys. Rev.* **D73** (2006) 064031, arXiv:hep-th/0512277 [hep-th].

[118] B. D. Chowdhury and S. D. Mathur, "Radiation from the non-extremal fuzzball," *Class. Quant. Grav.* **25** (2008) 135005, arXiv:0711.4817 [hep-th].

[119] B. D. Chowdhury and S. D. Mathur, "Pair creation in non-extremal fuzzball geometries," *Class. Quant. Grav.* **25** (2008) 225021, arXiv:0806.2309 [hep-th].

[120] B. D. Chowdhury and S. D. Mathur, "Non-extremal fuzzballs and ergoregion emission," *Class. Quant. Grav.* **26** (2009) 035006, arXiv:0810.2951 [hep-th].

[121] S. G. Avery, B. D. Chowdhury, and S. D. Mathur, "Emission from the D1D5 CFT," *JHEP* **10** (2009) 065, arXiv:0906.2015 [hep-th].

[122] S. G. Avery and B. D. Chowdhury, "Emission from the D1D5 CFT: Higher Twists," *JHEP* **01** (2010) 087, arXiv:0907.1663 [hep-th].

[123] J. L. Friedman, "Ergosphere instability," *Commun. Math. Phys.* **63** (1978) 243–255.

[124] N. Comins and B. F. Schutz, "On the ergoregion instability," *Proc. Roy. Soc. London* **A 364** (1978) 211.

[125] S. L. Braunstein, S. Pirandola, and K. Åżyczkowski, "Better Late than Never: Information Retrieval from Black Holes," *Phys. Rev. Lett.* **110** no. 10, (2013) 101301, arXiv:0907.1190 [quant-ph].

[126] A. Almheiri, D. Marolf, J. Polchinski, and J. Sully, "Black Holes: Complementarity or Firewalls?," *JHEP* **02** (2013) 062, arXiv:1207.3123 [hep-th].

[127] A. Almheiri, D. Marolf, J. Polchinski, D. Stanford, and J. Sully, "An Apologia for Firewalls," *JHEP* **09** (2013) 018, arXiv:1304.6483 [hep-th].

[128] S. D. Mathur and D. Turton, "Comments on black holes I: The possibility of complementarity," *JHEP* **01** (2014) 034, arXiv:1208.2005 [hep-th].

[129] S. D. Mathur and D. Turton, "The flaw in the firewall argument," *Nucl. Phys.* **B884** (2014) 566–611, arXiv:1306.5488 [hep-th].

[130] E. J. Martinec, "The Cheshire Cap," *JHEP* **03** (2015) 112, arXiv:1409.6017 [hep-th].

[131] S. D. Mathur, "A model with no firewall," arXiv:1506.04342 [hep-th].

[132] M. Cvetic and D. Youm, "General rotating five-dimensional black holes of toroidally compactified heterotic string," *Nucl. Phys.* **B476** (1996) 118–132, arXiv:hep-th/9603100 [hep-th].

[133] M. Cvetic and F. Larsen, "General rotating black holes in string theory: Grey body factors and event horizons," *Phys. Rev.* **D56** (1997) 4994–5007, arXiv:hep-th/9705192 [hep-th].

[134] Z. Carson, S. Hampton, S. D. Mathur, and D. Turton, "Effect of the deformation operator in the D1D5 CFT," *JHEP* **01** (2015) 071, arXiv:1410.4543 [hep-th].

[135] A. Schwimmer and N. Seiberg, "Comments on the N=2, N=3, N=4 Superconformal Algebras in Two-Dimensions," *Phys. Lett.* **B184** (1987) 191–196.

[136] O. Lunin and S. D. Mathur, "Three point functions for M(N) / S(N) orbifolds with N=4 supersymmetry," *Commun. Math. Phys.* **227** (2002) 385–419, arXiv:hep-th/0103169 [hep-th].

[137] E. J. Martinec and W. McElgin, "String theory on AdS orbifolds," *JHEP* **04** (2002) 029, arXiv:hep-th/0106171 [hep-th].

[138] E. J. Martinec and W. McElgin, "Exciting AdS orbifolds," *JHEP* **10** (2002) 050, arXiv:hep-th/0206175 [hep-th].

[139] R. Dijkgraaf, G. W. Moore, E. P. Verlinde, and H. L. Verlinde, "Elliptic genera of symmetric products and second quantized strings," *Commun. Math. Phys.* **185** (1997) 197–209, arXiv:hep-th/9608096 [hep-th].

[140] O. Lunin and S. D. Mathur, "Correlation functions for M(N)/S(N) orbifolds," *Int. J. Mod. Phys.* **A16S1C** (2001) 967–969.

[141] Z. Carson, S. Hampton, S. D. Mathur, and D. Turton, "Effect of the twist operator in the D1D5 CFT," *JHEP* **08** (2014) 064, arXiv:1405.0259 [hep-th].

[142] L. J. Dixon, J. A. Harvey, C. Vafa, and E. Witten, "Strings on Orbifolds," *Nucl. Phys.* **B261** (1985) 678–686.

[143] L. J. Dixon, J. A. Harvey, C. Vafa, and E. Witten, "Strings on Orbifolds. 2.," *Nucl. Phys.* **B274** (1986) 285–314.

[144] L. J. Dixon, D. Friedan, E. J. Martinec, and S. H. Shenker, "The Conformal Field Theory of Orbifolds," *Nucl. Phys.* **B282** (1987) 13–73.

[145] A. Adams, J. Polchinski, and E. Silverstein, "Don't panic! Closed string tachyons in ALE space-times," *JHEP* **10** (2001) 029, arXiv:hep-th/0108075 [hep-th].

[146] M. Gutperle, M. Headrick, S. Minwalla, and V. Schomerus, "Space-time energy decreases under world sheet RG flow," *JHEP* **01** (2003) 073, arXiv:hep-th/0211063 [hep-th].

[147] C. Vafa, "Mirror symmetry and closed string tachyon condensation," arXiv:hep-th/0111051 [hep-th].

[148] J. A. Harvey, D. Kutasov, E. J. Martinec, and G. W. Moore, "Localized tachyons and RG flows," arXiv:hep-th/0111154 [hep-th].

[149] D. Rasheed, "The Rotating dyonic black holes of Kaluza-Klein theory," *Nucl. Phys.* **B454** (1995) 379–401, arXiv:hep-th/9505038 [hep-th].

[150] F. Larsen, "Rotating Kaluza-Klein black holes," *Nucl. Phys.* **B575** (2000) 211–230, arXiv:hep-th/9909102 [hep-th].

[151] R. C. Myers and M. J. Perry, "Black Holes in Higher Dimensional Space-Times," *Annals Phys.* **172** (1986) 304.

[152] D. Katsimpouri, A. Kleinschmidt, and A. Virmani, "An inverse scattering formalism for STU supergravity," *JHEP* **03** (2014) 101, arXiv:1311.7018 [hep-th].

[153] C. Pope, "Lectures on Kaluza-Klein theory," *http://faculty.physics.tamu.edu/pope/* .

[154] S. Hollands and S. Yazadjiev, "Uniqueness theorem for 5-dimensional black holes with two axial Killing fields," *Commun. Math. Phys.* **283** (2008) 749–768, arXiv:0707.2775 [gr-qc].

[155] S. Giusto and A. Saxena, "Stationary axisymmetric solutions of five dimensional gravity," *Class. Quant. Grav.* **24** (2007) 4269–4294, arXiv:0705.4484 [hep-th].

[156] R. Emparan and A. Maccarrone, "Statistical description of rotating Kaluza-Klein black holes," *Phys. Rev.* **D75** (2007) 084006, arXiv:hep-th/0701150 [hep-th].

[157] T. Harmark, "Stationary and axisymmetric solutions of higher-dimensional general relativity," *Phys. Rev.* **D70** (2004) 124002, arXiv:hep-th/0408141 [hep-th].

[158] L. Andrianopoli, A. Gallerati, and M. Trigiante, "On Extremal Limits and Duality Orbits of Stationary Black Holes," *JHEP* **01** (2014) 053, arXiv:1310.7886 [hep-th].

[159] K. W., "Generation of stationary Einstein-Maxwell fields," *J. Math. Phys.* **14** (1973) 651.

[160] J. Lindman Hornlund and A. Virmani, "Extremal limits of the Cvetic-Youm black hole and nilpotent orbits of $G_{2(2)}$," *JHEP* **11** (2010) 062, arXiv:1008.3329 [hep-th]. [Erratum: JHEP05,038(2012)].

[161] I. Bena, S. Giusto, C. Ruef, and N. P. Warner, "A (Running) Bolt for New Reasons," *JHEP* **11** (2009) 089, arXiv:0909.2559 [hep-th].

[162] I. Bena, G. Bossard, S. Katmadas, and D. Turton, "Non-BPS multi-bubble microstate geometries," *JHEP* **02** (2016) 073, arXiv:1511.03669 [hep-th].

[163] Y. Chen and E. Teo, "Rod-structure classification of gravitational instantons with U(1)xU(1) isometry," *Nucl. Phys.* **B838** (2010) 207–237, arXiv:1004.2750 [gr-qc].

[164] R. Emparan and H. S. Reall, "Generalized Weyl solutions," *Phys. Rev.* **D65** (2002) 084025, arXiv:hep-th/0110258 [hep-th].

[165] N. Bobev and C. Ruef, "The Nuts and Bolts of Einstein-Maxwell Solutions," *JHEP* **01** (2010) 124, arXiv:0912.0010 [hep-th].

[166] A. A. Pomeransky, "Complete integrability of higher-dimensional Einstein equations with additional symmetry, and rotating black holes," *Phys. Rev.* **D73** (2006) 044004, arXiv:hep-th/0507250 [hep-th].

[167] B. Chakrabarty and A. Virmani, "Geroch Group Description of Black Holes," *JHEP* **11** (2014) 068, arXiv:1408.0875 [hep-th].

[168] R. G. Leigh, A. C. Petkou, P. M. Petropoulos, and P. K. Tripathy, "The Geroch group in Einstein spaces," *Class. Quant. Grav.* **31** no. 22, (2014) 225006, arXiv:1403.6511 [hep-th].

[169] P. Figueras, E. Jamsin, J. V. Rocha, and A. Virmani, "Integrability of Five Dimensional Minimal Supergravity and Charged Rotating Black Holes," *Class. Quant. Grav.* **27** (2010) 135011, arXiv:0912.3199 [hep-th].

[170] R. Emparan and H. S. Reall, "A Rotating black ring solution in five-dimensions," *Phys. Rev. Lett.* **88** (2002) 101101, arXiv:hep-th/0110260 [hep-th].

[171] I. Gradshteyn and I. Ryzhik, *Table of Integrals, Series, and Products*. Elsevier Science, 2014. https://books.google.co.in/books?id=F7jiBQAAQBAJ.

[172] L. Houart, A. Kleinschmidt, J. Lindman Hornlund, D. Persson, and N. Tabti, "Finite and infinite-dimensional symmetries of pure N=2 supergravity in D=4," *JHEP* **08** (2009) 098, arXiv:0905.4651 [hep-th].

[173] K. Izumi, "Orthogonal black di-ring solution," *Prog. Theor. Phys.* **119** (2008) 757–774, arXiv:0712.0902 [hep-th].

[174] R. Emparan and H. S. Reall, "Black Holes in Higher Dimensions," *Living Rev. Rel.* **11** (2008) 6, arXiv:0801.3471 [hep-th].

[175] H. Elvang and P. Figueras, "Black Saturn," *JHEP* **05** (2007) 050, arXiv:hep-th/0701035 [hep-th].

[176] J. V. Rocha, M. J. Rodriguez, O. Varela, and A. Virmani, "Charged black rings from inverse scattering," *Gen. Rel. Grav.* **45** (2013) 2099–2121, arXiv:1305.4969 [hep-th].

[177] A. Sahay and A. Virmani, "Subtracted Geometry from Harrison Transformations: II," *JHEP* **07** (2013) 089, arXiv:1305.2800 [hep-th].

[178] D. V. Gal'tsov and N. G. Scherbluk, "Improved generating technique for D=5 supergravities and squashed Kaluza-Klein Black Holes," *Phys. Rev.* **D79** (2009) 064020, arXiv:0812.2336 [hep-th].

[179] G. Compere, S. de Buyl, E. Jamsin, and A. Virmani, "G2 Dualities in D=5 Supergravity and Black Strings," *Class. Quant. Grav.* **26** (2009) 125016, arXiv:0903.1645 [hep-th].